UNCLASSIFIED

AD NUMBER
ADB208426
NEW LIMITATION CHANGE

TO

Approved for public release, distribution
unlimited

FROM

Distribution authorized to DoD only;
Specific Authority; 28 Aug 92. Other
requests shall be referred to Commander,
U.S. Army Medical Research and Materiel
Command, Attn: MCMR-RMI-S, Fort Detrick,
Frederick, MD 21702-5012.

AUTHORITY

U.S. Army Medical Research and Materiel
Command ltr., dtd January 21, 2000.

THIS PAGE IS UNCLASSIFIED

AD_____

CONTRACT NUMBER: DAMD17-92-C-2053

TITLE: Environmental Health Monitor: Advanced Development of Temperature Sensor Suite

PRINCIPAL INVESTIGATOR: Robert L. Talley, Ph.D.
                         T. Jeffrey Becker

CONTRACTING ORGANIZATION: Veritay Technology, Inc.
                           East Amherst, NY 14051-0305

REPORT DATE: 30 Jul 95

TYPE OF REPORT: Final, Phase II

PREPARED FOR: Commander
                 U.S. Army Medical Research and Materiel Command
                 Fort Detrick, Frederick, Maryland 21702-5012

19960405 052

DTIC QUALITY INSPECTED 1

REPORT DOCUMENTATION PAGE

Public reporting burden for this collection of information is estimated to average 1 hour per response, including the time for reviewing instructions, searching existing data sources, gathering and maintaining the data needed, and completing and reviewing the collection of information. Send comments regarding this burden estimate or any other aspect of this collection of information, including suggestions for reducing this burden, to Washington Headquarters Services, Directorate for Information Operations and Reports, 1215 Jefferson Davis Highway, Suite 1204, Arlington, VA 22202-4302, and to the Office of Management and Budget, Paperwork Reduction Project (0704-0188), Washington, DC 20503.

1. AGENCY USE ONLY (Leave Blank)	2. REPORT DATE 30 JUL 95	3. REPORT TYPE AND DATES COVERED Final, Phase II, July 1, 1993 - June 30, 1995

4. TITLE AND SUBTITLE	5. FUNDING NUMBERS
Environmental Health Monitor: Advanced Development of Temperature Sensor Suite	DAMD17-92-C-2053

6. AUTHOR(S)
Robert L. Talley, Ph.D.
T. Jeffrey Becker

7. PERFORMING ORGANIZATION NAME(S) AND ADDRESS(ES)	8. PERFORMING ORGANIZATION REPORT NUMBER
Veritay Technology, Inc. East Amherst, New York 14051-0305	VER-A20-002

9. SPONSORING/MONITORING AGENCY NAME(S) AND ADDRESS(ES)	10. SPONSORING/MONITORING AGENCY REPORT NUMBER
U.S. Army Medical Research and Materiel Command Fort Detrick, Frederick, MD 21702-5012	

11. SUPPLEMENTARY NOTES

Phase II Small Business Innovation Research (SBIR) Program

12a. DISTRIBUTION/AVAILABILITY STATEMENT Distribution authorized DOD Components only, Specific Authority, August 28, 1992. Other requests shall be referred to the Commander, U.S. Army Medical Research and Materiel Command, ATTN: MCMR-RMI-S, Fort Detrick, Frederick, MD 21702-5012	12b. DISTRIBUTION CODE

13. ABSTRACT (Maximum 200 words)

Heat stress is a significant contributor to both battlefield and non-battlefield injuries and performance degradation among both military and civilian personnel, particularly in hostile environments requiring protective attire. Recent field studies indicate that the performance of heat-strain decision aides and predictive models generally improves with the quality of meteorological inputs. The purpose of this Phase II Small Business Innovation (SBIR) Research Program has been to conduct advanced development of a self-contained suite of sensors capable of measuring, storing, and downloading upon command selected environmental temperature parameters related to heat-stress characterization.

One prototype sensor suite has been delivered that provides near real-time measurement of four environmental parameters (ambient temperature, relative humidity, wind speed, and radiant energy) in a form suitable for use as input to heat-strain predictive models. The battery-operated, pocket-sized, hand-held sensor suite features an innovative anemometer design that can be operated in a pulsed mode to conserve energy and extend operational life. This unique approach to wind speed measurement has been combined with system modularity, innovative design and packaging concepts, the incorporation of recent advances in electronics and the identification and integration of low-cost, commercial, off-the-shelf components to achieve desired reductions in unit cost, weight, size and power consumption.

14. SUBJECT TERMS			15. NUMBER OF PAGES 133
Environmental health monitor, Heat-stress monitor, Meteorological temperature sensor suite, Air-temperature sensor, Relative humidity sensor, Wind-speed sensor, Radiation (black-globe) sensor, Pocket-sized (miniaturized) device, Heat Strain			16. PRICE CODE

17. SECURITY CLASSIFICATION OF REPORT	18. SECURITY CLASSIFICATION OF THIS PAGE	19. SECURITY CLASSIFICATION OF ABSTRACT	20. LIMITATION OF ABSTRACT
Unclassified	Unclassified	Unclassified	Limited

NSN 7540-01-280-5500

FOREWORD

Opinions, interpretations, conclusions and recommendations are those of the author and are not necessarily endorsed by the US Army.

___ Where copyrighted material is quoted, permission has been obtained to use such material.

___ Where material from documents designated for limited distribution is quoted, permission has been obtained to use the material.

_X_ Citations of commercial organizations and trade names in this report do not constitute an official Department of Army endorsement or approval of the products or services of these organizations.

___ In conducting research using animals, the investigator(s) adhered to the "Guide for the Care and Use of Laboratory Animals", prepared by the Committee on Care and Use of Laboratory Animals of the Institute of Laboratory Resources, National Research Council (NIH Publication No. 86-23, Revised 1985).

___ For the protection of human subjects, the investigator(s) adhered to policies of applicable Federal Law 45 CFR 46.

___ In conducting research utilizing recombinant DNA technology, the investigator(s) adhered to current guidelines promulgated by the National Institutes of Health.

___ In the conduct of research utilizing recombinant DNA, the investigator(s) adhered to the NIH Guidelines for Research Involving Recombinant DNA Molecules.

___ In the conduct of research involving hazardous organisms, the investigator(s) adhered to the CDC-NIH Guide for Biosafety in Microbiological and Biomedical Laboratories.

Robert L. Talley, PI   7-30-95
                                             Date

The following is a list of employees who received pay under this contract and the percentage of time spent on this effort versus maximum hours possible during the contract period. No graduate degrees were received as a result of contract support.

Employee	Percentage	Employee	Percentage
T. Becker	50.5%	M. Munger	7.3%
K. Bernard	5.6%	P. Norris	44.3%
D. Dawidowicz	2.9%	D. Prather	2.9%
E. Fisher	2.0%	L. Repeta	<1%
M. Geise	<1%	C. Schwartzmeyer	2.9%
D. Ingraham	18.9%	J. Talley	<1%
D. Lung	6.4%	R. Talley	14.1%
L. Meyer	1.1%	L. Yaizzo	1.2%

TABLE OF CONTENTS

i

TABLE OF CONTENTS (CONT.)

LIST OF FIGURES

LIST OF FIGURES (CONT.)

LIST OF FIGURES (CONT.)

LIST OF TABLES

ACKNOWLEDGMENTS

1. EXECUTIVE SUMMARY

This report describes the advanced development of an Environmental Health Monitor: Temperature Sensor Suite under Small Business Innovation Research (SBIR) Contract Number DAMD17-92-C-2053. The compact, hand-held sensor suite employs microprocessor technology, commercial off-the-shelf sensors and sensor components, and an innovative wind speed measurement technique to achieve measurements of four basic meteorological input parameters: air temperature, humidity, wind speed, and radiant energy. The work was undertaken in conjunction with a U.S. Army Research Institute of Environmental Medicine (ARIEM) initiative to generate field-usable decision aids to improve heat-stress risk management.

Shown in Figure 1, the pocket-sized prototype sensor suite developed during this SBIR Phase II program is capable of providing local measurements of selected environmental temperatures for use as input to a variety of heat-stress predictive models. The prototype sensor exhibits the following characteristics:

- Low-power consumption achieved by using an innovative anemometer technique
- Easy-to-read display of raw data for local presentation
- Suitability for either hand-held or desk-top operation (i.e., individual or group)
- Battery operation; 72-hour mission life [This is equivalent to 16 hours continuous operation, or measurement of raw data approximately three times (a five minute process) per hour over a 72 hour period.]
- Light weight (about 150 grams)
- Elimination of need for field calibration
- Modular design; easy to upgrade or incorporate other sensors, if needed
- Non-interference among sensors and between sensors and case
- Small footprint (approximately the size of a cigarette pack).

Developmental and verification testing conducted both in wind tunnels and in outdoor conditions indicate excellent correlation to meteorological instruments with traceable calibrations to National Institute of Science and Technology (NIST) standards. Overall performance of the integrated prototype sensor suite satisfactorily demonstrated the ability of the sensor suite to sample environmental parameters and report data in real time. Additional field testing is recommended to ascertain suitability for use with heat-strain predictive models under field conditions.

1

Figure 1.   Photograph of Prototype Sensor Suite

2. INTRODUCTION

2.1   Enhancing the Performance of the Individual Soldier and Small Unit. The end of the Cold War has seen the proliferation of local warfare, increased potential for major regional conflicts, and widespread involvement of U.S. troops in operations other than war (OOTW). The Army warfighting doctrine continues to evolve toward lightened forces, increased tactical mobility, and an emphasis on increased protection for the individual warfighter in hostile environments. Simultaneously, shrinking defense budgets have resulted in force structure reductions, sharp curtailment of the development and production of new weapons, and increased emphasis on exploiting the economic and logistic advantages of dual-use technologies. Protecting and enhancing the individual soldier and the small fighting unit has never been of greater importance to the success of overall military objectives.[1]

Heat stress is a significant contributor to battlefield and non-battlefield injuries and performance degradation, particularly in hostile environments requiring protective attire. The U.S. Army Chemical School's P^2NBC^2 (Physiological and Psychological Effects of the NBC Environment and Sustained Operations on Systems in Combat) Program recently addressed a variety of issues associated with heat injury. Of particular interest was and is the impact of heat stress on the performance of soldiers attired in MOPP (Mission-Oriented Protective Posture) chemical protection. Work conducted under this program indicated general agreement between observed physiological response to heat stress and results predicted from the Heat-Strain Decision Aid, which has its foundation in the databases, predictive algorithms, and heat-strain prediction modeling efforts performed by the U.S. Army Research Institute of Environmental Medicine (ARIEM) and others over the past two decades. Recent field studies indicate that heat-strain predictive model performance generally improves with the quality of meteorological input. [Santee, et al., 1992; Pandolf et al., 1986; Kraning et al., 1991.]

2.2   Purpose of the Present Work. The specific purpose of this Phase II Small Business Innovation Research (SBIR) program has been to conduct advanced development of a prototype, pocket-sized temperature sensor suite capable of sensing, recording, and downloading on demand (for computational purposes) real-time measurements of four basic meteorological input parameters: air temperature, humidity, wind speed, and radiant energy. Primary emphasis has been placed on achieving reduced power consumption, modularity of component parts, integration of commercial off-the-shelf items, and reduced size and weight.

---

[1] *Department of the Army, Army Science and Technology Master Plan for Fiscal Year 1995, December 1994.*

2.3   Background of Previous Work. The importance of temperature as a contributing factor to worker performance and productivity has long been recognized (as indicated by the incorporation of the WBGT approach in ISO Standard 7726).[2] Heat accumulation is the result or product of the contributing factors of stress, (such as environment and activity); hence, it is an indicator of strain. When the body is subjected to more heat than it can dissipate, less blood goes to the active muscles, the brain, and other internal organs. People working in conditions imposing heat stress get tired sooner, become less alert, and are less able to use good judgment. The most serious heat-related illness is heat stroke; its effects can include confusion, irrational behavior, convulsions, coma, even death. Heat stroke can severely damage the blood-clotting mechanism and liver and kidney functions. The lungs can accumulate fluid, the central nervous system can be damaged irreversibly, and virtually all other organs and tissues sustain injury. Moreover, heat stroke can develop quickly without overt signs of heat exhaustion [Kilbourne, 1988, cited in EPA/OSHA Guide, 1993].

Heat-injury risk management protocols in both military and civilian settings are predicated on the assumption that if prevailing heat stress can be adequately quantified, appropriate countermeasures can be implemented.[3] Countermeasures include altering work/rest cycles, increasing water intake, attempting to achieve gradual acclimatization, and monitoring environmental conditions and individual responses to working in protective gear or in hot climates.

Heat stress may arise from a variety of physiological and environmental factors that act independently or interactively to affect the balance of heat production or loss experienced by an individual.

In 1988 Goldman compiled an exhaustive list of indices striving to achieve a numerical expression integrating the various factors contributing to heat stress, and concluded that the most promising approach for the resolution of heat stress problems was through prediction modeling. Significant

> *"...the most promising approach for resolution of heat stress problems is through prediction modeling. Such modeling can build on the concept that heat stress results from an imbalance between demands imposed on the worker by the task and the environment, and the worker's capacity to eliminate the heat load as modified by clothing."*
>
> *---Ralph F. Goldman, "Standards for Human Exposure to Heat," in Environmental Ergonomics, Sustaining Human Performance in Harsh Environments, Edited by Igor B. Mekjavic, Eric W. Banister, and James B. Morrison (Philadelphia: Taylor & Francis, 1988), p. 99-104.*

---

[2] *International Standard (ISO) 7726, "Thermal Environments-Instruments and Methods for Measuring Physical Quantities," First Edition-1985-07-01, UDC 331. 043.6:53.08. Reference No. ISO7726-1985(E).*

[3] *TB Med 507, 1980; GTA 8-5-45, 1985; FM 21-10, 1988; NIOSH, 1986; EPA/OSHA Guide EPA-750-b-92-001, 1993; ISO 7726.*

advances in database generation and predictive algorithm development have occurred in the wake of Goldman's observations [e.g., McNally, R.E., et al., 1990; Kraning, K.K., 1991; Pandolf et al., 1986; Gonzalez, et al., 1985, 1988, 1992].

The next level of model refinement and application of intervention strategies may be dependent to a significant extent on achieving an improved understanding of the dynamic nature of the thermal environment as it impacts human performance. Appendix A provides a discussion of several issues impacting the dynamic thermal environment and approach used for assessing the impact of heat stress on the individual soldiers.

This report documents the advanced development of a prototype temperature sensor suite small and light enough to be carried by the individual soldier (or used in small fighting units) without interference with military objectives, yet robust enough in its design to gather, store, and download real-time meteorological data for use as input in predictive heat-strain models.

Several candidate conceptual configurations were developed during the first year of the program, incorporating both off-the-shelf components and innovative sensor and integrated module design elements. Component, sensor, and module bench-level testing protocols were developed and preliminary testing of candidate sensor elements/modules was conducted.[4] An integrated module configuration was subsequently selected for prototype development on the basis of its ability to accommodate performance objectives within the constraints imposed by sensor operation, system support requirements, and size/weight/power limitations. This configuration was subjected to extensive additional component-level and system-level iterative testing and design refinement, culminating in verification testing under controlled conditions in the environmental test chamber located at Research Triangle Institute, Research Triangle Park, North Carolina, and the delivery of a prototype sensor suite configured to generally achieve the systems objectives given in Figure 2.

---

[4] R.L. Talley and C.K. Akers, "Environmental Health Monitor: Advanced Development of Temperature Sensor Suite," Phase II Mid-Term Report, July 30, 1994.

PARAMETER	REQUIREMENTS
Wind Speed	0.5 - 4.5m/s at $\pm$ 0.5m/s 4.5 - 6.5m/s at $\pm$ 10%
Temperature	5 - 65°C at $\pm$ 0.6°C
Humidity	0 - 100% RH at $\pm$ 4.5%
Solar/Radiant - Globe	5 - 77°C at $\pm$ 0.6°C

Figure 2.   **System Characteristics of Prototype Temperature Sensor Suite**

3. OBJECTIVES AND APPROACH

3.1   Objectives. The objective of this Phase II SBIR program was to conduct advanced development of a self-contained temperature sensor suite for potential use with an environmental health monitor (EHM). This sensor suite was miniaturized for hand-held use in the field, and was designed to be capable of measuring, storing and downloading (upon command) the following environmental parameters: ambient air temperature, relative humidity, radiant energy, and wind speed.

3.2   Approach. Veritay adopted a systems engineering approach to the design and development of the sensor suite, including the following:

- Identifying the overall methodology to be employed;
- Delineating the criteria for sensor selection, test and performance;
- Identifying state-of-the-art sensor technologies and candidate commercial off-the-shelf sensors and components whenever possible;
- Postulating and developing innovative approaches to fill technology gaps, as possible, within the scope of this program;
- Selecting and conducting tests for sensor components and subsystem evaluation;
- Selecting, designing and fabricating integrated sensor modules and system support modules; and
- Conducting integrated system calibration, operation and validation tests.

4. METHODS

4.1   Overall Methodology. Veritay has adopted a systems methodology to generate a small (i.e., nominally the size of a cigarette pack), lightweight (i.e., about 150 grams), battery-operated, sensor suite capable of measuring four basic environmental parameters: air temperature, humidity, wind speed, and radiant energy.

Recent technological advances (e.g., chip technology) and state-of-the-art, off-the-shelf components have been identified and appraised for suitability to meet desired sensor suite design goals and requirements, such as configuration, operation non-interference among sensors, electronics, system support and size/weight/power limitations. It has been the goal of this approach to generate a system exhibiting the following characteristics:

- Light weight
- 72-hour mission life
- Display for local presentation of data
- Modularity
- Suitability for hand-held or desk-top operation (individual or group use)
- Small foot print.

This section provides a technical discussion of the methodologies used to (1) identify currently available candidate sensor technologies and sensor suite components; (2) test sensor components, systems, and subsystems; (3) develop sensors and sensor modules for incorporation into a system configuration having a small footprint and light weight; (4) downselect candidate components and subsystems; (5) conceptualize, design and develop an overall system configuration; and (6) fabricate breadboards, brassboards, and prototype.

4.2   Criteria for Selection and Test. The objective of the sensor selection/test portion of the effort was to identify and test commercially available, original equipment manufacturer's (OEM) sensors and/or sensor components. The search and testing effort was used as the basis for performing trade-off analyses to determine the optimum combination of sensors and configuration to meet the overall performance, size, weight, and power requirements. Ease of sensor integration, cost, and projected availability were also considered. Although no performance criteria were specified in the contract, the following performance objectives for each of the measurement parameters of interest were adopted in conjunction with discussions with the technical activity:

• Wind Speed	0.5 to 4.5 m/s at ±0.5 m/s
	4.5 to 6.5 m/s at ± 10%
• Temperature	5 to 65°C at ±0.6°C
• Humidity	0 to 100% RH at ±4.5%

- Solar/Radiant
  Globe   5 to 77°C at ±0.6°C

4.3 Survey of Potential Sensor Technologies and Commercially Available Sensor Elements and Components. A top-down systems approach to design and development was adopted—with an ancillary goal of incorporating off-the-shelf technology whenever appropriate. Veritay subcontracted Akers Associates to (1) perform a comprehensive review of the literature to identify new sensing technologies suitable for integration into the sensor suite, and (2) to perform a comprehensive survey of commercial off-the-shelf sensor elements and/or components.

The search methodology used by Akers Associates to identify potential new technologies suitable for integration into the sensor suite included a computer database search using the following key words:

> Anemometer, wind speed
> Relative humidity, humidity, absolute humidity
> Solar detection, radiant detection, thermal detection.

Several technologies were identified, each having distinct advantages and disadvantages; a summary of this literature search is given in Appendix B. One of the primary reasons for conducting this search was to ensure that no new approaches or technologies were overlooked when selecting candidate technologies for integrated use in the sensor suite (particularly if commercial, off-the-shelf sensors/elements proved to be unobtainable for any given parameter of interest).

Veritay also asked Akers Associates to conduct a survey of off-the-shelf sensors, sensor components, calibration equipment, and data acquisition systems to identify cost-effective, commercially available items suitable for incorporation into the sensor suite. Environmental parameters searched included sky radiation (solar and radiant), wind speed, relative humidity, and ambient air temperature. In addition to conducting both computerized and manual literature searches (including the Thomas Register, American Chemical Society Laboratory Guide, Sensor Magazine Supplier Guide, etc.), Akers conducted interviews by telephone and/or made personal inspections of vendor products that appeared promising. Akers then prepared a master file cataloging relevant data and equipment literature received. The list of commercially available sensor technologies and sources compiled by Akers is given as Appendix C to this report.

Subsequently, Veritay subcontractor Mr. Alexander E. Martens, Executive Director of the Upstate New York CTC, the local office of the National Aeronautics and Space Administration (NASA) Northeast Region Technology Transfer Center (RTTC) conducted a validation review of the literature and a survey of activities at various

government research centers, universities, and private companies to ensure that no potentially useful technology had been overlooked or developed subsequent to the initial survey. This rather extensive survey (Appendix D) concluded that "Veritay's solutions to the measurement of at least wind speed measurement and, possibly, of total solar radiation are probably unique (though two references regarding the use of thermistors in an anemometer are included) and are, for a number of reasons, especially well suited for the application on the EHM [Environmental Health Monitor]" [Martens, 1995, p.2]. This conclusion of Martens' regarding probable uniqueness of Veritay's solution to making these measurements pertains to the combined use of a low energy, hot-bead anemometer mounted on a well-known miniaturized black globe. Several types of miniature black globes already exist.

4.4 Approach to Experimental Test Design. To evaluate the ability of sensor candidates to meet performance criteria under various environmental conditions and to determine potential interference effects (either among sensors/sensor components or between sensors and the body of the unit), Veritay identified two experimental methodologies:

1. Perform initial sensor characterization testing using laboratory bench apparatus capable of generating a variety of environmental characteristics

    The use of laboratory bench-type apparatus to perform initial sensor characterization tests (e.g., to determine if precision, accuracy, and operational characteristics of OEM sensors/components were within acceptable ranges) was determined to be a cost-effective and preferable alternative to expensive full-up environmental test chamber testing in certain instances. For example, bench type testing was used to quickly eliminate candidate OEM sensors/components and/or configurations when single parametric measurements were decision factors. This type of testing was also conducted to permit rapid evolutionary development of potential sensor configurations incorporating various combinations of off-the-shelf and customized sensors/components/electronics.

2. Perform certain testing in an environmentally controlled test chamber

    This approach had the advantage of permitting all parameters (e.g., relative humidity, temperature, wind speed) to be maintained under constant control. Since this type of testing is very costly, it was determined that it would be reserved for evaluating synergistic effects and for conducting validation testing.

It was also determined that solar/radiant evaluations would be performed under outdoor conditions, rather than attempting to duplicate the solar spectrum in an artificial environment. Validation testing of the integrated system was performed using both the outdoor environment and the environmental test chamber located at Research Triangle

10

Institute, Research Triangle Park, North Carolina (Appendix E). This test facility is described in Section 5.3.1.

4.5   Equipment Used to Test Sensors and Sensor Components. To achieve cost-effective sensor selection, fabrication, and breadboard and brassboard testing (prior to the validation testing which was performed at Research Triangle Park), Veritay configured the test equipment and developed the procedures described in the following subsections.

4.5.1   Bench-top Environmental Chamber. A bench-top environmental chamber was developed to provide a quick assessment of thermistor temperature sensors and candidate humidity sensors. Details of the bench-top chamber design are shown in Figure 3. As illustrated, the test environment was contained within a 12-inch-diameter, 11-½-inch high, nalgene "bell jar" seated over a plastic lid seal. Through-ports on the lid facilitated installing the sensor instrumentation and chamber plumbing lines. Humidity generation and air flow control was provided by a two-speed, cool-mist, ultrasonic humidifier. Chamber temperature above ambient was controlled by a 1500-Watt heater coil, which was inserted into a 1-1/2-inch PVC tube in line with the fan and humidifier air flow. Both humidity and temperature were adjustable, thereby permitting a wide range of relative humidity values to be generated. Corrugated polyethylene hose was used to connect chamber ducts to the humidity generator and PVC heater core. Hose disconnects were fabricated from schedule 40 PVC fittings to accommodate various hook-up arrangements between the humidity chamber and generator.

The chamber humidity was varied from 15% RH to 90% RH at ambient temperatures during preliminary testing. Temperatures above 65°C were achievable at the maximum heater power. Insulative material was wrapped around the outside of the nalgene jar, the connecting polyethylene hoses and the PVC plumbing lines to prevent moisture condensation on the walls of the air line tubing when tests were run at high humidity and temperature values.

4.5.2   Environmental Wind Tunnel. Figure 4 presents a schematic drawing of the environmental wind tunnel, which was used to make preliminary evaluations and calibrations of candidate sensors, and to determine their suitability for integration into the sensor suite. The environmental wind tunnel is a closed-circuit tunnel with stable, controlled air flow through a transparent, 7-inch-inside-diameter by 18-inch-long test section. The tunnel was of sufficient size and was suitable for calibrating both individual or groups of wind speed sensors against standard instruments. It was used to assess the influence of wind, temperature and humidity on the performance of groups of sensors. The wind speed capability of the tunnel covered the range from about 0.5 to 6.5 meters/sec.

11

TOP VIEW

SENSOR PORTS (5)

SIDE VIEW

12" DIA. NALGENE
VACUUM CHAMBER

1-1/2" PVC 45°
AIR RETURN

CHAMBER SUPPORT
TABLE

1500W HEATER
CORE

ADJUSTABLE
TRANSFORMER

1-1/2" PVC "T"
DIFFUSER VENT

1-1/4" CORRUGATED
POLYETHYLENE HOSE

ULTRASONIC COOL-MIST
HUMIDITY GENERATOR
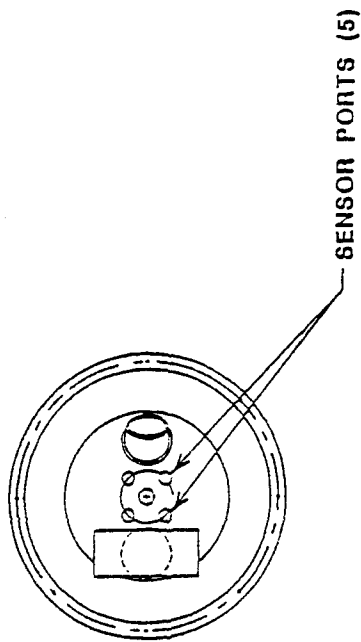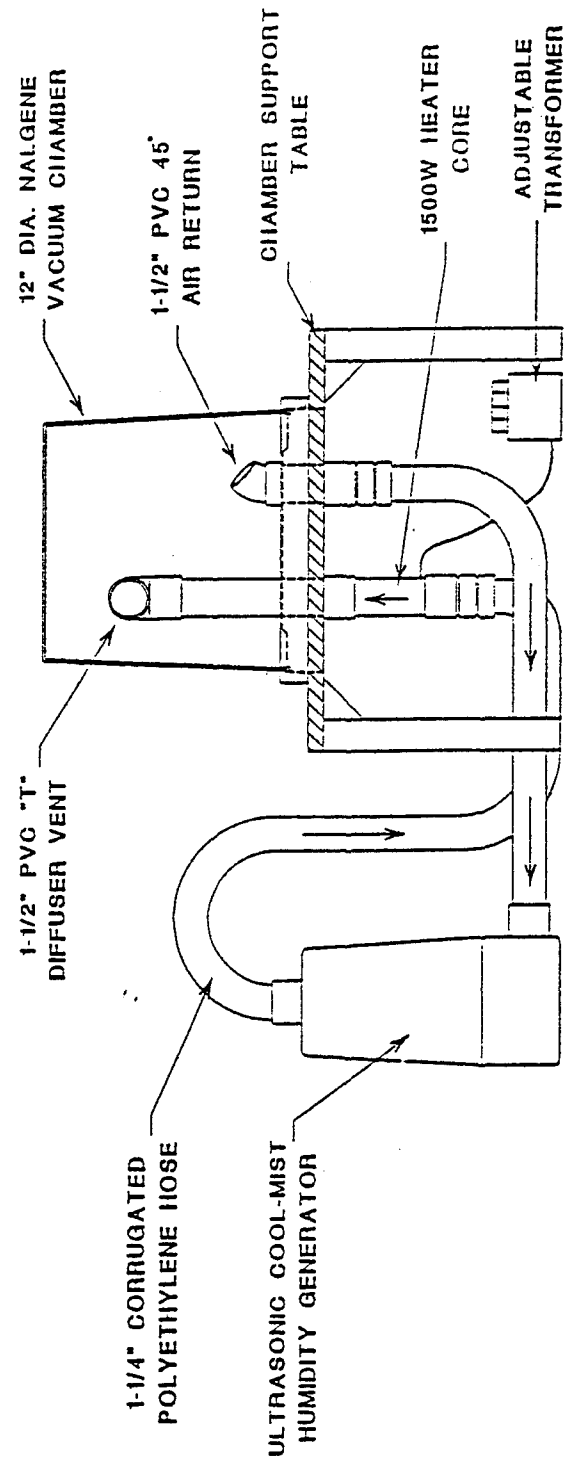
Figure 3. Laboratory Bench Chamber

SCALE

| 1.00m |
| 0.50m |
| 36.00" |
| 24.00" |
| 12.00" |

PLUMBING PORTS TO TENNY

MAT. GALVANIZED SHEET METAL

FLOW VANE ELBOWS

NOTE:
OUTSIDE OF BOX & DUCT INSULATED EXCEPT FOR TEST SECTION

AIRFLOW BAFFLE

BOX CONSTRUCTION 2X4 & PLYWOOD INTERIOR COATED WITH POLYURETHANE

ULTRASONIC HUMIDIFIER IN/OUT PORTS

SQUARE TO ROUND ADAPTER

PLASTIC DUCT

HEAT EXCHANGER

CLEAR PLASTIC TEST SECTION

MAT. GALVANIZED SHEET METAL

ADJUSTABLE BAFFLE

ADJUSTABLE BAFFLE

CENTRIFUGAL BLOWER

AIRFLOW BAFFLE

AIRFLOW

13

Figure 4. Environmental Test Chamber

The wind in the tunnel was generated by a centrifugal blower, which was driven by a shaded-pole, two-speed electric motor operating on 115 volts AC. An adjustable baffle plate was incorporated for restricting the volume flow of air to achieve selected values of wind speed. A variac controller was used for making minor adjustments of the blower motor speed, and, thereby, the wind speed.

The tunnel featured temperature control of the air flow over the range of about +5°C to +65°C, within approximately ±0.5°C. Tunnel air temperature was increased by passing air through a hot-water-driven, radiator-type heat exchanger located at the outlet of the air-mixing plenum. Two temperature-controlled heating units (not shown in Figure 4) external to the tunnel were used to condition the water temperature. These, together with insulated flexible hoses and a pump, circulated approximately three (3) liters of water through the radiator, and allowed the tunnel structure and air inside the tunnel to come to temperature equilibrium---typically in less than an hour. One of the water heaters used was a 1000-Watt Laude® immersion heater emplaced in an insulated water plenum. The second (hooked in series), was a 500-Watt heating unit contained in a Veritay-owned Tenny Junior®, high/low temperature environmental test chamber, together with a second fin-type, water-flow-through heat exchanger unit located inside this test chamber.

The tunnel air flow was cooled using the second of the preceding heat exchangers and elements of the water-based system. This was accomplished by bypassing the immersion heater, directly using the previously noted heat exchanger in the environmental chamber, and employing the refrigeration capability of this same environmental chamber.

The environmental chamber itself has a self-contained Tenny Hermitcool® Refrigeration system, which is a cascade system incorporating two compressors with accurately calibrated capillary tubes in lieu of mechanical expansion valves, and using the non-flammable refrigerants Freon R12 and R503. The operating temperature range of the environmental chamber extends from -80°C to +177°C, and temperature control capabilities within the chamber are claimed to be ±0.3°C over the range of -65°C to +177°C.

The time response, stability and control aspects of attaining and maintaining heating, cooling, or ambient air temperatures within the calibration wind tunnel were aided by extensive use of insulation throughout the tunnel. Closed cell foam insulation panels were installed inside and outside the air mixing plenum, and flexible cellular foam insulation contained within an aluminum foil wrap was applied to the outside of all galvanized and plastic air duct components--except the clear test section of the tunnel, which was encased with a three-inch-thick fiberglass insulation removable jacket.

Provisions were made to vary the humidity of the air flowing in the tunnel, to the extent that the humidity of the air could be increased slowly over selected ranges, while holding the air temperature nearly constant. Although this approach did not strictly provide direct humidity control, it permitted performance comparison of sensors with standard sensor units as the humidity levels of interest were reached. From an experimental standpoint, the use of this technique enabled much more humidity-temperature data to be acquired in a timely manner than would otherwise have been possible in a test unit of the size of this calibration wind tunnel.

A commercially available ultrasonic humidifier unit provided an unheated effluent of fine spray droplets into turbulent air flow within the mixing plenum and was used for low temperature humidity tests. At higher temperatures, a dual-element electric hot plate was used to assist the evaporation of water in two conventional 10½-inch x 14-inch steel pans within the mixing plenum. Relative humidity was adjusted by varying the temperature of the water.

4.5.3 Reference Instrumentation. Test apparatus and supporting test equipment used for the purposes of evaluating sensors was monitored using instruments conforming to either ISO standards or NIST-traceable standards. The Testoterm Model 452 and its associated environmental test probes was the sole reference for tracking temperature, relative humidity and wind speed measurements in all of the test evaluations performed. Table 1 contains a complete list of test equipment and the experiments in which they were employed.

4.5.4 PC Data Acquisition System (DAS). Monitoring of the wind tunnel environment was accomplished using the Testoterm instrument via an RS-232 interface in conjunction with an IBM-compatible AT personal computer (PC) system. The PC system was also used to monitor the sensor devices under test using the MetraByte DASCON-1 multifunction analog and digital I/O expansion board interface. The DASCON-1 is primarily used for analog data acquisition purposes. The features of the DASCON-1 include 12-bit resolution, ± 2.0475 full-scale input (0.0005 resolution), 4-channel multiplexer and a digitizing rate of 30 channels per second.

Computer control of both the wind tunnel and sensor acquisition systems was implemented using program code existing at Veritay. The software, written in Microsoft® QuickBASIC, facilitated program changes for adaptation to various test procedures. It also provided a means of converting, scaling, timestamping and formatting data for subsequent spreadsheet data analysis.

4.5.5 Outdoor Black Globe Thermometer Test Configuration. Preliminary testing of four analog black globes was conducted in an outdoor environment to evaluate the performance of the ⅞-inch diameter globe selected for use in the sensor suite package. A 6-inch and 1⅝-inch IST black globe thermometer (BGT) served as black globe

references. For the early tests, all four globes were positioned in an array and mounted on a 9-feet-high rooftop of a mobile test facility. Later, the array of globes and associated sensors was mounted at a height of 48 inches above ground level as shown in Figure 5, and was placed in an open area, on short grass turf. This was done

EQUIPMENT	DESCRIPTION	APPLICATION
Testoterm 452 Using Test Probes:	Expandable Environmental Measuring Instrument	Probe Interface Instrumentation
9540	Mini-Vane Anemometer	Initial reference for tunnel wind speed testing
1049	Telescoping "Hot-Bead" Anemometer	"Hot-Bead" energy analysis
9760	Dual-Function Probe: RH and Temperature	Reference for bench and tunnel fixtures used in RH and temperature measurement
1045	Three-Function Probe: RH, Temperature and "Hot-Bead" Anemometer	Tunnel wind speed reference
1549	Non-telescoping "Hot-Bead" Anemometer	Integrated Black Globe, "Hot-Bead" interference tests
Fluke 87	3 ½ Digital Multimeter	Power Supply Voltage Measurement
Fluke 8050A	4 ½ Digital Multimeter	Calibration of signal conditioning circuitry
H.P. 34401A	6 ½ Digital Multimeter	Anemometer Thermistor measurement and PC DAS circuit calibration
LeCroy 6810	Waveform Digitizer	Anemometer energy consumption evaluation
B&K 1660	Triple Output Power Supply	Powered circuitry for for "Hot-Bead" Energy analysis

Table 1. Test Instrumentation and Equipment

primarily to provide for a more realistic test environment and to minimize the effects of reflected solar and long wave surface radiation interferences stemming from surrounding buildings, asphalt and the aluminum flashing of the rooftop surface on which the early test fixture was situated. The remounted sensor array was located in

SIDE VIEW

1549 PROBE (WIND SPEED)

7/8" WAND 5

15.5"

15.5"

1 5/8" IST

31"

6"

WAND 6 TEMP REF

31"

THERMISTOR
SUN SHIELD

9760 PROBE
(RH/TEMP)

CEMENT BLOCKS (4)

SHORT GRASS

48"

END VIEW
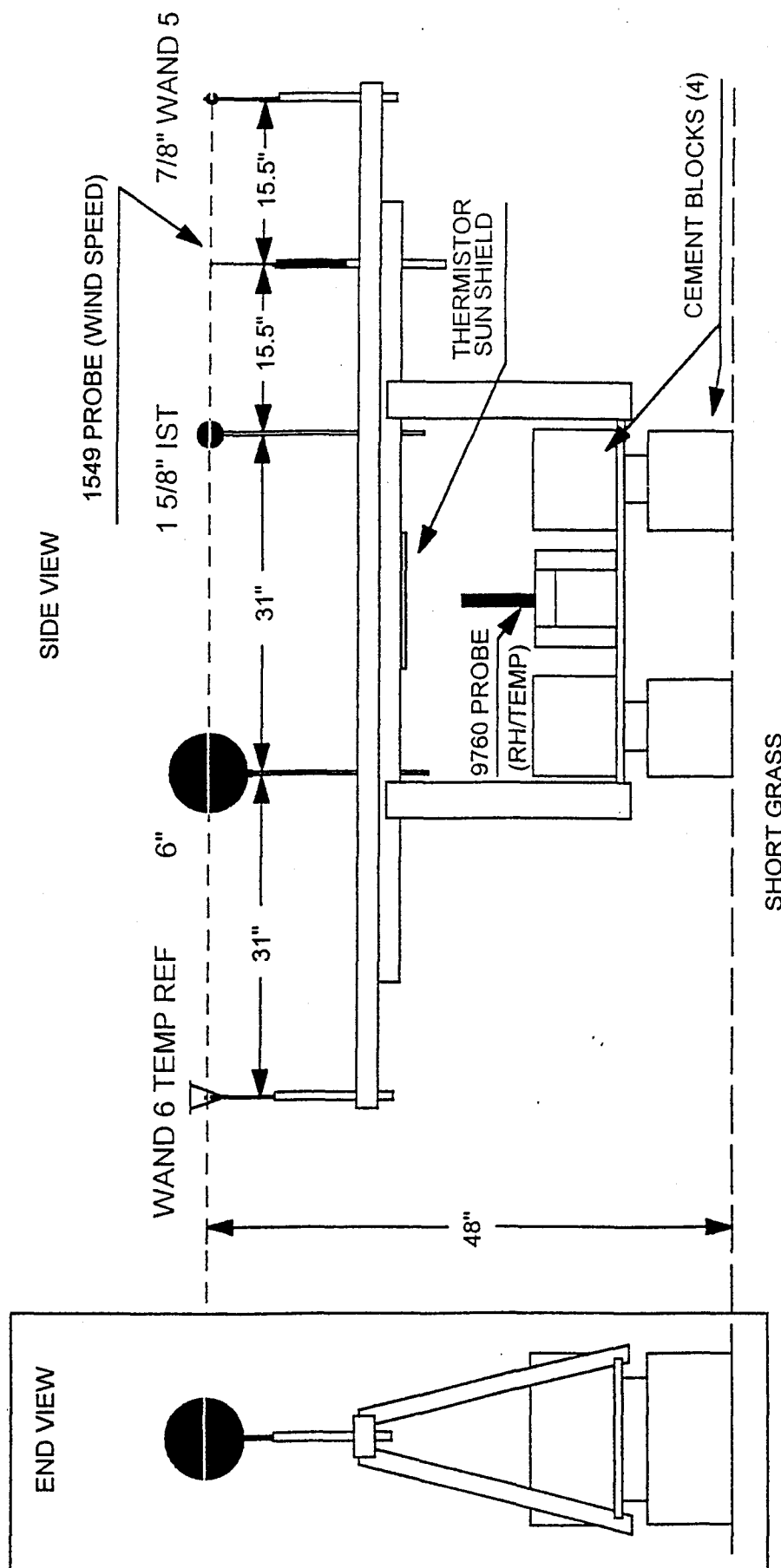
Figure 5. Ground Level Black Globe Test Array

17

an area with no obstructions in the upwind and downwind directions for distances in excess of about 100 feet, and no large obstructions (e.g., trees) for distances of about 300 feet. In both cases, the length of the test fixture assembly was positioned in the northwest-southeast direction with the prevailing winds directed nearly perpendicular to the assembly from the southwest. A multi-channel data acquisition system, illustrated in Figure 6, was used to scan the individual black globe sensors. Temperature data for each globe channel was acquired using an HP-34401A multi tester and subsequently logged by a PC computer via serial communications interface. The Testoterm 1045 multifunction probe was used as the reference for wind speed, relative humidity and temperature and these were recorded simultaneously, along with the BGT data. Readings were taken every 10-30 seconds and timestamped for future reference.

```
┌─────────────────────────────────┐   ┌─────────────────────────────┐
│  MULTIPLE BLACK GLOBE TEST       │   │  TESTOTERM PROBES:          │
│  FIXTURE WITH BARE-BEAD          │   │  1049 (WIND SPEED)          │
│  TEMPERATURE REFERENCE           │   │  9760 (HUMIDITY)            │
└─────────────────────────────────┘   └─────────────────────────────┘
                │                                    │
                ▼                                    ▼
┌─────────────────────────────────┐   ┌─────────────────────────────┐
│  COMPUTER CONTROLLED             │◄──│  PC/AT                      │
│  RELAY BOX                       │   │                             │
└─────────────────────────────────┘   └─────────────────────────────┘
                │                                    ▲
                ▼                                    │
┌─────────────────────────────────┐                 │
│  DIGITAL MULTIMETER             │◄────────────────┘
│                                  │
└─────────────────────────────────┘
```
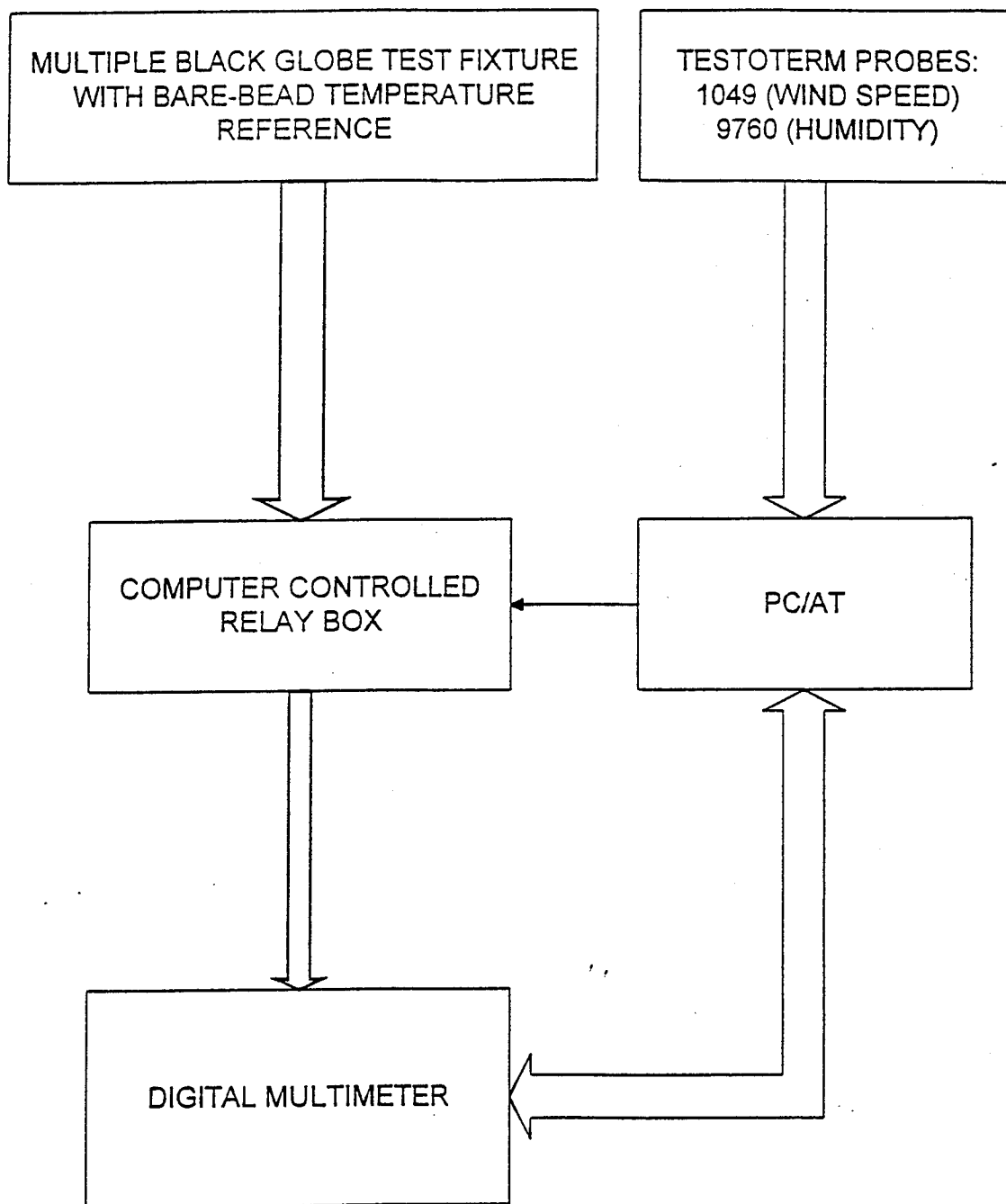
Figure 6. BGT Data Acquisition Test Fixture

5. TEST RESULTS

Test results are presented in four subsections:

    5.1   Candidate Sensor Evaluation
    5.2   Preliminary Subsystem/Module Evaluation
    5.3   Integrated System and Calibration/Control Testing
    5.4   Validation Testing.

5.1   Candidate Sensor Evaluation. Based on the technical review and analysis of Original Equipment Manufacturers (OEM) sensor elements, potential candidates were evaluated to select which sensors should be included in the integrated Environmental Health Monitor—Advanced Temperature Sensor Suite.

The performances of individual sensors were evaluated, and the interference effects of selected combined sensor elements were explored to assess the potential for using sensors in close proximity in a miniaturized integrated sensor suite.

Considerable effort was made to locate theoretical models to serve as bases for fitting experimental performance data from both individual sensors and combined sensor elements directly to existing theory, or as alternatives to serve as theoretically sound bases for determining correction factors or establishing performance related correlations. These efforts were only partially successful.

Both performance characterizations and sensor evaluations were based rather heavily on direct experimental results and observations. Standard theoretical models or analytical expressions were used whenever possible for correlation of baseline responses of various thermistors with each corresponding temperature of concern (including dry bulb air temperature, black globe temperature, and hot-bead anemometer temperature limits), or of humidity sensor response with imposed or natural relative humidity levels of interest. The basic temperature and humidity sensor measures and correlations are noted in the next two subsections (5.1.1 and 5.1.2) of this report.

More complex steady-state and time-dependent heat transfer models, such as those discussed by Incropera and DeWitt (1985), were also examined to relate the temperature responses of sensors and spheres to ambient temperatures and wind speeds.

The straight forward radiant and convective heat transfer model presented in the International Standard ISO 7726 was examined and used in relating both miniature and standard black globe temperatures to one another, and to the corresponding mean radiant temperature, characteristic of a uniform black body temperature which would

20

radiate the same average energy as that actually received by the sensor from the environment.

5.1.1 Temperature. The thermistor was identified as the ambient air temperature sensor of choice under this contract because of its simplicity in use, its power and signal conditioning requirements, its reliability, and its ready availability. Several OEM stock products are capable of meeting the temperature range of interest (i.e., 0°C to 64°C with accuracies better than 0.5°C).

All of the thermistor sensors that were used in both breadboard and prototype sensor suite support module assemblies were precalibrated at three nominal temperature points: 0, 35 and 70°C. The calibration was performed by placing several thermistors inside a 9-inch-long x 6-inch-wide x 6-inch-high steel enclosure. The enclosure itself was placed inside Veritay's temperature-controlled Tenny Jr.® conditioning oven, and allowed to equilibrate at least 30 minutes at each temperature setting. Temperature of the test environment was monitored by the Testoterm temperature reference probe, Model No. 9760. Thermistor resistance was acquired by a HP 34401 multi-tester using the instrument's internal 100-μA constant current source. Three unique calibration constants, A_0, A_1 and A_3 were derived for each thermistor tested using the three known temperature points, the corresponding resistances, and the following natural log fit equation:

$$In \ R_T = A_0 + A_1/T + A_3/T^3 \hspace{3cm} (1)$$

Thermistor calibration constants were verified at two additional temperature points, nominally 25 and 55°C using equation (1). The results indicated that the curve fit determination was accurate to within better than 0.1°C.

5.1.2 Relative Humidity. The output response was obtained for three candidate sensors as a function of relative humidity. The relative humidity was varied at three different temperature values (35°C, 45°C, and 55°C). It should be noted that although relative humidity measurements were taken at temperatures below 35°C, relative humidity values greater than 90% were not achievable as a result of condensation problems on the test chamber walls and reference probe instrumentation at temperatures much below 35°C. Figure 7 provides a plot of the data taken using the Hy-Cal humidity sensor (Model IH-3602-A); these data were within a 4.5% experimental error when compared to the Testoterm reference humidity sensor, demonstrating that the commercially available Hy-Cal was suitable for incorporation into the sensor suite.

For completeness, it is noted that the other two sensor types examined were a Panametrics HC-2, and a Thunder Scientific PC-21-1C (02). Our test results for the

21
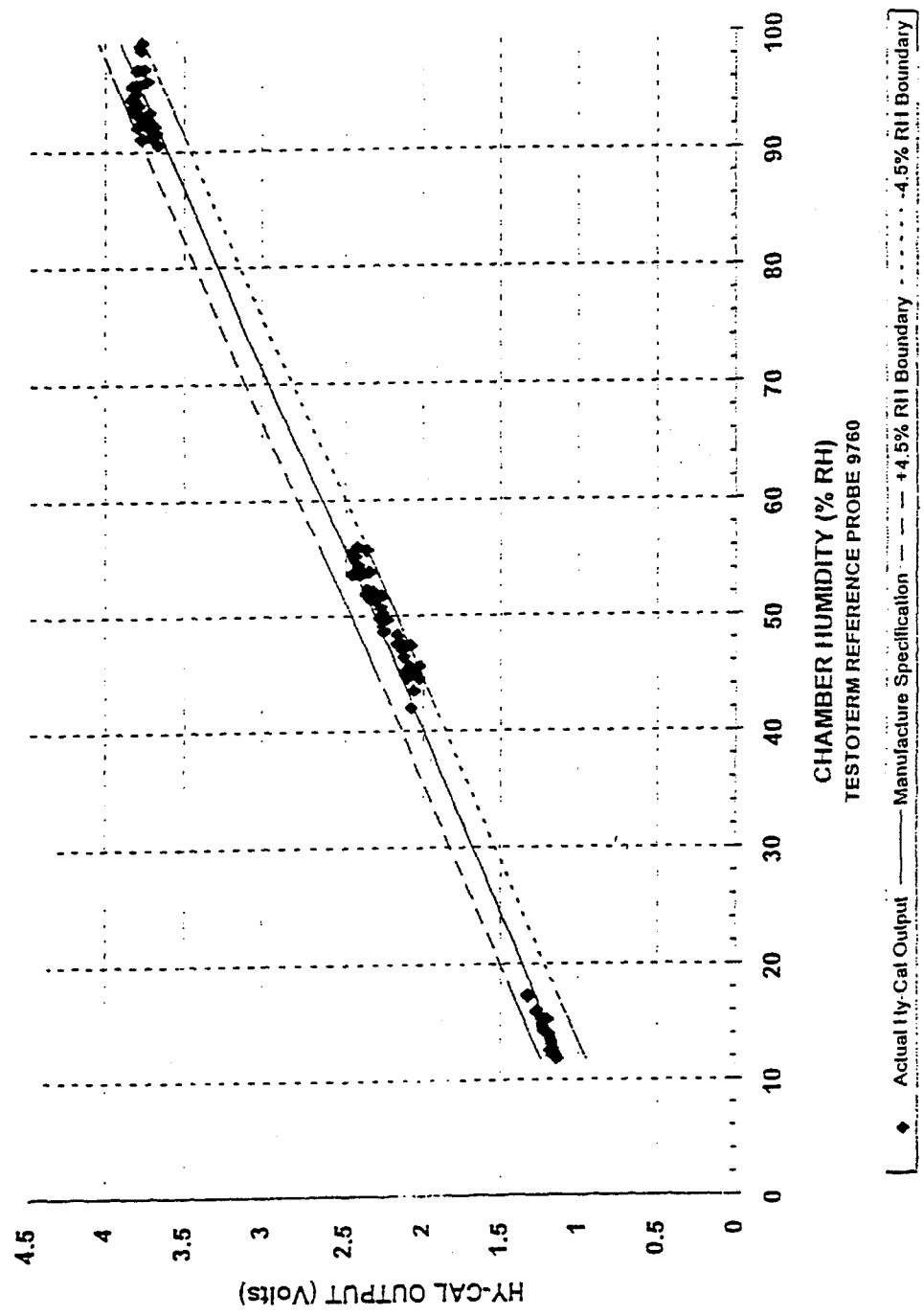
Figure 7. Output Response for HY-CAL IH-3602-A Humidity Sensor

former indicated that the response curve might not be linear, but more importantly, the spread of the data was beyond the 4.5% variation from the Testoterm reference humidity sensor. For the latter sensor, such test results indicated that this sensor was not temperature compensated, making additional support electronics necessary to counter these temperature effects in order to determine relative humidity within acceptable error. On the basis of these results, both of these sensors were omitted from further consideration as candidates for inclusion in the sensor suite.

To determine if off-the-shelf Hy-Cal sensors from different lots could be reliably used as replacement sensors without the need for additional calibration, Veritay obtained Hy-Cal IH-3602-A sensors from three different lots and tested them under different wind speed and relativity humidity conditions using the calibrated wind tunnel. Figure 8 depicts data taken at low (<20%), medium (40-50%) and high (80-90%) relative humidities as a function of wind speed. The test result show excellent consistency among sensors to within less than 3%RH units.

The Testoterm "mini-vane" anemometer, Model Number 9540, was used as the wind speed reference for these tests. The Testoterm dual probe, Model 9760, served as the reference for temperature and relative humidity. The Testoterm reference probes were inserted through the wall of the tunnel test section to a depth of two (2) inches and were situated radially at the midpoint of the test section. The three Hy-Cal sensors were aligned as shown in Figure 9 and located approximately four (4) inches downstream from the reference probes near the center of the test section.

The signals from each Hy-Cal sensor were signal conditioned with amplifiers situated on a patch panel located outside the test section. The PC DAS system was used to simultaneously record the three (3) Hy-Cal sensors and Testoterm reference data at one-second intervals. Tests were conducted at nominal wind speeds of 2, 3, 4.7, 6.3 and 7.1 m/s. Each wind speed level was maintained for a minimum of four (4) minutes to permit sensor equilibration.

A calibration was performed on (5) five Hy-Cal IH-3605-A wafer-type sensors to verify their performance in conjunction with the manufacturer's specification. The bench chamber for these tests was instrumented with a NIST-traceable, Hy-Cal IH-3602-A humidity sensor, the Testoterm 9760 probe as a temperature reference, and the five (5) Hy-Cal IH-3605-A sensors. All sensors and the temperature reference were placed in a 3.5-inch linear array seven (7) inches above the floor of the chamber. Humidity was introduced into the chamber by damp paper towels and air was circulated by a 3-inch DC fan. One of the tested sensors was shown to be defective (and was replaced by the manufacturer), while the remaining four (4) proved to be within the $\pm$ 2% specification claimed by the manufacturer. The replacement wafer humidity sensor (Hy-Cal Wafer 4) was a factory-calibrated unit. Figure 10 provides a graphical comparison of the sensor outputs from (1) calibrated wafer sensors type IH-3605-A,

23
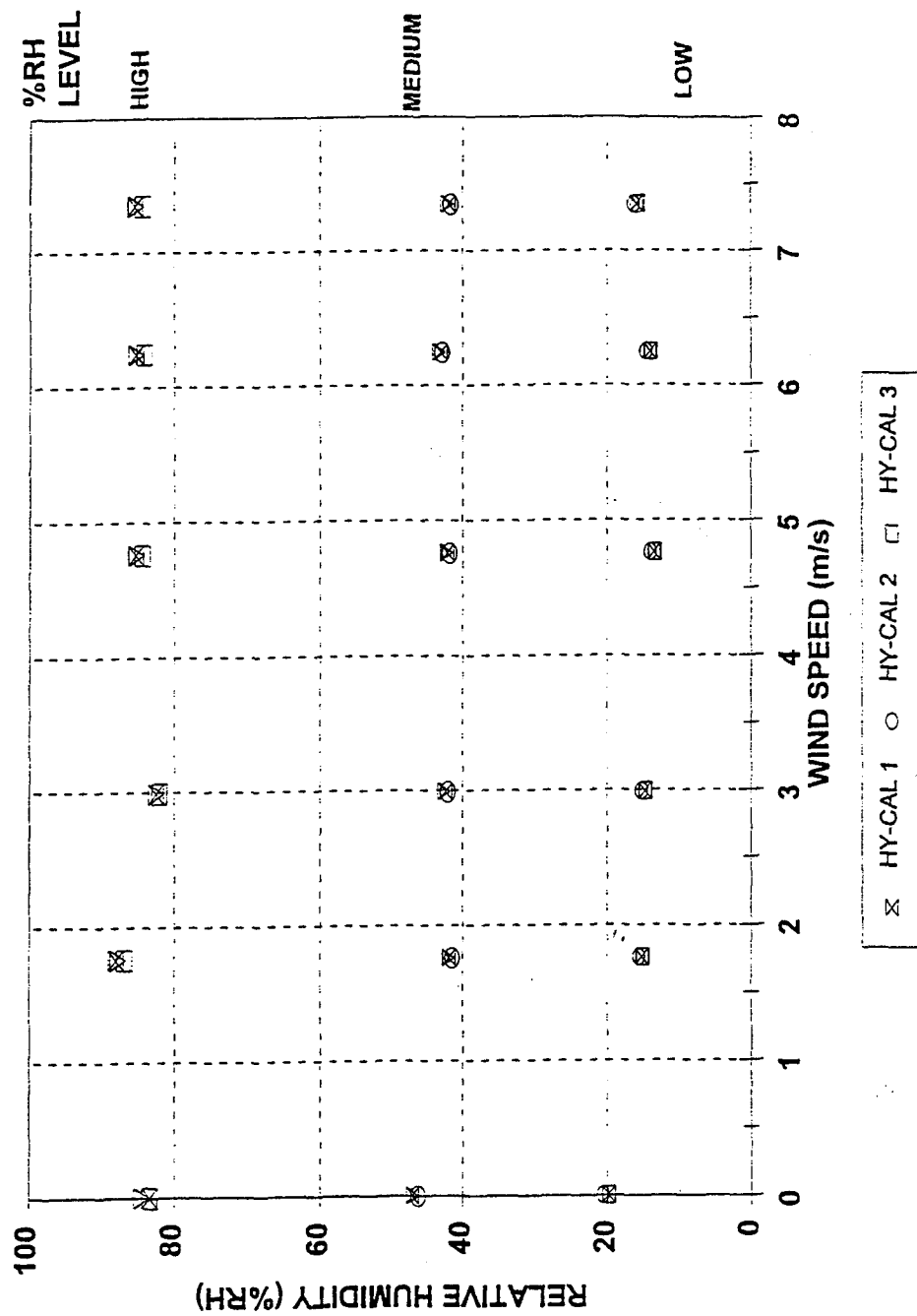
Figure 8. Comparison of HY-CAL IH-3602-A Sensors in Environmental Wind Tunnel

TESTOTERM
PROBES

9760

2.0"

9540

☐ ☐ ☐

HY-CAL SENSORS
(4" DOWNSTREAM)

AIRFLOW INTO PAGE
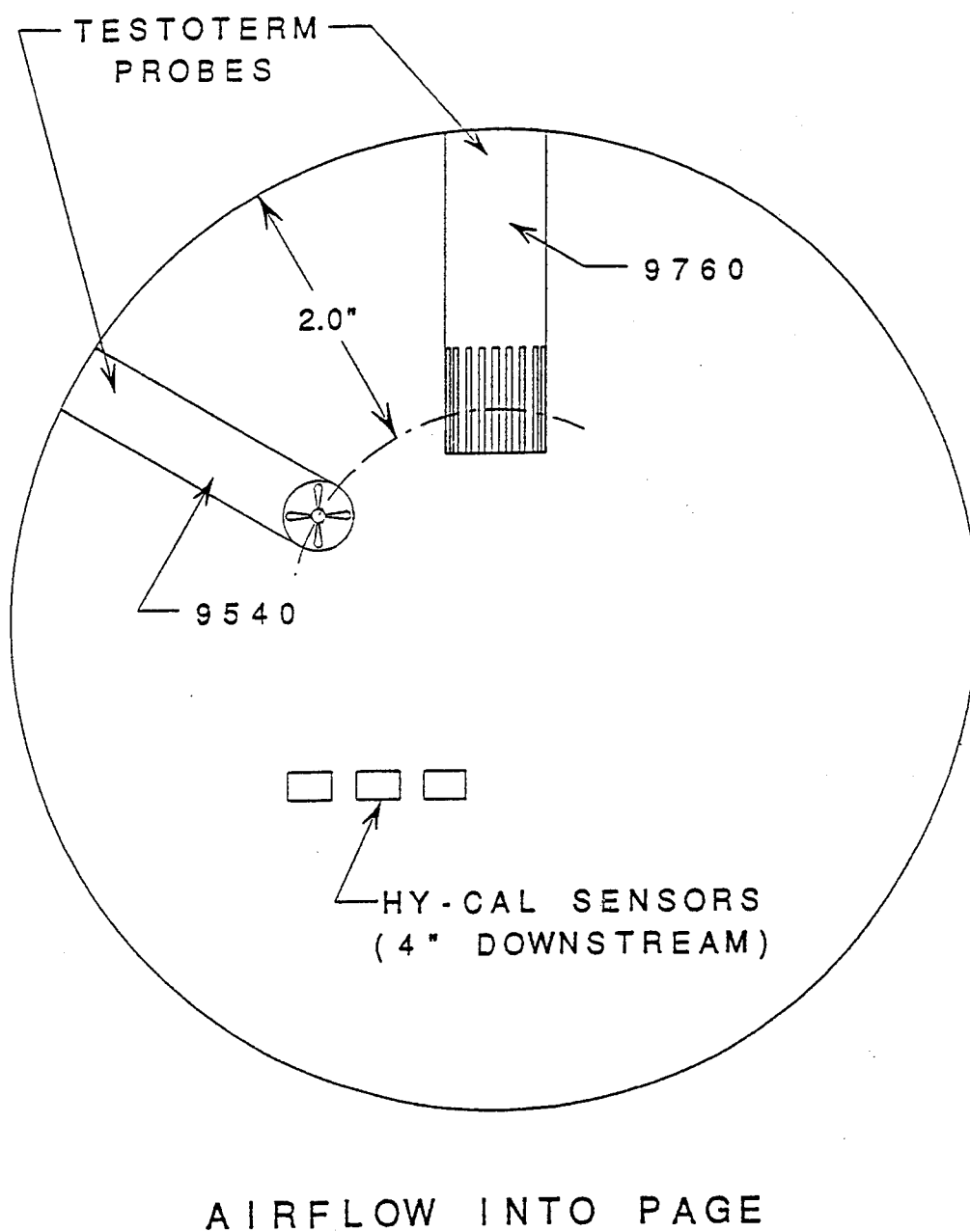
Figure 9. Orientation of Reference Probes and HY-CAL Sensors in Test Section
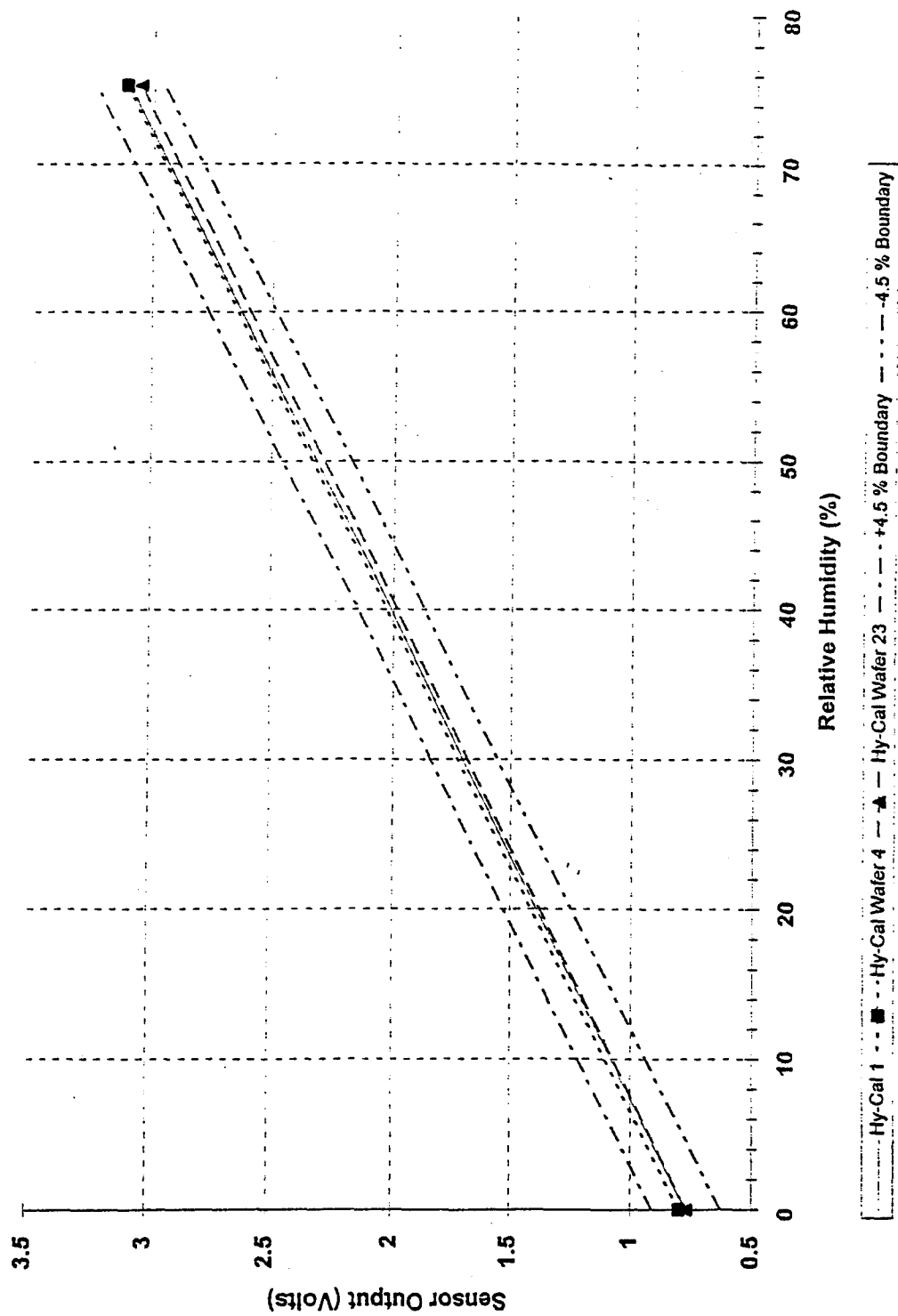
Figure 10.   Comparison of Manufacturer Specifications for HY-CAL IH-3602-A Sensor (HY-CAL 1) and HY-CAL IH-3605-A Sensors (WAFERS 4 and 23)

Nos. 4 and 23, and (2) calibrated sensors type IH-3602-A (shown earlier together with its 4.5% RH data boundaries). All three of these sensors indicate close agreement with one another (i.e., within 3 percent).

Two of the Veritay-calibrated wafer-type sensors which were mounted in sensor suite support modules were re-evaluated separately in a low-humidity desiccated environment and a high-humidity saturated salt environment simultaneously with the aforementioned NIST-traceable Hy-Cal IH-3605-A sensor. The response of both wafer-type sensors was within 2%RH units at both extremes when compared to the Hy-Cal standard.

5.1.3 Wind Speed

Basic Test Results. While the standard, hot-bead anemometer can permit omni-directional wind speeds to be measured, the power consumption necessary to constantly maintain the temperature of the hot-bead 100°C above ambient air temperature was not consistent with the objectives of this program (particularly the goal of reducing power demands). The primary power drain in such a system could be traced to the wind speed measurement sensor.

To reduce anemometer power requirements, an innovative technique was devised. The anemometer was pulsed with a given amount of energy to raise the hot-bead temperature to a given value above ambient. When the temperature reached this pre-set value, the power was reduced to a very small "read" level, and the decay curve of the hot-bead being cooled by the wind was observed.

This pulsed hot-bead approach was initially explored using a bare thermistor bead with a diameter of 1.09mm (0.043 inch). The bead was mounted on the end of a tapered Torlon® tube with outside and inside diameters of 3.18-mm (0.125 inch) and 1.09 mm (0.043 inch), respectively. The thermistor leads were connected to a twisted pair of 30-gauge magnet wire, held in place within the tube by epoxy. The tube provided a mechanical mount for the thermistor and provided essential thermal shielding of the lead wires---particularly against convective cooling by wind.

Two such thermistor probes, designated Wand 1 and Wand 2 were fabricated and tested to establish feasibility of this pulse-heated anemometer.

It was recognized early that it would be convenient to mount this pulsed hot-bead anemometer on top of the black globe to achieve a compact unit. However, such a configuration had the potential for interference between the sensor elements of the integrated black globe thermometer and the hot-bead anemometer. A brief investigation was conducted to examine this potential interference.

27

The first series of experiments was performed to observe the effects on wind speed measurement by placing a ⅞-inch-diameter black globe at three (3) different positions beneath a separate Testoterm model 1549 continuously energized hot-bead anemometer. Figure 11 shows the observed wind-speed measurement of the hot bead at different distances from the black globe surface. The hot-bead was evaluated flush with the globe surface and at separation distances of 3.2 mm (0.125 inch) and 6.4 mm (0.25 inch) from the globe surface. The Testoterm model 1549 hot-bead anemometer used in these tests was normalized to the Testoterm model 9540 minivane wind speed reference so that accurate wind speed measurements could be obtained. Preliminary data indicated that the wind speed taken by the hot-bead anemometer mounted in this fashion was approximately eight (8) percent below the reference wind speed over the range of concern, up to 6.5m/s for the case in which the hot-bead was mounted about 3.2 mm (0.125 inch) from the globe surface.

What is perhaps more striking was that the measured wind speed increased slightly as the bead separation distance from the sphere surface increased to 3.2 mm (0.125 inch), and then decreased as the probe was separated further to 6.4 mm (0.250 inch). This most likely represents in part, the combined effect of wind speed variation with distance from the sphere surface of (1) an increasing wind speed within the boundary layer, together with (2) a decreasing wind speed of potential flow about the sphere outside the boundary layer. (see Milne - Thomson, 1955). As the wind speed increases, the tendency of the boundary layer is to decrease in thickness adjacent to the sphere; at the same time one would expect the wind speed of potential flow to increase at the corresponding velocity point in the new boundary layer. The net effect would be expected to show a slight decrease in indicated wind speed at a given separation distance from the sphere surface. This, in part, is what is observed and illustrated in Figure 11, even though the overall effect indicates that the maximum indicated wind speed with distance from the sphere still occurs at the same radial distance - a somewhat surprising result. It is possible that this experimental finding can be confirmed theoretically, but this was not done under this effort.

The experimental result that the wind speed indicated by the hot-bead was approximately a fixed percentage of the actual wind speed was most encouraging, as this indicated that the hot-bead unit could likely be related to the actual wind speed using a simple empirical relation---perhaps using even a constant scaling factor.

A second set of experiments was performed to observe the effect of heating the adjacent hot-bead anemometer on the measured black-globe temperature. Figure 12 illustrates the ⅞-inch, integrated-black-globe/hot-bead assembly that was evaluated inside a closed chamber at ambient temperature. The interior of the integrated black globe was instrumented with one 10K and one 100K thermistor-type temperature sensor. Both thermistors were situated radially just above the surface of a ¼-inch-diameter acrylic tubing support, and were located at the equator of the black globe.
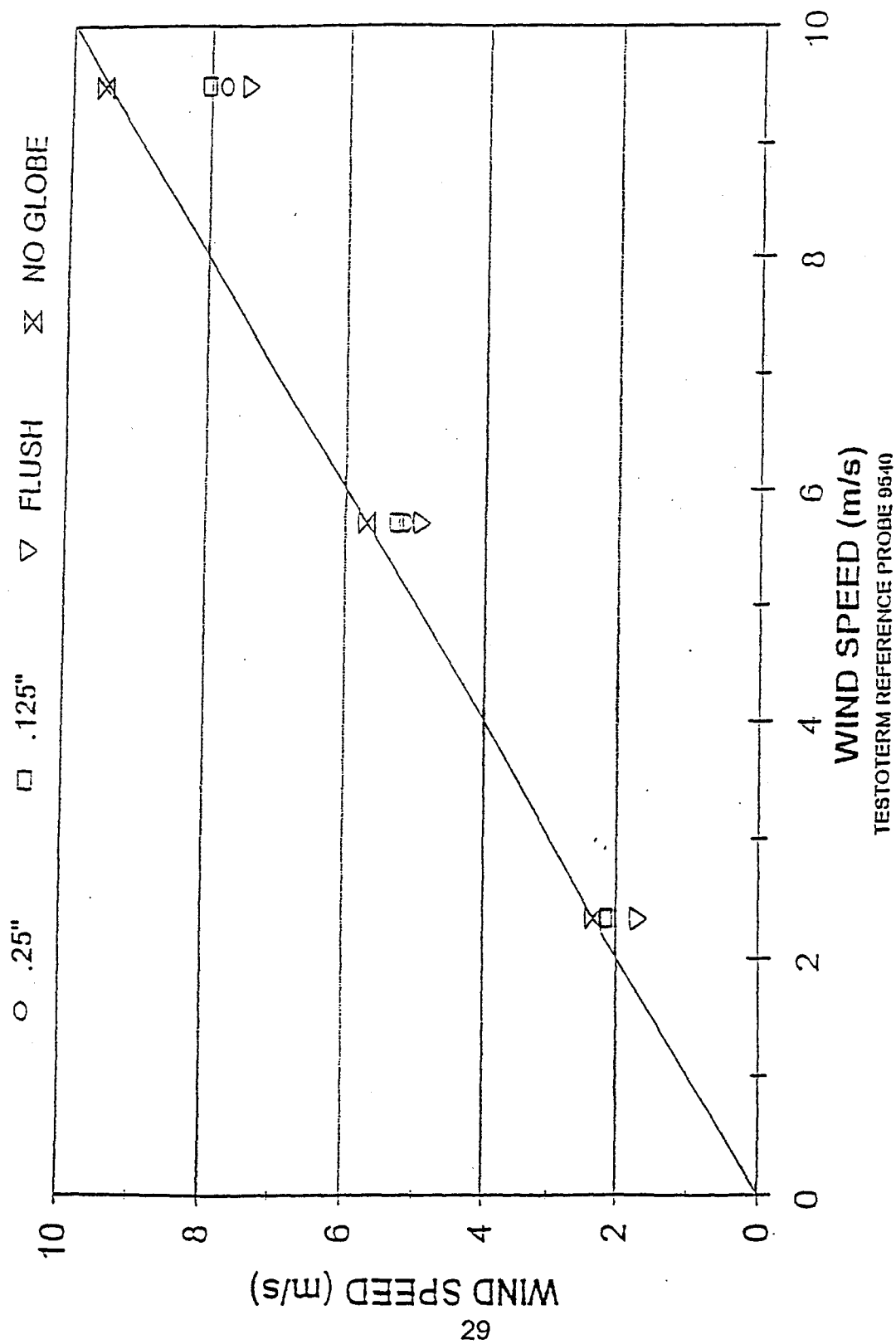
Figure 11. Effect of 7/8-inch Black Globe Orientation to Hot-Bead on Wind Speed Measurements

SLIDING TORLON SHAFT

.875" DIA. MINIATURE BLACK GLOBE
(COPPER)

10K AND 100K THERMISTORS
(THRU .070" HOLES)

HOT BEAD ASSEMBLY

(OVERALL LENGTH: 7.5")

.250" DIA. CLEAR PLASTIC TUBING
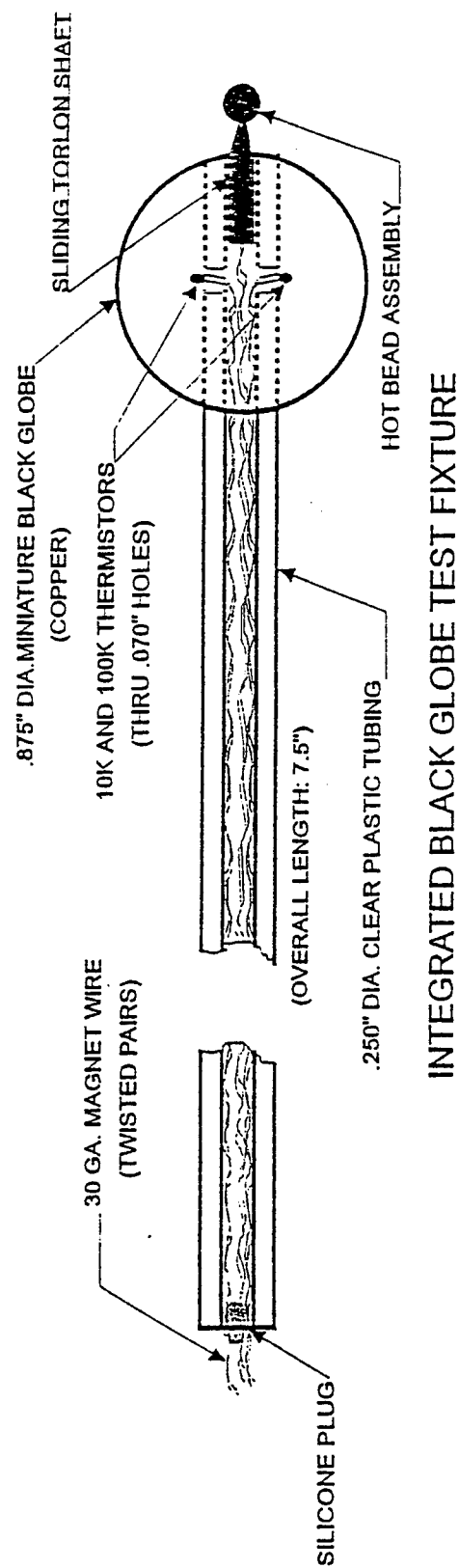
INTEGRATED BLACK GLOBE TEST FIXTURE

30 GA. MAGNET WIRE
(TWISTED PAIRS)

SILICONE PLUG

Figure 12. Integrated BGT/Wind Speed Assembly Sensor

30

The hot-bead anemometer portion consisted of a 0.043-inch-diameter, 200-ohm thermistor bead, which was potted inside of a 0.125-inch-diameter solid aluminum ball with a thin layer of thermally conductive epoxy. The ball was affixed atop a tapered Torlon® shaft, which joined the acrylic tubing support. All lead wires exited the back end of the acrylic tube and were connected to the appropriate instrumentation. The resistance of each thermistor was monitored using a precision ohmmeter, which used a constant current source exceeding not more than 100 µAmps. The hot-bead thermistor was heated continuously with an average power of approximately 24mW over an 18-minute interval. The resultant temperature change within the black globe for the first six (6) minutes of continuous anemometer bead heating is illustrated in Figure 13. As observed, both thermistors tracked within approximately 0.02°C and indicated a 0.6°C temperature elevation.

This temperature elevation has not proven to be a problem, since the actual operation of the anemometer is in a pulsed-duty mode of several seconds over the duration of about three (3) minutes, rather than in a continuous mode over a duration of either three (3) minutes or six (6) minutes, as shown in Figure 13.

Both the 10K and the 100K thermistors exhibited almost negligible self-heating effects in the black globe at ambient temperature. The 100K thermistor was selected for further use, however, since it consumed only one-tenth (1/10) the power of the 10K device for a comparable temperature measurement.

A comparison of the energy consumed by the Testoterm hot-bead anemometer in both continuous and pulsed modes is illustrated in Figure 14. In the continuous mode, the anemometer constantly heats the hot-bead to hold it at a given temperature. The result is a constant energy demand. In the pulsed mode, the anemometer is heated to the same set point, and then allowed to cool by turning the heating mechanism off. In the cooling phase, a small amount of energy is required to monitor the hot-bead temperature. Figure 14 illustrates the energy saved by using the pulsed mode of operation.

Aluminum-Encased Versus Bare-Bead Anemometer Although the cooling curves for the aluminum-encased thermistor bead exhibited almost linear characteristics, the aluminum-bead anemometer consumed approximately 30% more energy than the bare-bead version. Even with this additional energy, the aluminum-bead temperature was not elevated to the full 20°C above ambient. Also, because the half-life temperature change for the aluminum-bead was small, the corresponding voltage change was near the noise threshold of the test instrumentation. It was evident that this signal-to-noise margin would be incompatible with the 10-bit resolution of the data acquisition system (DAS). In light of this, wind-speed testing focused on the use of the bare-bead assembly, which---although having a nonlinear response---proved to have a greater output resolution and considerably faster response time. It was for these reasons that

31
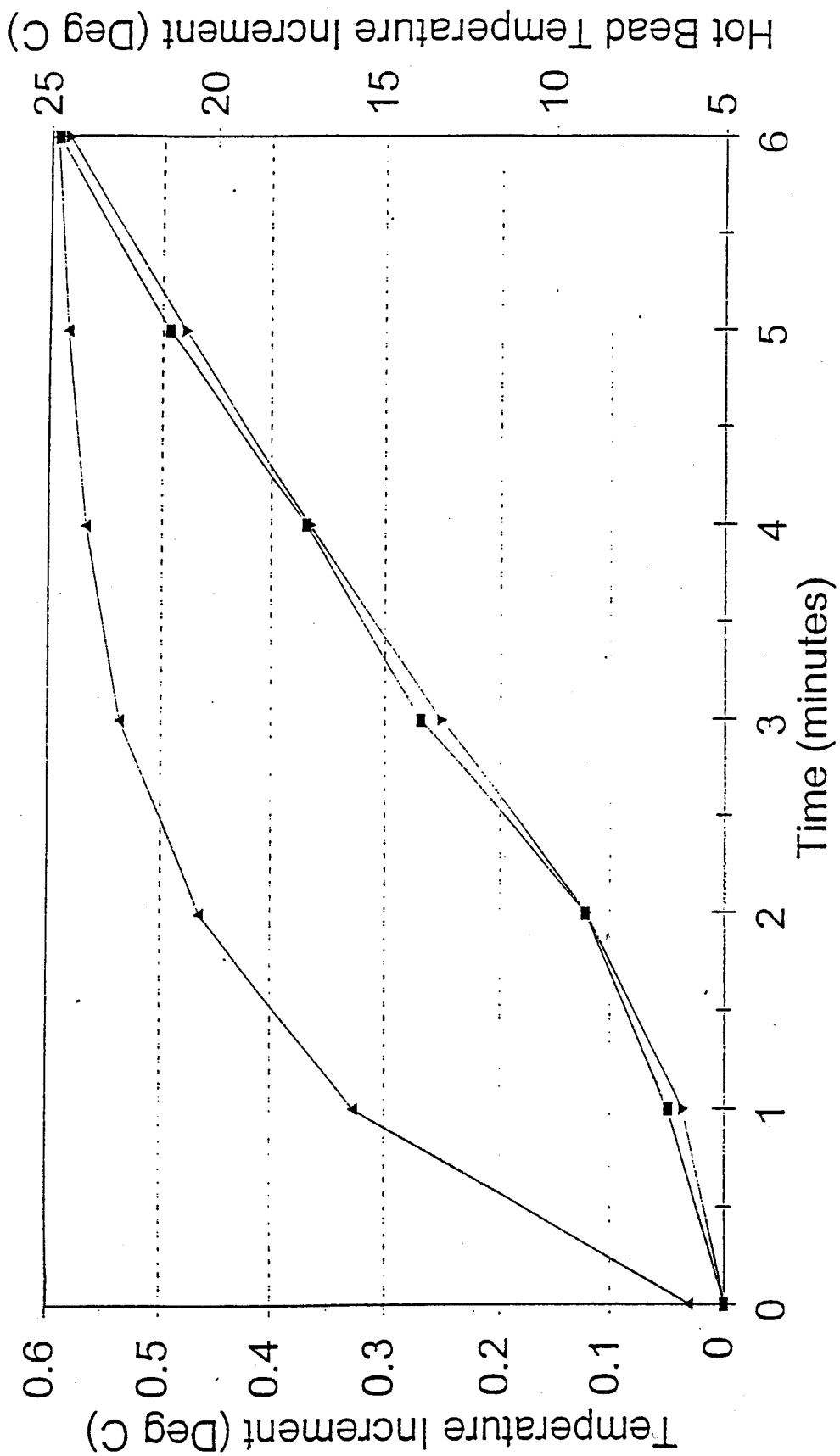
Figure 13. Effect of the Heated Anemometer on the Interior Temperature of the 7/8-inch Diameter BGT

ENERGY CONSUMED FOR 1049 PROBE UNDER PULSED AND CONTINUOUS OPERATION
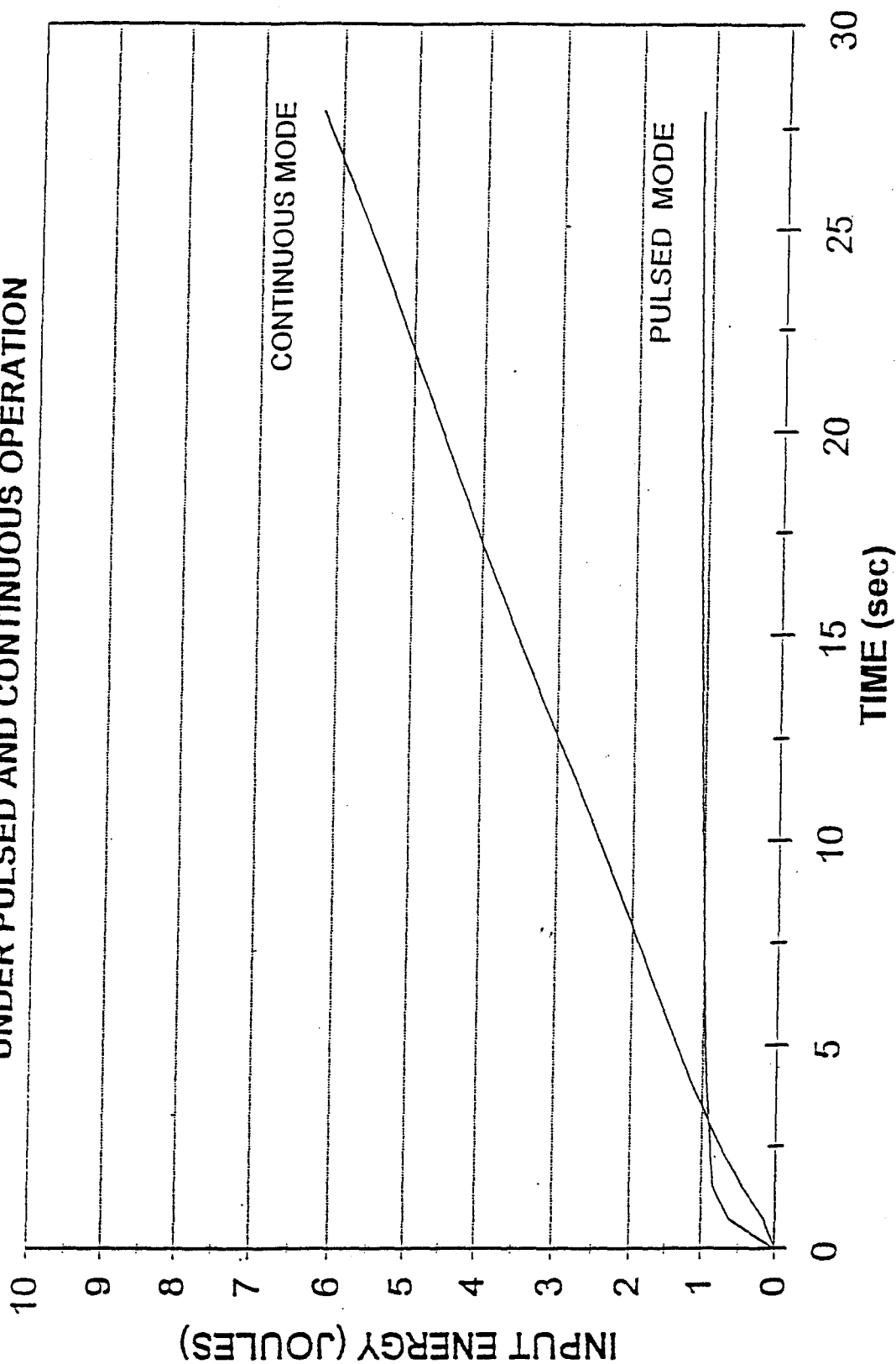
Figure 14. Comparison of Energy Consumed Between Continuous and Duty-Cycled Anemometer Probe

a bare-bead anemometer and not an aluminum-encased anemometer was incorporated into the current sensor suite support module. Any potential gains which might be achieved in ruggedness by use of the aluminum-encased bead rather than the bare-bead in the anemometer does not appear at present to offset the loss in response time and temperature change increment relative the noise threshold of the bare-bead. This tradeoff is not well quantified at present, but the bare-bead unit has been shown to operate reasonably well. The non-linear response of the bare-bead verses a more nearly linear response of the aluminum encased bead has little impact on this decision with the data handling system to be used.

Open and Closed Tunnel Test Results. Two tests were performed in the 7-inch-diameter environmental test chamber using an integrated, 7⁄8-inch-diameter, black-globe/bare-hot-bead anemometer assembly (see Figure 15, Wand 5). The first test was conducted with the tunnel in the typical closed system configuration, while the second utilized an open configuration, which allowed outside ambient air to enter the chamber's mixing plenum. The opening of the chamber to the outside ambient conditions was an attempt to minimize the heating effects arising from air/blade and bearing friction of the fan motor assembly that typically caused temperature variations in the closed-loop tunnel configuration. The relatively uniform ambient temperature of Veritay's underground test facility was used with the intent of maintaining an even tunnel temperature.

Test chamber conditions were monitored using the Testoterm model 1549 hot-bead anemometer and temperature reference. Both the anemometer under test (i.e., Wand 5; see Figure 12) and the reference probe were situated radially, two (2) inches from the inside wall of the test section of the test chamber. No data were taken from the pictured Wand 2.

To promote environmental stability around the anemometer under test, the reference probe, and the test section, an insulative box was constructed over the probes and test section, and was sealed beneath the test section by 5/16ths-inch-thick foil-lined bubble insulation shown in Figure 15. Bubble insulation material was also used around the cylindrical test section for additional isolation from the outer environment. An additional change to the environmental test chamber included the insertion of a honey comb air flow straightener 24 inches upstream of the test section of the tunnel.

The air flow straightener consisted of many 0.2-inch-diameter plastic straws fashioned in a honeycomb configuration. This flow straightener was introduced to minimize turbulence and promote laminar air flow through the 7-inch-diameter test section of the tunnel.

Each test was performed separately and consisted of heating the anemometer bead thermistor with a 25-mA constant current pulse until it reached a nominal 20°C above

34
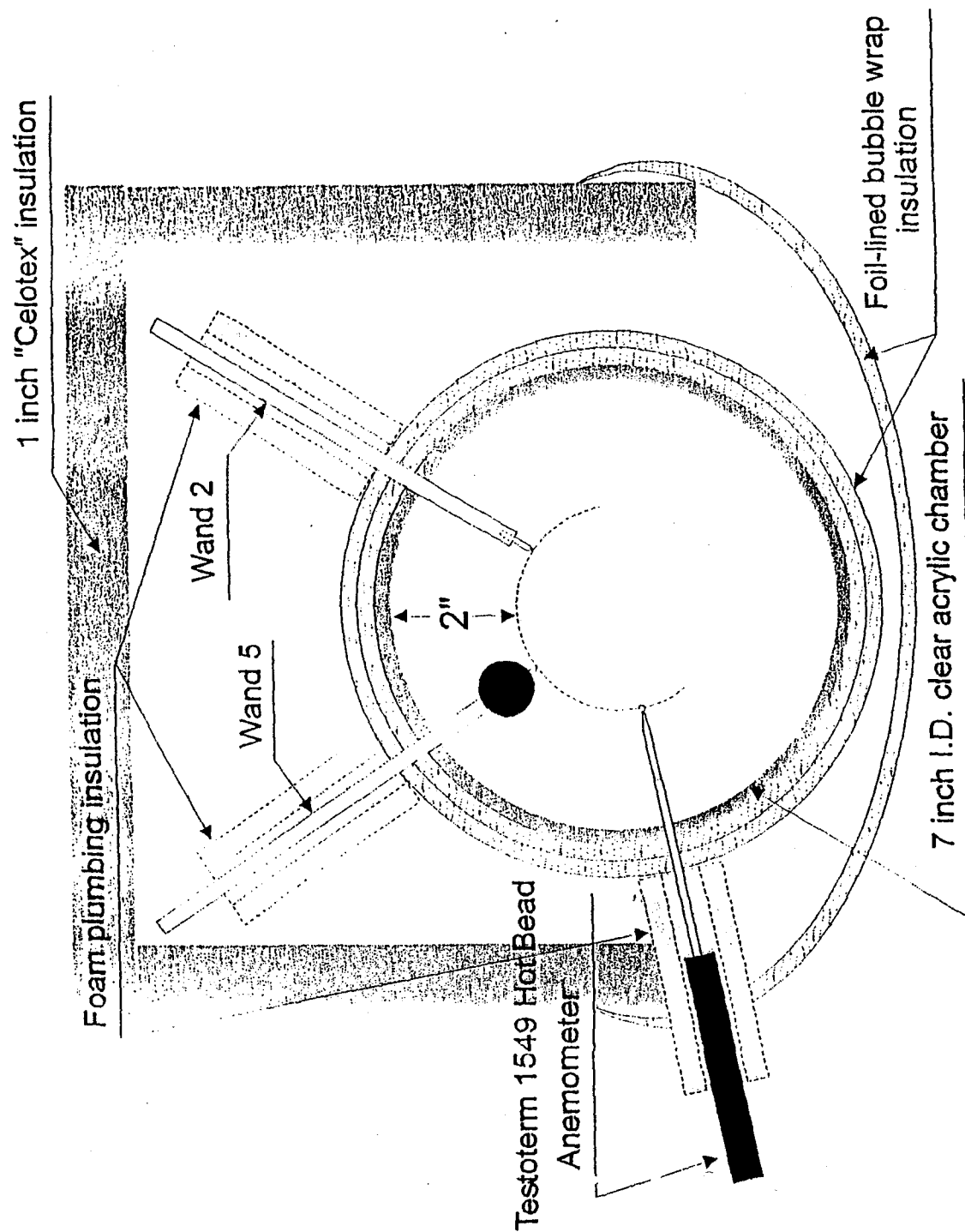
Figure 15. Cross-Section of Wind Tunnel Chamber (Air Flow Into Page)

35

the initial tunnel ambient condition of each test. The bead was then allowed to cool. The thermistor bead resistance, a function of temperature, was monitored during the cooling portion of the cycle using a 100-μA constant current source in series with the bead. The corresponding voltage drop across the bead was coupled to a circuit consisting of two voltage comparators, one preset to a voltage corresponding to 15°C above the initial chamber condition, the other to 7.5°C above. When the bead cooled to the +15°C temperature, a 10-digit counter was triggered on. As the bead cooled further to the +7.5°C level, the counter was gated off. The counter then displayed a number representative of the time it took the bead under test to cool from 15°C above the initial ambient chamber condition to 7.5°C above (i.e., the half-life cooling time). For each test, eight (8) pulses were obtained at each wind speed level ranging from 0 to 6 m/s in one (1) m/s increments. Additionally, the closed circuit test included a wind speed level (with corresponding cooling data) of 6.5 m/s, while the open circuit test included data at a 6.3 m/s wind-speed level. These two levels represent the maximum wind speed attainable for each test. Tunnel ambient temperature data was recorded via the Testoterm reference prior to the first and eighth pulses of each eight-pulse sequence. It should be noted that once the voltage comparators were set prior to each test, no additional adjustments were made despite an approximate two- (2) degree drift of tunnel ambient temperature for each test.

Figures 16 and 17 show the wind speed results for the integrated black-globe-temperature (BGT)/Wind-speed sensor for both the closed and open chamber configurations, respectively. Each graph shows an eight (8)-pulse average of half-life cooling times and an average of the two (2) temperature readings at each wind-speed level. The time sequence in which wind speed data were recorded occurs right-to-left on both curves. Test results of the "open" tunnel configuration indicated that temperature was not maintained as anticipated. The curve illustrates the tendency of the cooling time interval to become comparatively longer in duration as the ambient tunnel temperature increases, while the wind speed decreases. A similar effect was noticed for the closed tunnel test where the effects of a decreasing temperature and decreasing wind speed caused the overall shape of the curve to be slightly compressed as compared to the open tunnel results. In other words, a warmer ambient temperature gives rise to a longer cooling time interval and vice-versa. The variations in the observed wind speed cooling interval as a function of temperature is probably an artifact of the hot-bead conditions. As expected, this effect was minimized later when operation of the hot-bead anemometer was dynamically compensated for changing ambient conditions by the DAS controller.

Several additional early tests of candidate pulsed-anemometer probes were conducted to explore, develop and characterize both a suitable probe configuration and probe performance for use in the overall sensor suite. Inasmuch as these test results were developmental, they are not included here. However, test results for the pulsed

36

Reference: Testoterm model 1549
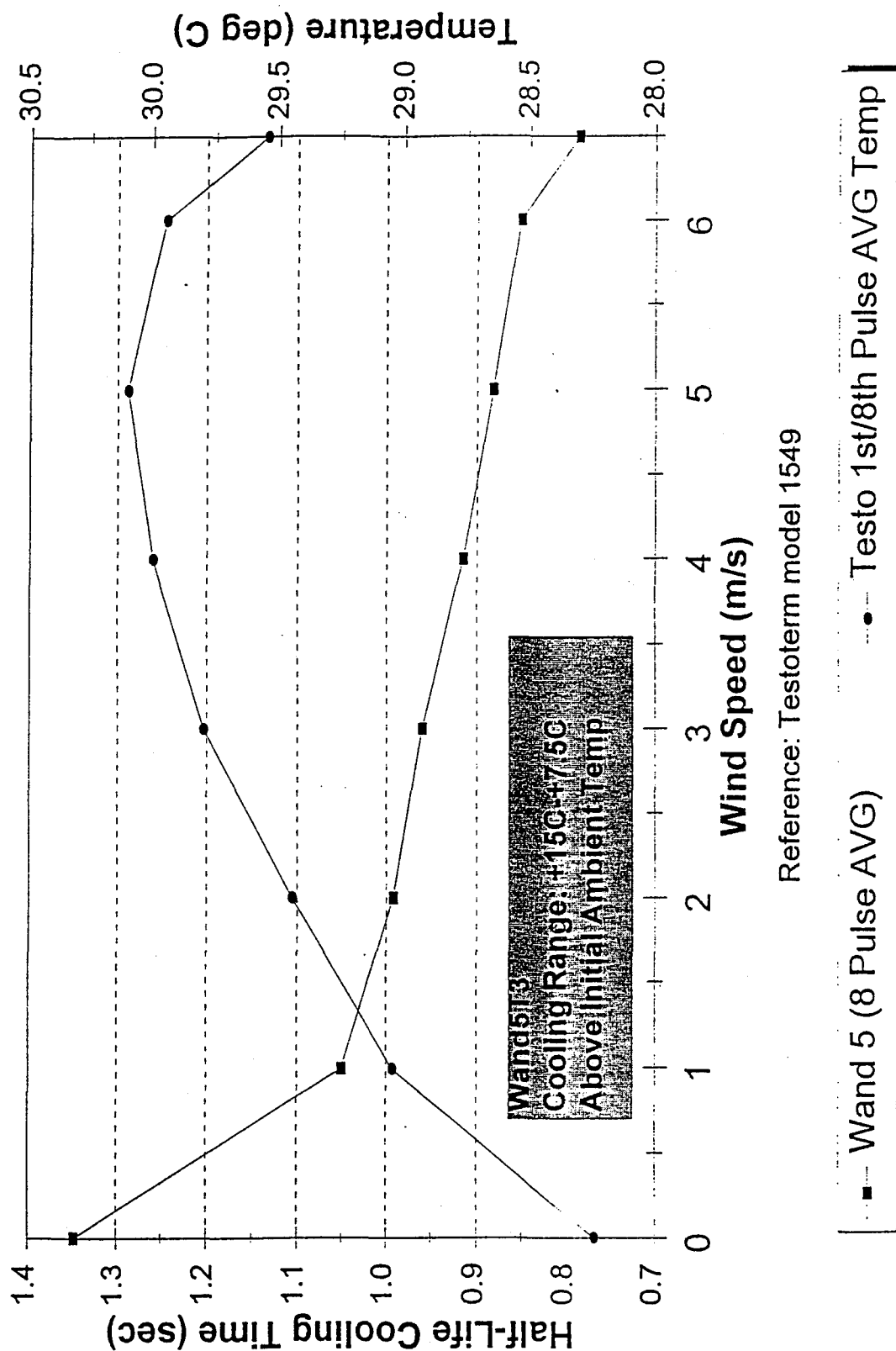
Figure 16. Closed Circuit Tunnel—Wind Speed Performance Test
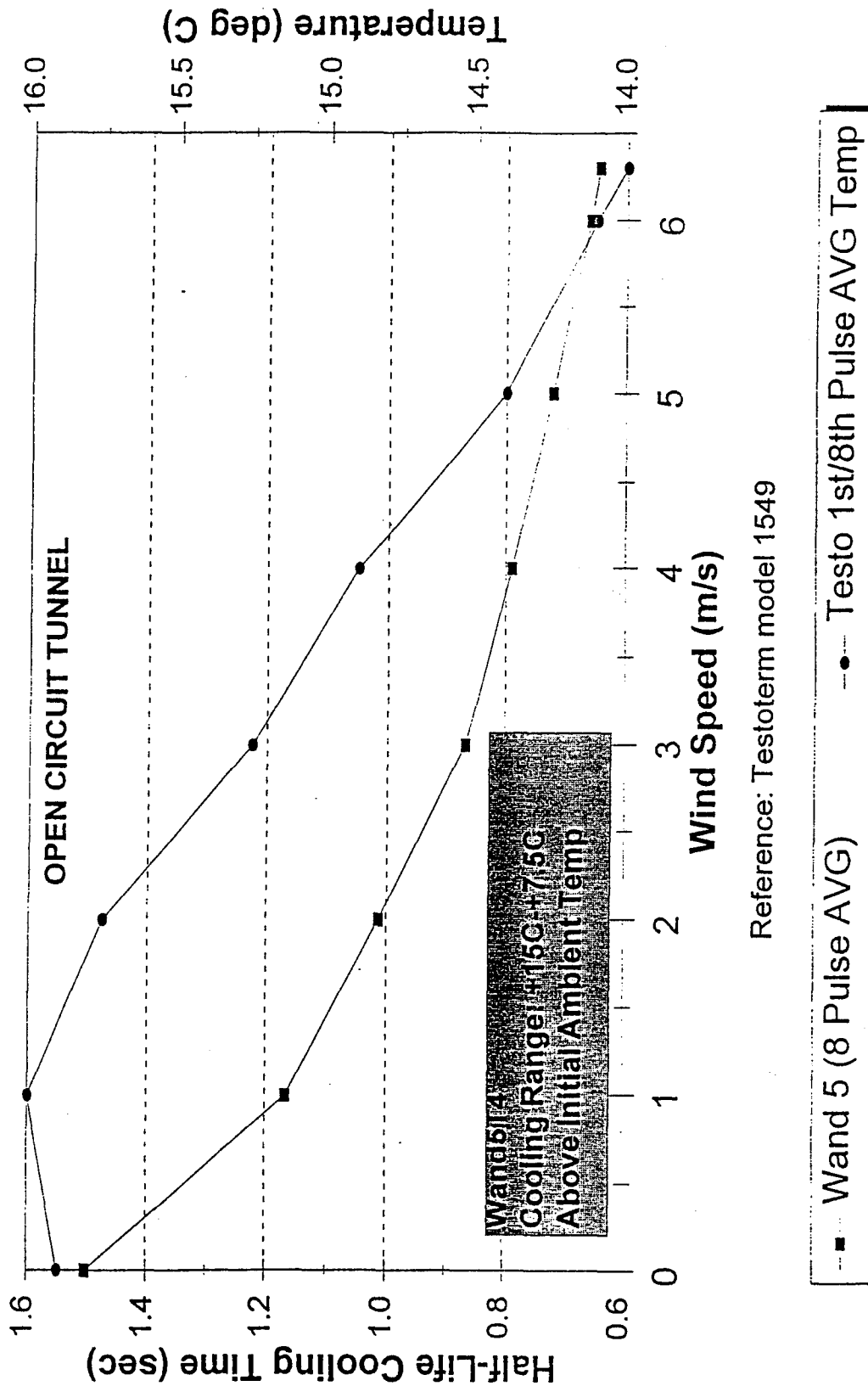
Figure 17. Open Circuit Tunnel—Wind Speed Performance Test

anemometer incorporated in the final sensor suite are included later in this report in Section 5.3, "Validation Testing."

5.1.4 Radiant Energy. Several sensor types were considered for measuring mean radiant energy, including radiometers, black globes, thermometers, and novel concepts requiring various degrees of advanced development.

Investigations revealed that no radiometer-type sensors other than the black globe currently exist that appear to be capable of achieving integration over a sufficiently wide angular field of view to be directly useful in the sensor suite.[5]

The black globe radiometer was, therefore, adopted as the radiation sensor for use under this program both to achieve angular integration of the incoming radiation from a variety of directions, and to determine the "mean radiant temperature $(\overline{T}_r)$," which is the variable used by most thermal physiologists in studies involving heat stress. This type of radiation sensor will therefore provide the input used in virtually all existing thermal models. However, the size of the standard black globe sphere used in such heat stress studies typically has been six (6) inches [15 cm] in diameter. In turn, the mean radiant temperature has usually been determined with this standard size black globe radiometer. Since this globe size was too large for use in this application, a smaller diameter globe was required for use in the sensor suite. As a result, a 7/8-inch- (22.2-mm) diameter black globe sensor was selected for use here.

As a result of down-sizing of the black globe radiometer device an effort was initiated to correlate the globe temperatures measured for the 7/8-inch and the standard 6-inch diameter globes under identical operating conditions of radiation, wind, humidity, and ambient temperature. As noted earlier in Section 4.5.5, it was expected that the greatest degree of realism could be achieved if the several candidate environmental parameters were measured simultaneously outdoors under natural environmental conditions during daylight hours. Such tests were conducted using the set of three (3) black globe thermometers with diameters of 7/8 -inch (22.2mm), 1 5/8 -inch (41.3mm) and 6-inch (150mm). The 1 5/8-inch globe sensor tested was a commercial black globe thermometer manufactured by IST Corporation. It was included as a possible second black globe unit for correlation with the 7/8-inch unit, if required. In the final analysis it was not used for this purpose. All of these globe sensors together with reference wind, ambient temperature and relative humidity sensors were exposed to the natural environment during outdoor tests.

---

[5] *One concept that promised to achieve the requisite angular integration was a global radiation sensor that used a novel coating technology with alternating black and white bands. Preliminary investigation of this concept indicated that development well beyond the scope of this contract would have been required to achieve implementation. Therefore, it did not warrant further consideration under this contract.*

Although several such outdoor tests were conducted, the results of some tests were complicated by unforeseen weather problems (such as clouds, mist, rain, etc.) before sufficient data were gathered to warrant detailed data analysis. The results of two successful tests, conducted at significantly different ambient temperatures, using the latest version of the 7/8-inch globe employed on the actual sensor suite are included here. These results form the basis for the current black globe calibrations in the final sensor suite. As with the other sensors incorporated in this sensor suite, the sensors themselves are replaceable on a one-to-one basis without re-calibration. If for some currently unforeseen reason re-calibration is needed, this can be readily accommodated by a straightforward change in the software program---without requiring hardware modifications.

The temperature-time data for Test No. 14 and Test No. 15 are shown in Figure 18 and Figure 19, respectively. The "curves" in these figures are derived from measured data points taken every ten (10) seconds during the tests for each sensor. The curves represent the measured ambient air temperature (T_a), the measured 6-inch black-globe temperature (T_G), and the measured 7/8-inch black globe temperature (T_g), each as a function of time.

The overall relation between temperatures registered by the 6-inch and the 7/8-inch globes over the range of temperatures and temperature variations was developed on the basis of the relative thermal balance between the black globes and their environment. Because of the undetermined heat losses inherent in the globes and support apparatus, a complete heat transfer analysis was neither feasible nor practical at best. Instead, an empirical approach was developed to simplify the thermal characteristics, yet still provide an accurate representation of the scaling of globe temperature. This method considers the thermal balance equation [ISO 7726, Annex B] of the form:

$$h_{rg}(\overline{T_r^4}-T_g^4)+h_{cg}(T_a-T_g)=0, \qquad (2)$$

where:

$h_{rg} = \sigma\epsilon$ is the coefficient of radiation between the enclosure and the globe,

σ is the Stefan-Boltzmann constant, and ϵ is the emissivity of the black globe (typically 0.95 for matt black paint);

$\overline{T_r}$ is the mean radiant temperature in degrees Kelvin;

$h_{cg} = 6.3\dfrac{v_a^{0.6}}{D^{0.4}}$ is the coefficient of heat transfer for the case of forced convection,

40
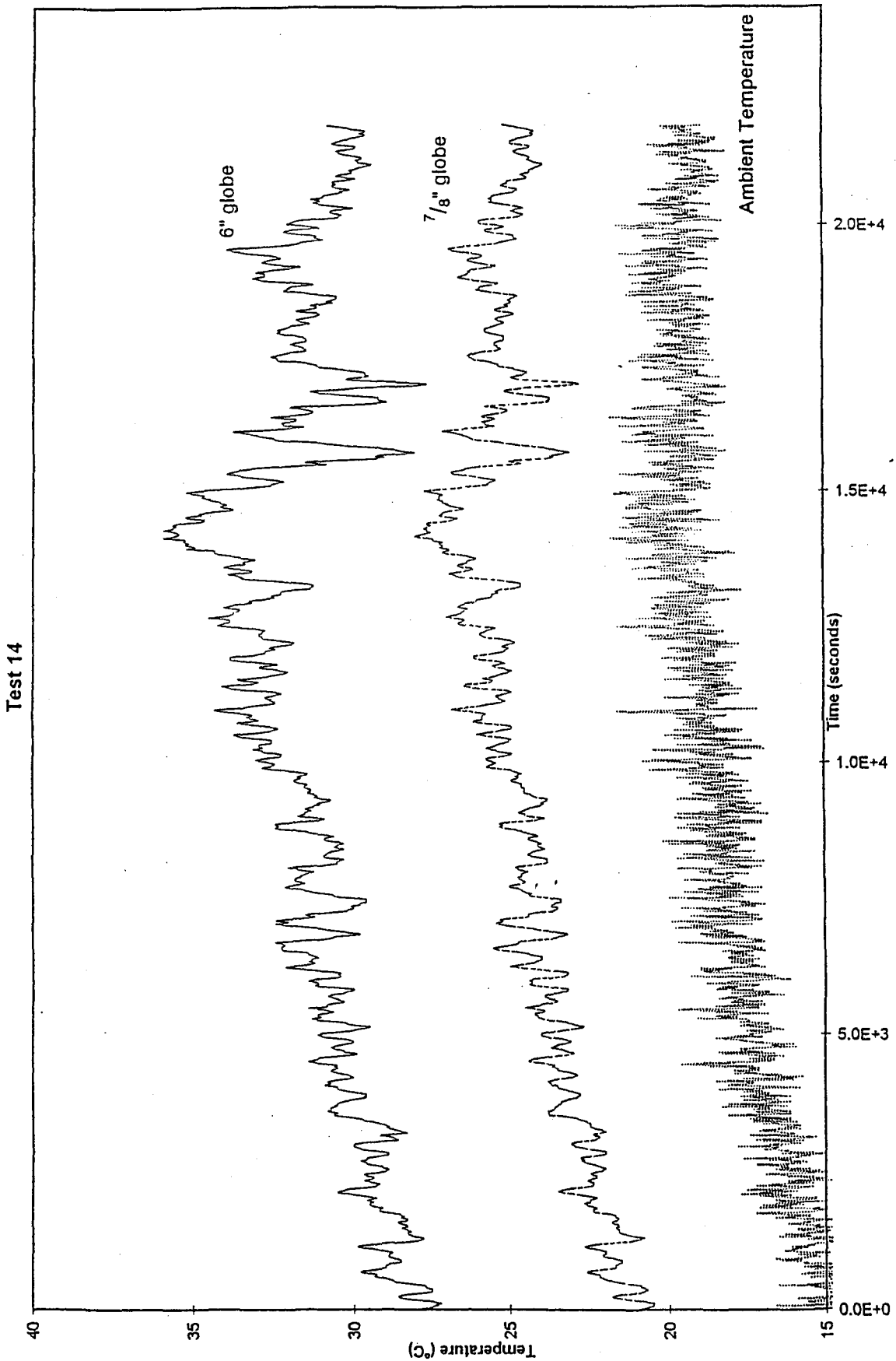
Figure 18. Temperature-Time Data Traces for Outdoor Measurements During Black Globe Test No. 14
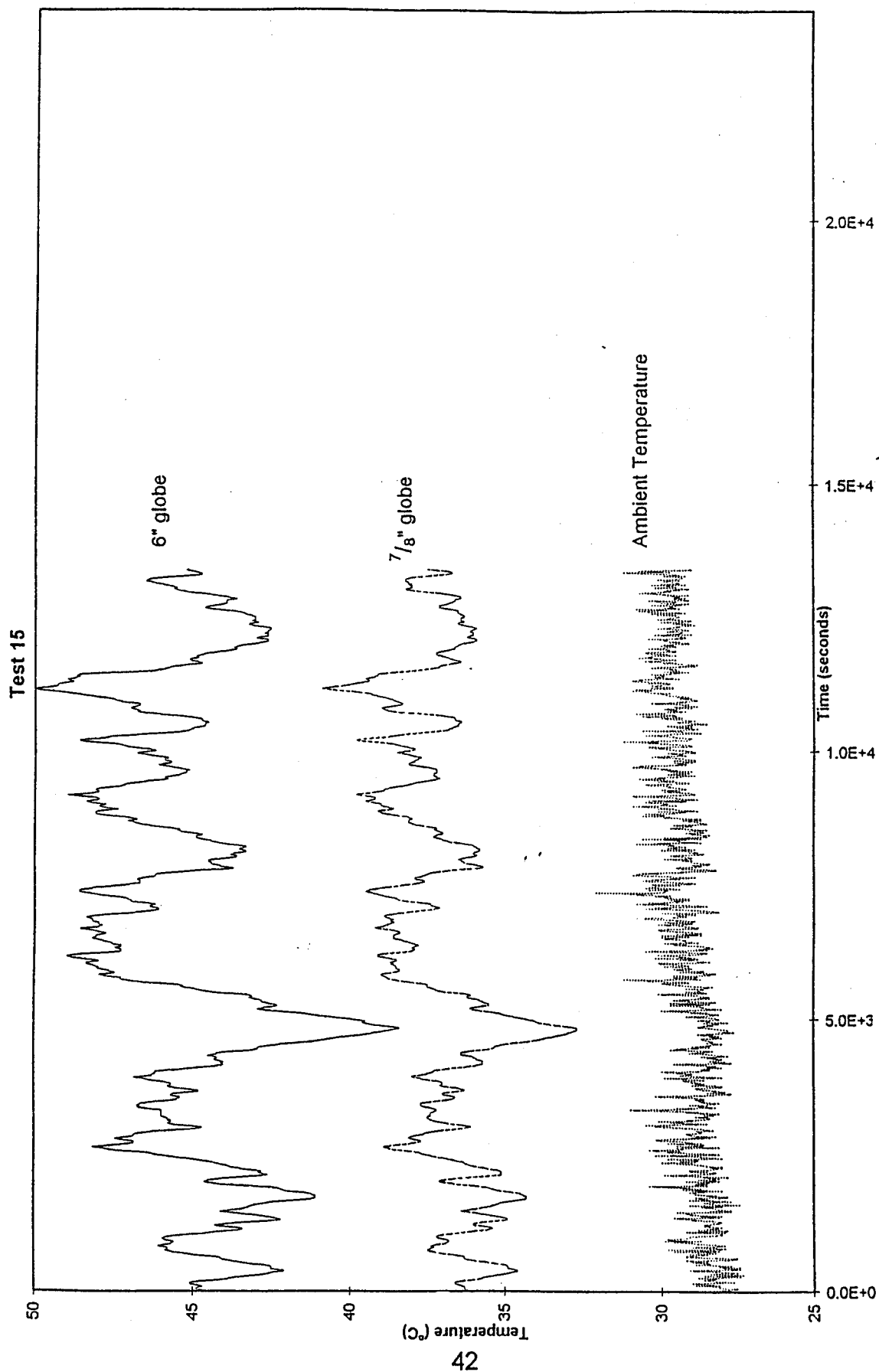
Figure 19. Temperature-Time Data Traces for Outdoor Measurements During Black Globe Test No. 15

42

v_a is the wind speed and D is the diameter of the globe;

T_a and T_g are the ambient and globe temperatures (degrees Kelvin) respectively.

A correlation between the 6-inch globe and $7/8$-inch for both globe temperature and mean radiant temperature was derived using the data obtained from the black globe tests in conjunction with the above equation.

Initially, a direct comparison was made between the 6-inch and the $7/8$-inch globe temperatures, but a better correlation was achieved by comparing the difference between the internal temperature of each globe (T_g) and the outside ambient temperature (T_a), or T_g-T_a. Relating the two globe temperatures in this manner required the assumption that both of the devices experienced the same ambient temperature, wind speed and radiant exposure. This can be illustrated by rearranging equation (2) and equating the mean radiant energy for the two cases:

$$k_G(T_G - T_a) + T_G^4 = k_g(T_g - T_a) + T_g^4, \qquad (3)$$

where:

T_G and T_g are the temperatures of the 6-inch and the $7/8$-inch globes respectively,

k_G and k_g are the lumped heat transfer coefficients, in essence differing by the same ratio as between the globe diameters raised to the 0.4 power (assuming both globes exist in a common environment).

The procedure for relating the globes involved plotting T_G-T_a for the 6-inch globe as a function of T_g-T_a for the $7/8$-inch unit. A linear relationship between these differences was obtained using curve fitting software. The $7/8$-inch globe to 6-inch globe correlation was then found by adding T_a to the curve fit expression. The T_G^4 and T_g^4 terms in the previous equation could not be explicity handled in the curve fit algorithm and required a numerical methods approach. An iteration was performed by substituting the correlated globe temperature data back into the above equation; however, no noticeable improvement to the correlation was observed in the refitted data.

The individual curve fits obtained for both test 14 and 15 showed that the $7/8$-inch globe temperature, appeared to correlate rather well with the 6-inch globe temperature. More important however, was the fact that the curve fit expressions obtained by each were quite similar, considering the different weather conditions in which they were performed.

43

Although the data was limited, a more general relationship for converting the ⅞-inch globe temperature to the 6-inch globe was formed by averaging the individual terms of the curve fit expression for each of the two tests; the result was as follows:

$$T_G = 1.667T_g - 0.677T_a + 3.67.$$ (4)

This conversion was applied using the measured ⅞-inch globe temperature and compared to the actual results obtained for the 6-inch globe in tests 14 and 15. Results of this comparison are shown in figures 20A, 20C, and 20B, 20D (expanded segment).

The relationship for mean radiant temperature was more straightfoward than the globe temperature correlation. It was derived directly using the thermal balance equation in the form:

$$\overline{T}_r = [T_g^4 + \frac{h_{cg}}{h_{rg}}(T_a - T_g)]^{\frac{1}{4}}.$$ (5)

The conversion for scaling the mean radiant temperature of the ⅞-inch $\overline{T}_{rg}$ to the 6-inch $\overline{T}_{rG}$ was also based on a linear fit. As in the case of the globe temperature, a general correlation between the measured 6-inch and the scaled mean radiant temperature was obtained by averaging the curve fit expressions associated with each test. The effective scaling factor,

$$\overline{T}_{rG} = 0.911\overline{T}_{rg} + 37.8,$$ (6)

was used to scale the computed mean radiant temperature of the ⅞-inch globe. A comparison of the scaled mean radiant temperature for the ⅞-inch globe and its 6-inch counterpart are illustrated in figures 21A, 21C, and 21B, 21D (expanded segment) for tests 14 and 15 respectively.

44
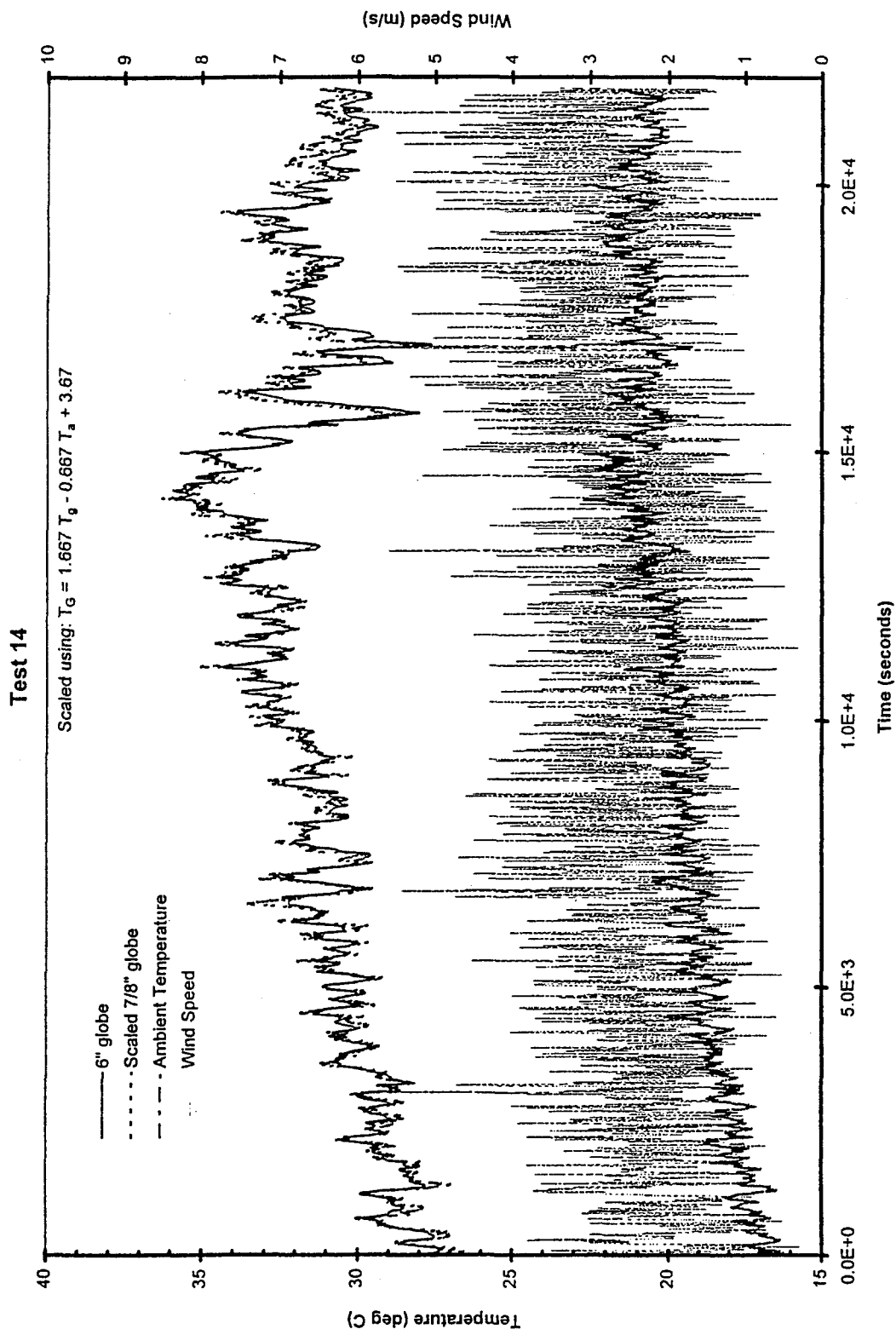
Figure 20A. Comparison of Measured and Scaled 6-inch Black Globe Temperatures for Test No. 14

45
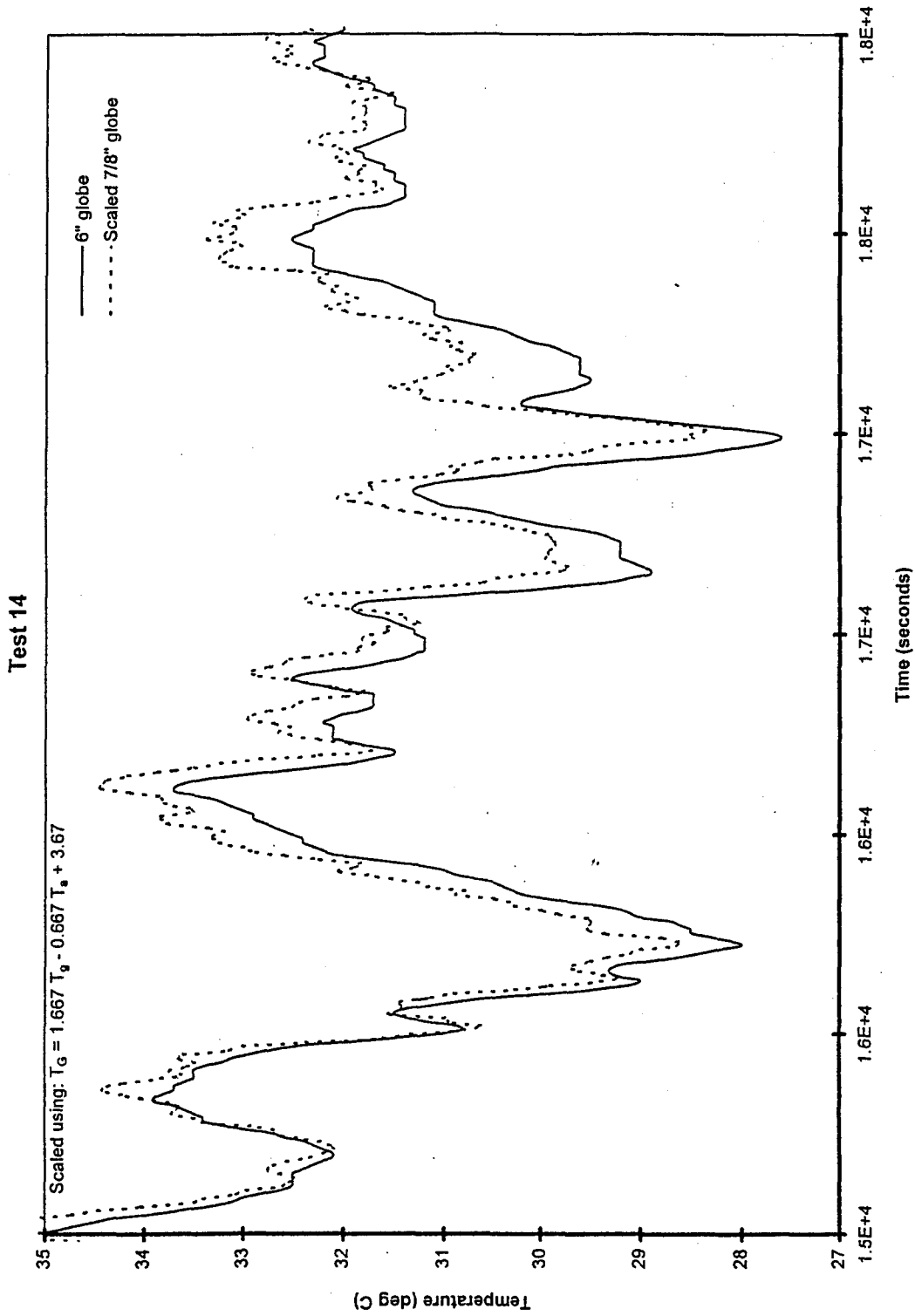
Figure 20B. Comparison of Measured and Scaled 6-inch Black Globe Temperatures for Test No. 14 (Expanded Segment)

46
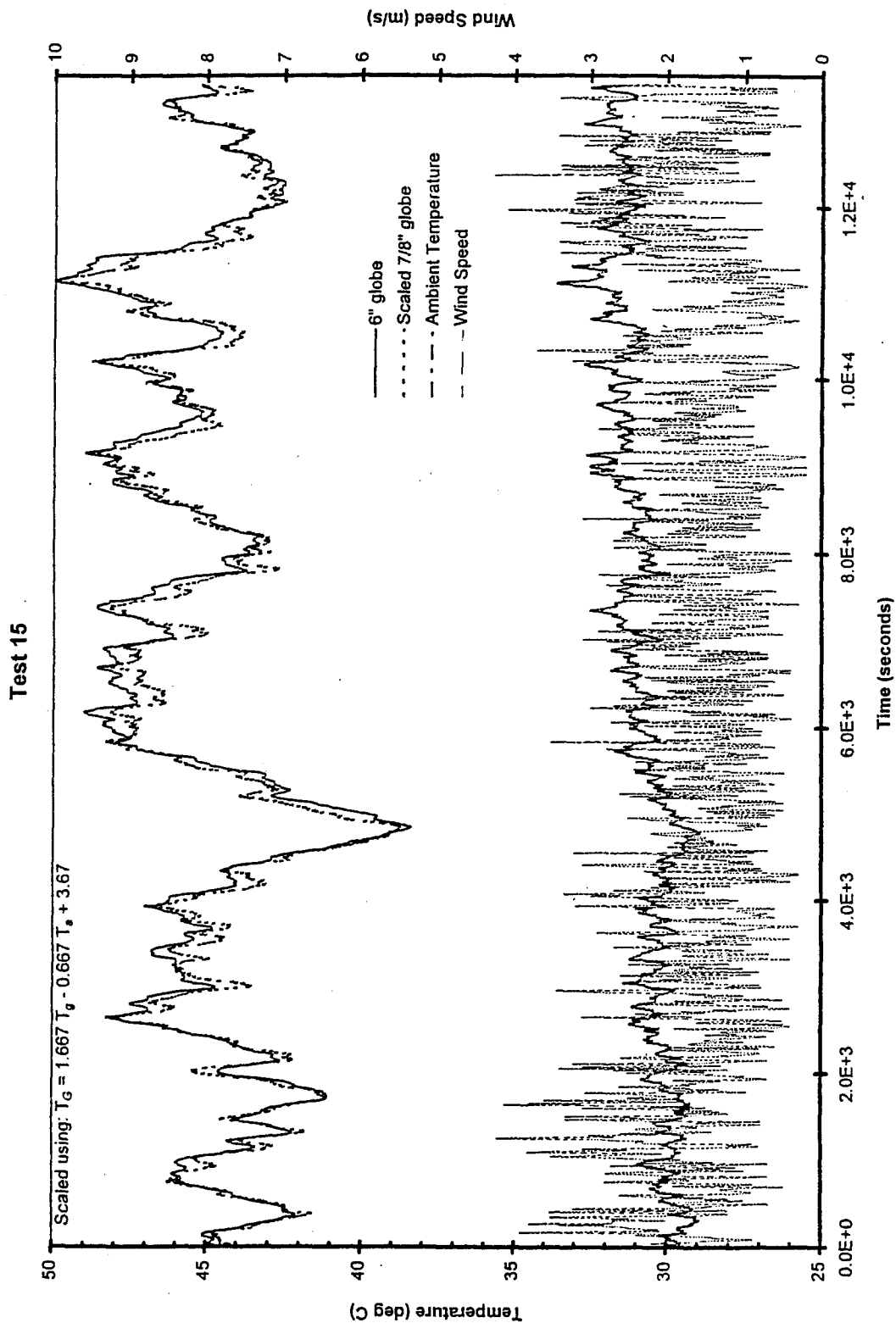
Figure 20C. Comparison of Measured and Scaled 6-inch Black Globe Temperatures for Test No. 15

47
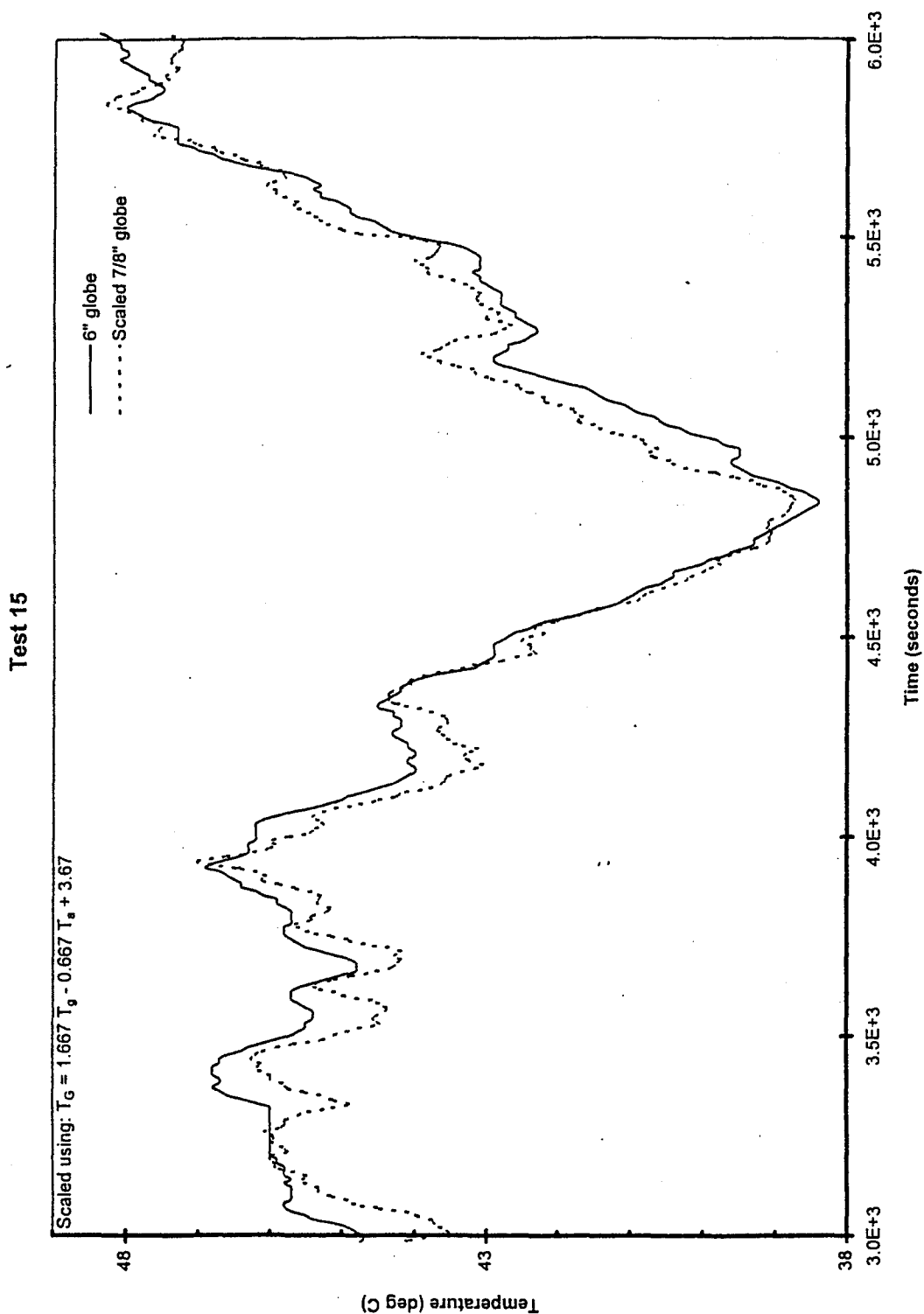
Figure 20D. Comparison of Measured and Scaled 6-inch Black Globe Temperatures for Test No. 15 (Expanded Segment)
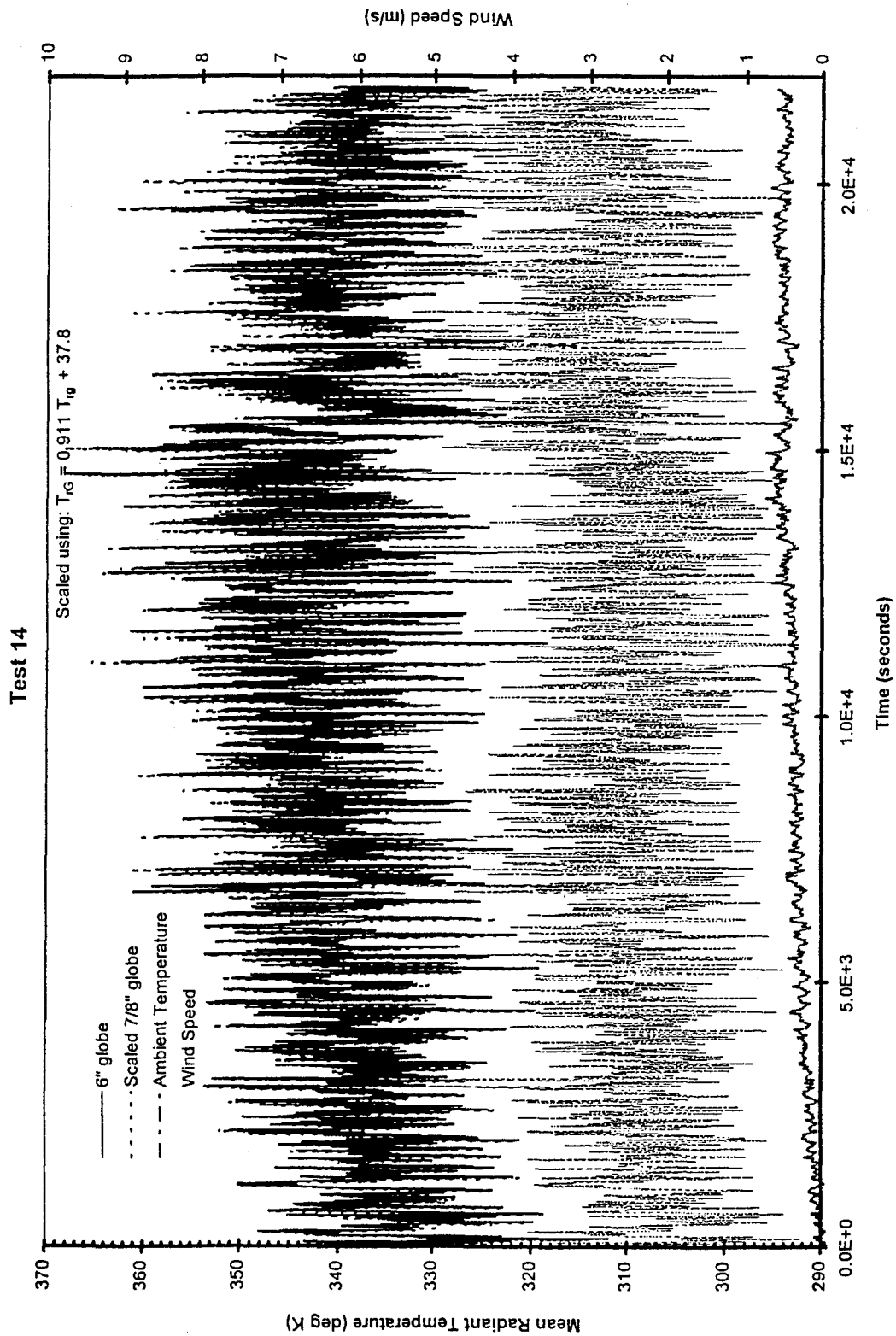
Figure 21A. Comparison of Measured and Scaled 6-inch Black Globe Mean Radiant Temperatures for Test No. 14

49
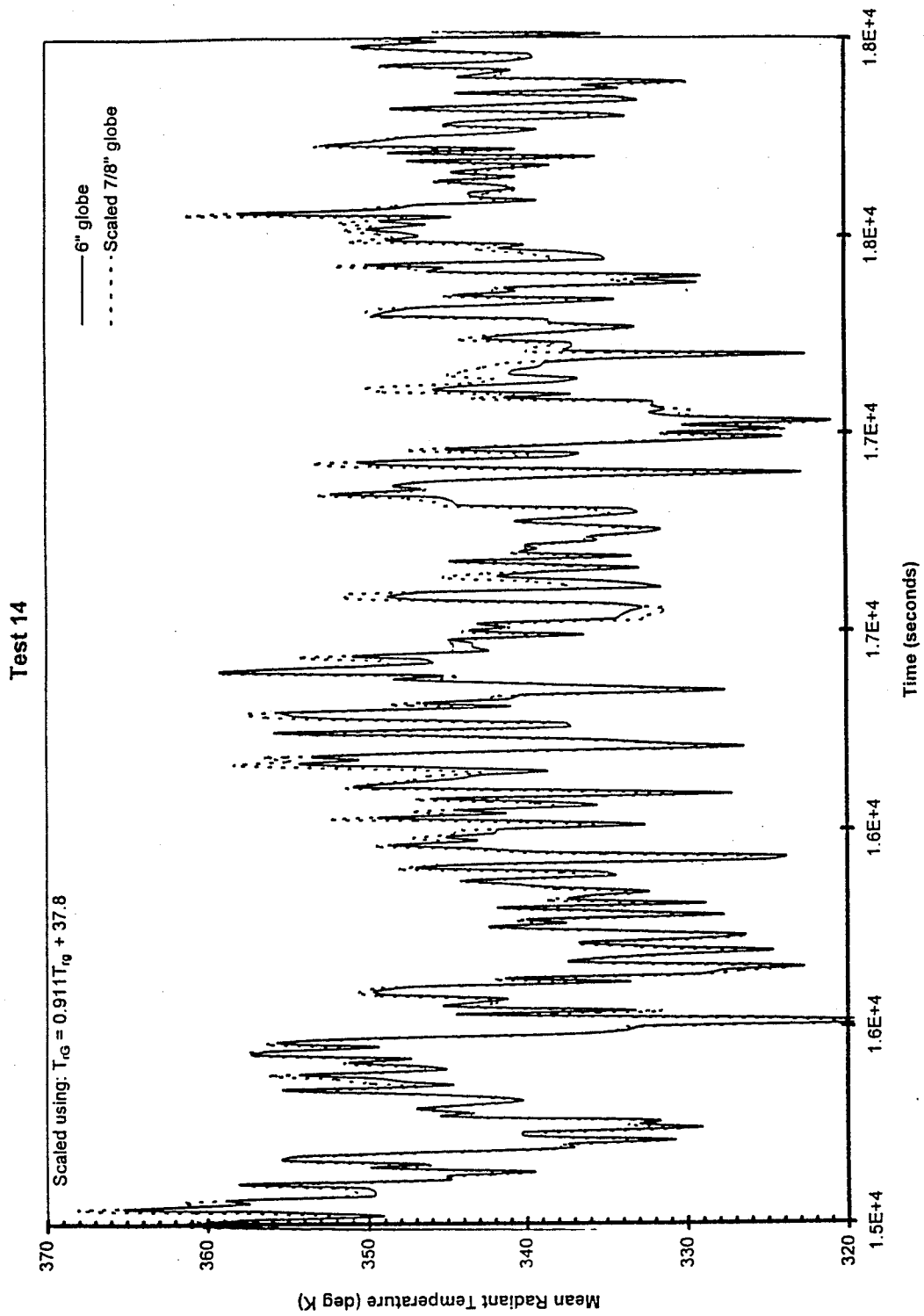
Figure 21B. Comparison of Measured and Scaled 6-inch Black Globe Mean Radiant Temperatures for Test No. 14 (Expanded Segment)

50
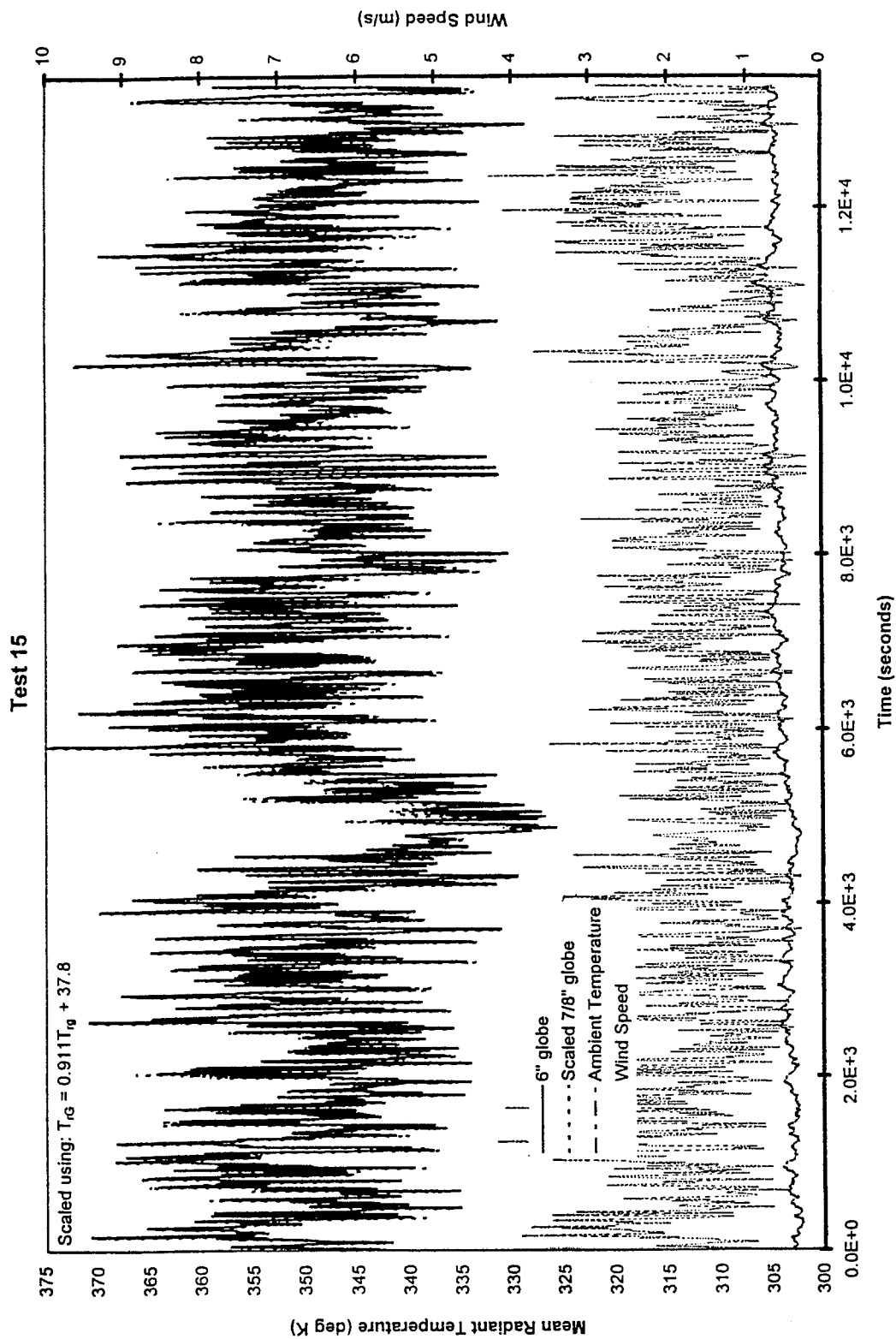
Figure 21C. Comparison of Measured and Scaled 6-inch Black Globe Mean Radiant Temperatures for Test No. 15

51
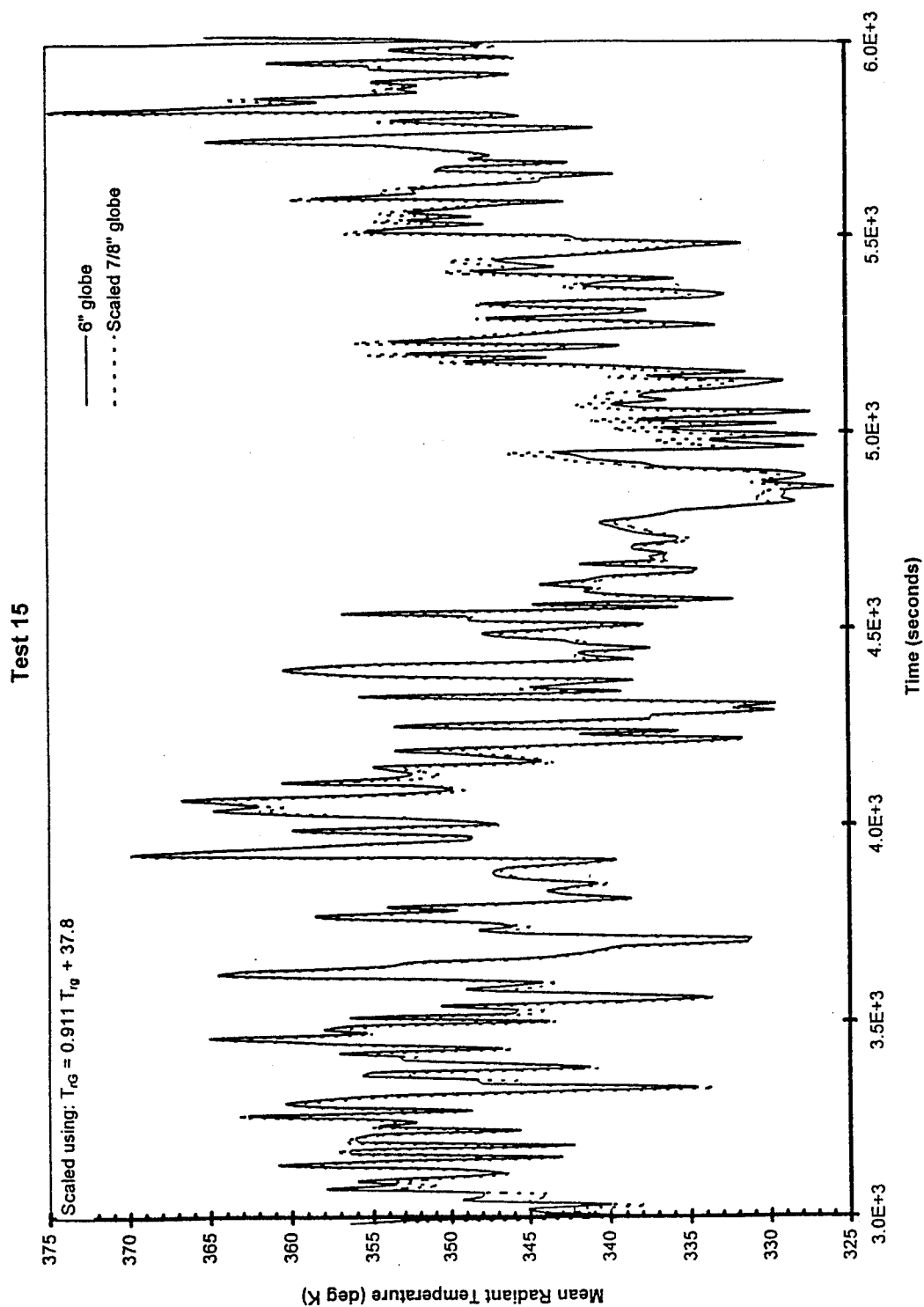
Figure 21D. Comparison of Measured and Scaled 6-inch Black Globe Mean Radiant Temperatures for Test No. 15 (Expanded Segment)

Fortunately, the response time of temperature changes for the smaller globe appears to be essentially the same as for the 6-inch globe, so that no specific time-delay feature needs to be taken into account explicitly. If there were exact scaling of all the hardware features between the two globes, one would expect the smaller globe to respond more quickly. The scaling is certainly not exact.

Generally, the scaled temperatures compare favorably over part of the test runs, but not necessarily over the entire run. The magnitudes of the major peaks are emphasized in the scaling technique used, so the largest temperature variations are rather well represented. The main discrepancies tend to be in regions where the temperature variations are not nearly so large. It is possible that slightly improved values in the scaling algorithm could help improve the temperature agreement. At present, the agreement illustrated is generally better than one (1)°C and is believed to represent a useful representation of 6-inch black-globe temperatures.

5.2   Subsystem Sensor Suite/Module Description

5.2.1 Candidate Integrated Sensor Modules. Several candidate sensor modules were considered. The most promising and innovative were examined to determine their relative abilities to address such important trade-off considerations as size, weight, cost, and power objectives; operation and performance requirements; and manufacturing costs and constraints. The two modules evaluated for integration into the sensor suite are described here and depicted graphically in Figure 23.

5.2.1.1   Black Globe and Anemometer Sensor. This candidate sensor module consisted of a miniature black globe having a diameter of ⅞ inch (22.2mm). The globe itself was made of thin copper that had been treated with a flat black paint on the surface to absorb radiant energy. A thermistor was placed inside the globe and was used to measure interior temperature. A linearizing thermistor voltage divider circuit was used to take advantage of the full-scale accuracy and resolution of the DAS analog-to-digital converter (ADC). The net amount of radiant energy absorbed by the black globe was a function of the temperature difference between the black globe interior temperature and the ambient temperature.

The black globe was modified by attaching an anemometer hot-bead probe on top of the black globe. This was accomplished by having a plastic tube placed through the globe and by mounting the anemometer on the tube at the top of the globe using a thermally insulated mount. The lead wires exit the globe via the other end of the tube. The hot-bead anemometer extended from the top of the globe by approximately 0.040 to 0.050-inch (1.0 to 1.3 mm). To minimize wind-flow and temperature-reading

HOT BEAD ANEMOMETER

BLACK GLOBE

AMBIENT TEMPERATURE AND RELATIVE HUMIDITY VENT WINDOW

SENSOR SUITE SUPPORT MODULE

FOLD

SSSM SOCKET

DAS UNIT

ITEM

MENU

PWR / ENTER

END VIEW
SHOWING BATTERY IN PLACE

BATT.

CASE SCREW

SIDE VIEW

BATTERY
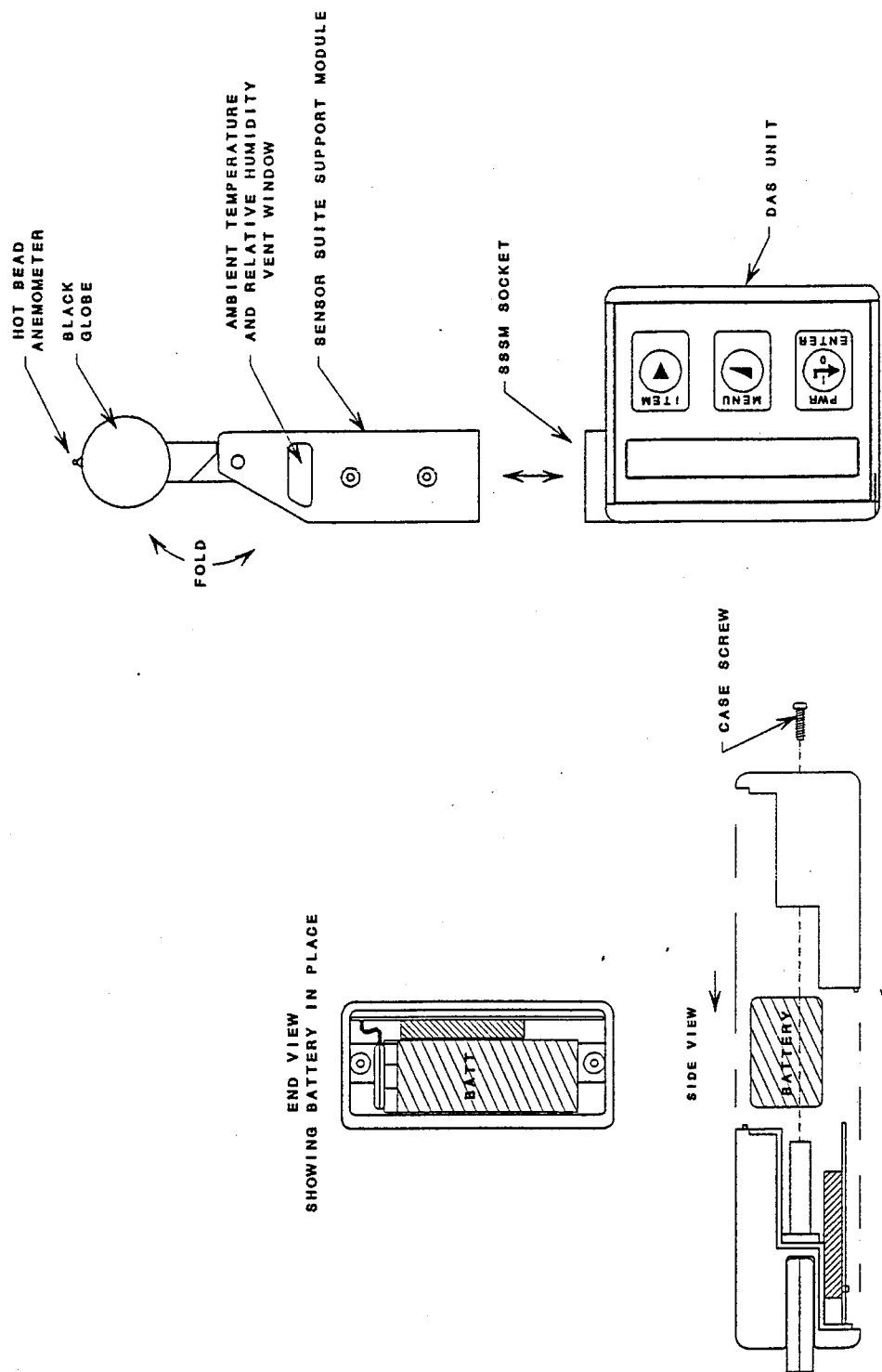
Figure 22. Complete EHM Unit Shown with Sensor Suite Unit and DAS Support Module (Right),
DAS Internal View (Left)

54

0.043" HOT BEAD
THERMISTOR

UPPER SEAL

BGT
THERMISTOR
BEAD

0.875"
BLACK GLOBE

LOWER SEAL

HY-CAL
HUMIDITY SENSOR

WINDOW

AMBIENT TEMP
THERMISTOR BEAD

PRINTED CIRCUIT BOARD
(THERMISTOR LINEARIZING
AND ANEMOMETER CIRCUITS)

1.000
SCALE

MODULAR
CONNECTOR
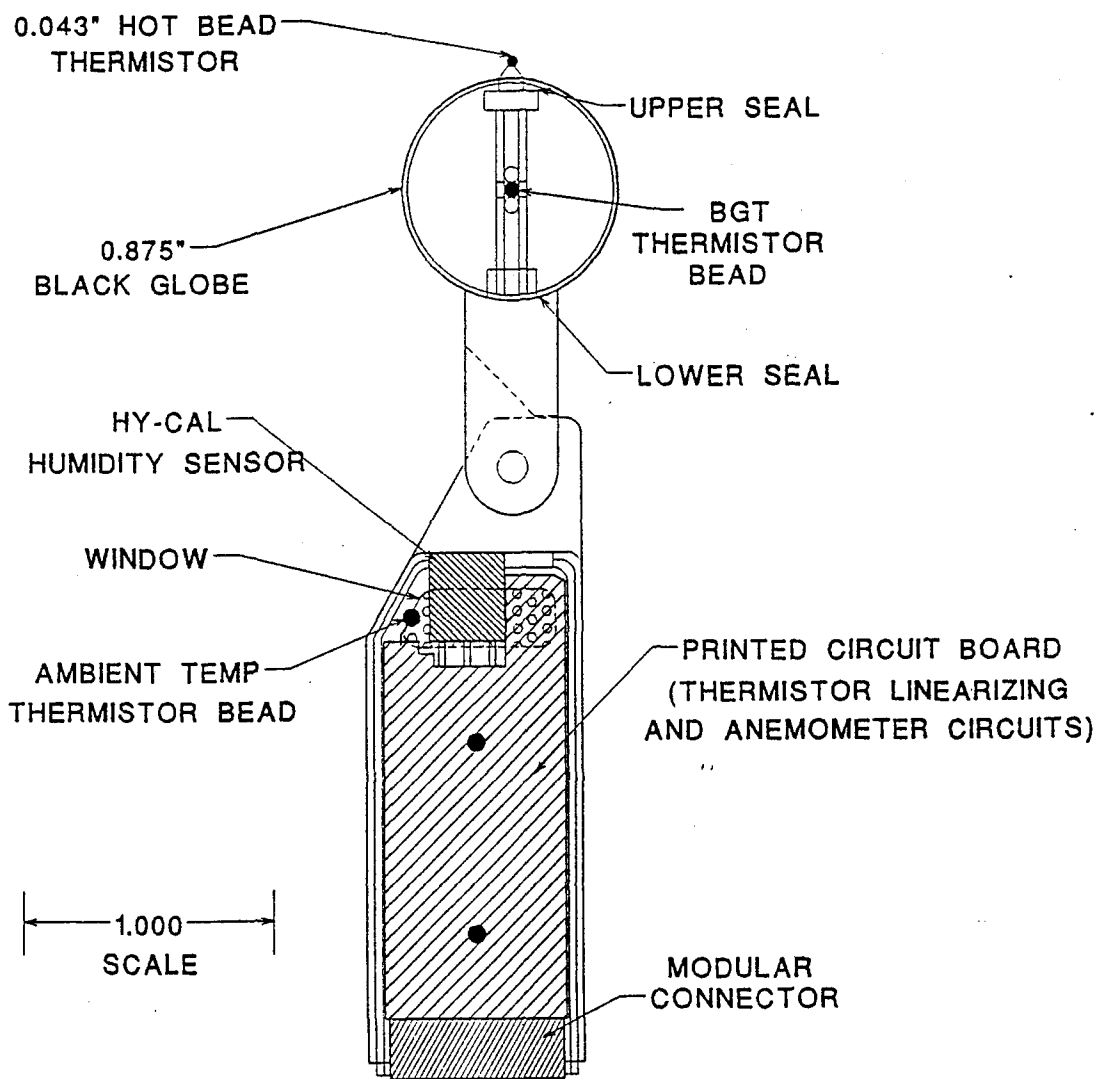
Figure 23. Cross Sectional View of Sensor Suite Support Module

interference from the case, the black globe/anemometer module configuration was located at the end of an arm extending as far as possible from the case.

5.2.1.2   Ambient Air Temperature and Relative Humidity Sensors. In this configuration, the ambient temperature thermistor and solid-state relative humidity (RH) sensors were grouped together in a sensor module. These discrete sensors were located in the extendable arm in the final integrated sensor system. The integrated circuit converted the output from the relative humidity sensing element to an analog signal that directly corresponded to the observed RH. The same linearizing divider circuit used for the black globe thermistor measurement was employed for the ambient temperature measurement.

5.2.2 System Support Module. The sensor suite support module is shown in Figure 23. The assembly features a pivoting arm to extend the integrated anemometer/black globe sensors above the main section of the module. A vent window on the side of the enclosure provides air circulation across the humidity and ambient temperature sensors located within the main section of the module. A 16-pin,2mm dual row type interconnect at the bottom of the assembly serves to connect the power supply voltages, voltage references and instrumentation lead wires between the sensor suite support module itself and DAS control unit. These connections are illustrated in the block diagram, Figure 24. The electronic circuitry within the module is minimal and contains only the necessary components required for biasing and/or conditioning each sensor in order to provide a full-scale output for subsequent interfacing to an Analog-tp-Digital converter (ADC) located on board the DAS controller unit. In particular, a linearizing voltage divider configuration is used in conjunction with all of the thermistor sensors employed. This technique effectively linearizes the response of the thermistor device to match the input scaling and resolution of the ADC. The ambient temperature and black globe linearinzing dividers are reference to 5.000 volts and provide a full scale level of approximately 3.5 volts at their respective ADC channel inputs. The Hycal humidity sensor is a self contained, linear integrated circuit device whose output is fed directly to its corresponding ADC channel. It is also powered from the 5.000 volts reference supply.

The remaining circuitry in the sensor suite module is dedicated to the operation of the hot bead anemometer sensor. The anemometer features a pulsed, duty-cycle operation, which is directly controlled by one of the Pulse Width Modulation (PWM) outputs of the microcontroller. This method permits adjustment of the energy delivered to the anemometer thermistor bead during the heating cycle. It also provides the capability of simultaneously reading the bead temperature during the heating process so that an accurate set-point temperature above ambient can be obtained without excessive overshoot. During the read sequence and cooling interval, the output of the anemometer's thermistor/linearizing voltage divider is amplified and fed directly to its respective ADC channel.

56
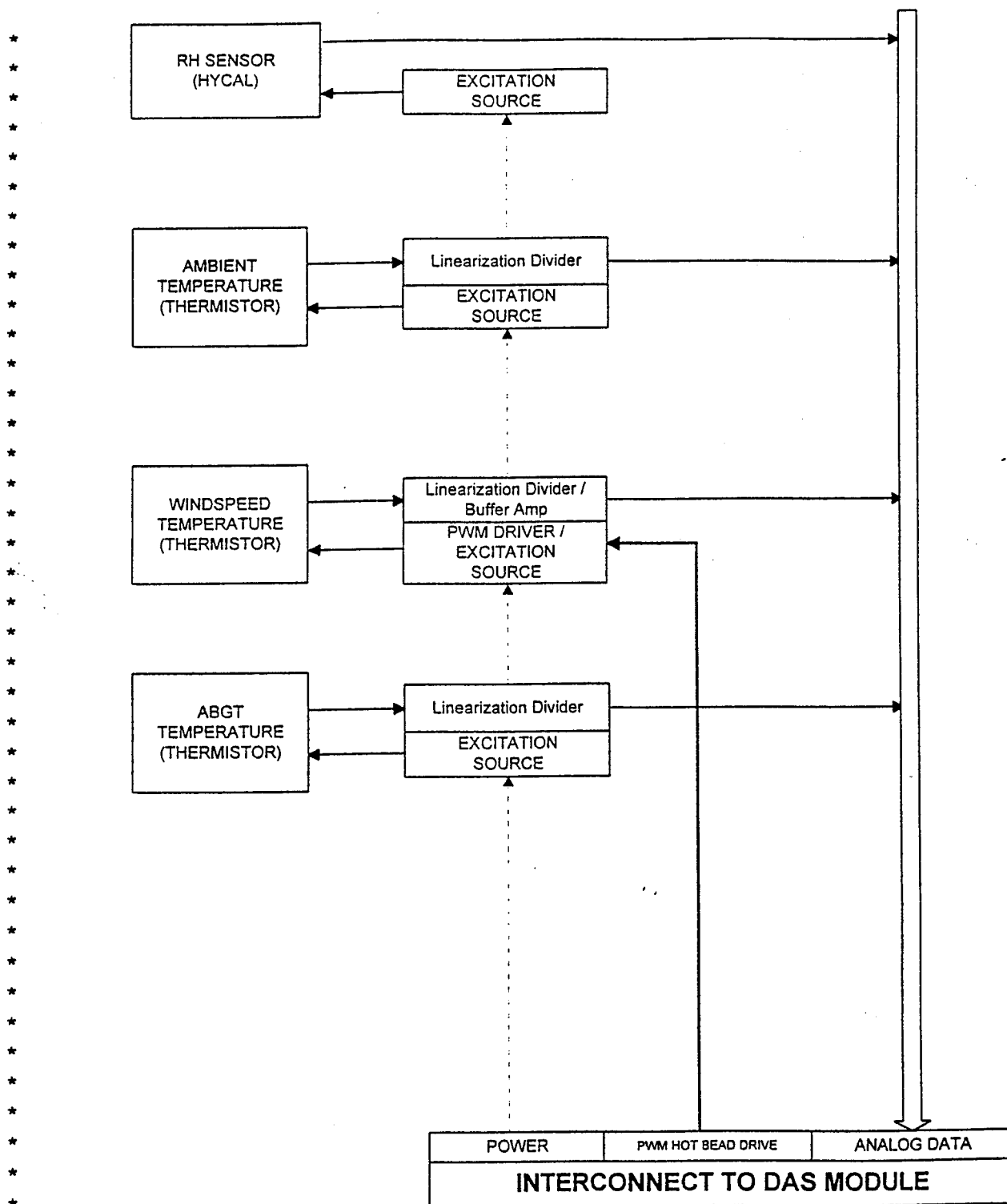
Figure 24. Block Diagram of Sensor Suite Support Module

The voltage output from each sensor is routed to the ADC via an eight-channel internal multiplexer on board the microcontroller unit and then converted using software into corresponding temperature, humidity and wind speed readings.

All functional requirements and sensor module data acquisition needs are incorporated within the DAS support module section of the instrument. These include:

- Conversion of battery source to regulated power supplies;
- Reading user command inputs via multifunction keypad;
- Routing and digital conversion of analog sensor data;
- Data manipulation and temporary storage;
- Display of raw output data via liquid crystal display (LCD) driver module; and

5.3   Validation Testing. Validation testing of the Sensor Suite Support Module was conducted at the wind tunnel facility of Research Triangle Institute, Research Triangle Park, NC. Because of the limitations imposed on Veritay's wind tunnel, tests at RTI focused primarily on wind-speed performance of the integrated Black Globe Thermometer (BGT)/pulsed hot-bead anemometer under various temperature, humidity conditions. Two sensor suite devices were evaluated using the Testoterm 1549 anemometer probe as the wind-speed reference.

5.3.1 RTI Wind Tunnel Facility. Figure 25 illustrates the layout of RTI's large wind tunnel, better described as a "wind room," with a seven-foot-diameter, 40 horsepower (HP) vane-axial fan centrally located within a 28-ft x 50-ft sealed environment. The fan assembly, situated above floor level, is even with a six-foot wide, raised platform runway that serves as the test area. Air output generated from the fan passes through a six-foot-diameter honeycomb air-flow straightener and then is directed down the runway, expanding freely into the room, where it is deflected along the walls and then recirculated back into the fan intake. To facilitate testing, feed-throughs at the base of the raised platform provide access to instrumentation lines between the test area and adjoining control room.

5.3.2 Wind Tunnel Evaluation and Sensor Suite Testing. Validation testing was conducted during two separate sessions at the RTI facility. The first session included an investigation of the capabilities and performance of the wind tunnel environment. It also included preliminary sensor suite and breadboard validation testing. Validation of the actual prototype sensor suite module was conducted during the second session. Because the large wind tunnel facility is designed for relatively heavy equipment and human subject testing, certain characteristics pertaining to air-flow generation, influences of conditioning equipment and room geometry were of utmost concern for the proper evaluation of the EHM sensor suite instrumentation. These included:

58
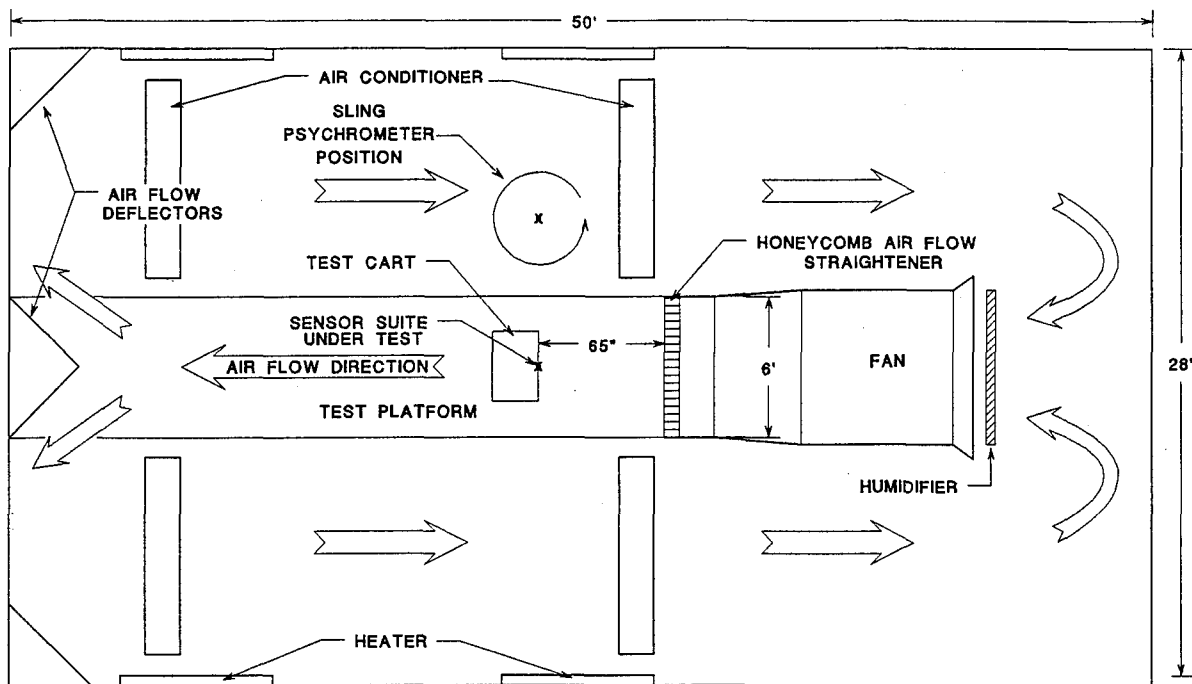
TOP VIEW
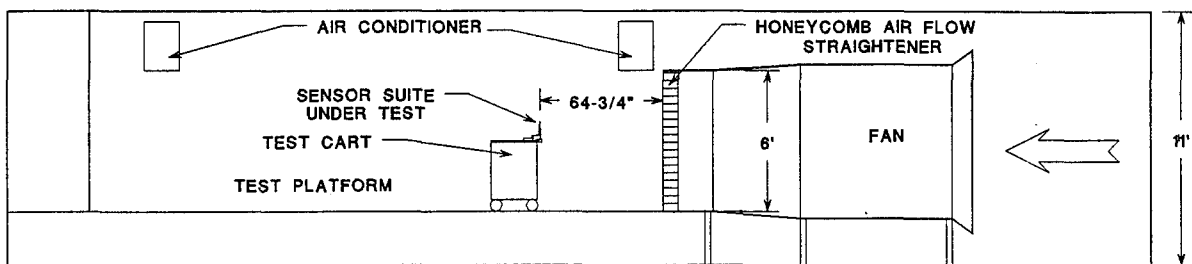
SIDE VIEW

Figure 25. Wind Tunnel Test Facility at Research Triangle Institute

59

- Determination of the minimum attainable wind speed;
- Determination of the wind profile for the designated test region;
- Effects of cooling, heating and humidity equipment on the air-flow pattern around the test region; and
- The limits of and ability to maintain humidity and temperature conditions.

To ascertain the various parameters associated with the wind tunnel, the Testoterm reference instrument standard was used to examine these critical areas.

The wind-speed profile was assessed at controlled temperature of approximately 22°C. A ¾-inch-diameter rod was used to support the Testoterm 1549 hot-bead anemometer reference probe and was situated perpendicular and horizontal to the fan's axis, approximately 65 inches down wind from the honeycomb flow straightener (refer to Figure 26). The bead of the anemometer probe sat approximately ten (10) inches above the rod. An adjustable clamp was used to position the reference probe along the rod, parallel to the honeycomb straightener. Significant wind turbulence was observed, especially at lower wind velocities. This was primarily caused by nearby air-conditioning circulating fans, which were being used to maintain temperature and humidity conditions. As a result, the wind speed averaging capability of the Testoterm instrument was required to obtain a steady wind speed measurement during the initial tunnel assessment, and subsequent validation tests. Using a twenty-second velocity average measurement provided by the Testoterm reference, wind speed was recorded in one-inch increments over a three-inch span on either side of the anemometer under test. Results from this test showed that there was approximately ±0.25 m/s maximum variability over the six-inch span. This did not appear to present a major problem since it was well within the proposed ±0.5 m/s wind speed specification. Temperature variability in the wind tunnel was minimal and was attributed to the room's large air mass. It varied typically a few tenths of a degree over the duration of the test. Humidity control was the most difficult environmental factor to simulate, primarily because of the extremely humid climate of RTI's locale. As a result, humidity testing was focused on the mid to upper values of relative humidity. Table 2 summarizes the maximum and minimum wind speeds, humidities and temperature ranges achieved at the RTI wind tunnel facility.

64-3/4"

10"

AIR FLOW

SENSOR SUITE
SUPPORT MODULE
UNDER TEST

RIBBON CABLE

DATA ACQUISITION
INTERFACE

SUPPORT ROD

SUPPORT CLAMP

FAN CENTER
OF ROTATION

HONEYCOMB
AIR FLOW
STRAIGHTENER
(FAN OUTPUT)

TEST CART
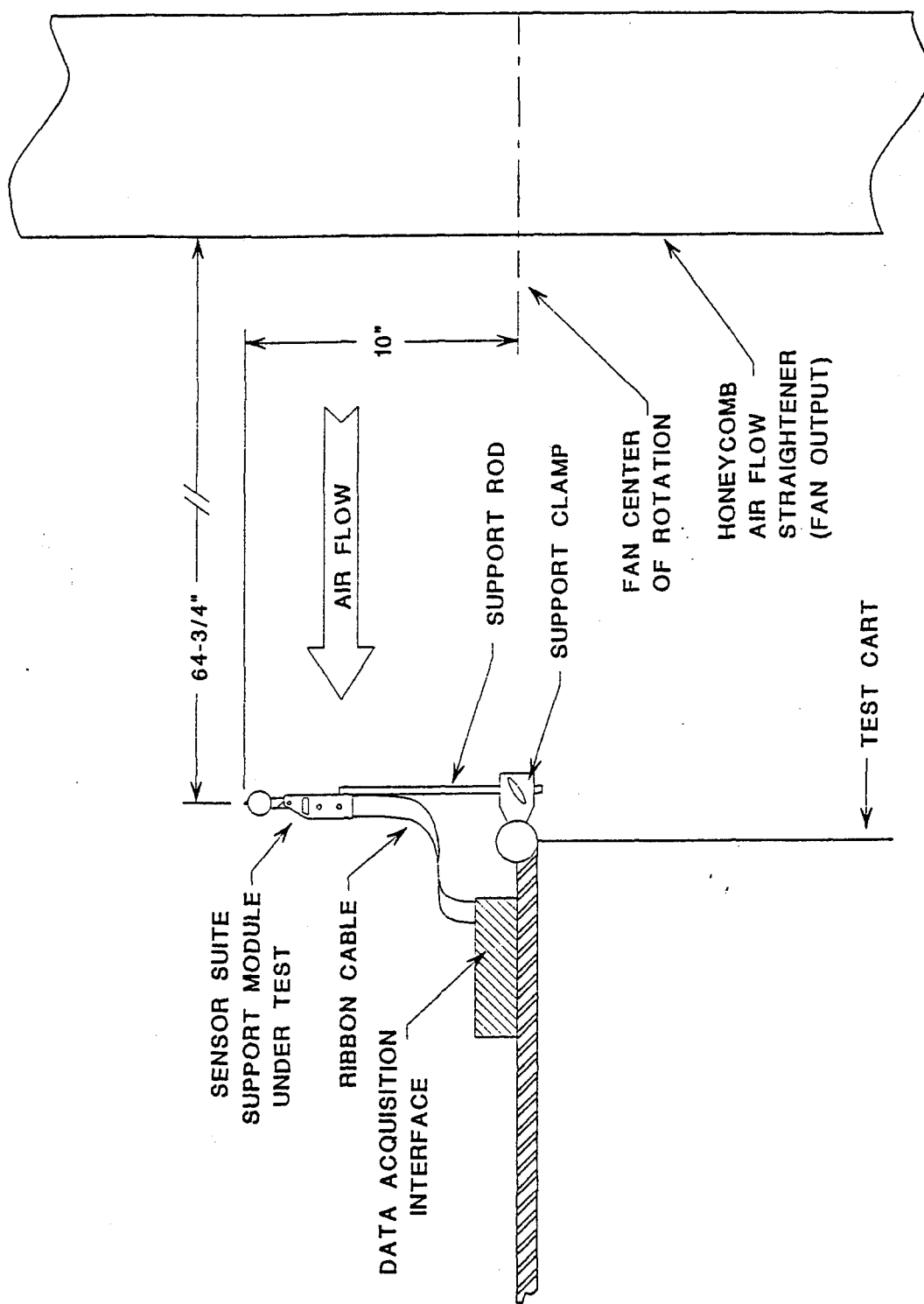
Figure 26. Side View Detail of Sensor Suite Support Module Test Arrangement at RTI

61

Wind Speed

Range	Velocity(m/s)
Low	1
High	10

Humidity and Temperature

Humidity ▸ Temperature▾	High	Low
High	84% RH @ 45°C	39% RH @ 39 °C
Low	66% RH @ 5°C	55% RH @ 4 °C

Table 2. Wind Speeds, Humidities, and Temperatures Achieved at RTI

Validation testing of the EHM sensor suite circuitry was performed initially in breadboard form using the ⅞-inch-diameter, integrated black globe/anemometer (IBGA) test probe sensor assembly, Wand 5. A test matrix was developed focusing on the half-life cooling rate of the IBGA sensor bead for a variety of wind speeds and temperature and humidity extremes. The test matrix was divided into individual tests sets that were representative of the wind tunnel's humidity and temperature at various environmental conditions. Each of these sets was subdivided into four (4) nominal wind velocities ranging from one meter per second to seven meters per second. Table 3 summarizes the average temperature and humidity conditions of the wind tunnel environment for each test set conducted for the breadboard version of the sensor suite module using the Wand 5 IBGA test probe.

Test Set	Average Temperature Testoterm 1549 (°C)	Average Humidity Sling Psychrometer (%RH)
1	4.3	58
2	11.7	88
3	36.9	47
4	41.7	84
5	23.6	70

Table 3. Average Temperatures and Humidities for Test Sets of Breadboard Units at RTI

In all tests conducted during this session, the Wand 5 IBGA assembly, acting as the device under test (DUT), was situated on the ¾-inch diameter support rod approximately 2.5 inches from the Testoterm reference probe. Both probes were oriented in front of the honeycomb air-flow straightener such that the fan axis was centered between them as shown in Figure 27. A test cart located just behind the two test probes was used to support the DAS test-fixture breadboard, separate control interface hardware and Testoterm reference instrumentation. A computer located within the wind tunnel's control room facility was employed as a means of modifying program parameters of the DAS test fixture and monitoring the performance of the pulsed anemometer DUT via the breadboard controller. Temperature was recorded using the Testoterm reference before and after each wind-speed setting. Sensor suite temperature and humidity parameters were also obtained, along with sling psychrometer measurements, prior to each test run. The half-life cooling interval for the pulsed-cycled, hot-bead anemometer was acquired on the basis of a twenty-cycle sample average. Each sample (or cycle) was initiated from inside the control room at approximately 25-second intervals. This permitted a quick review of the temperature and humidity conditions of the environment before the start of the next cycle. During this period, lasting approximately twelve (12) minutes, the actual average wind speed was obtained using the Testoterm reference probe. This average included both air flow from the tunnel and turbulence from nearby conditioning fans. Since both the DUT and Testoterm were in close proximity, this average reflected the effective wind speed as experienced by the hot bead.

Testing of the actual prototype sensor suite support module (Sensor Suite No.2) was conducted in a similar manner. Additional test points were taken at a nominal two (2) m/s and ten (10) m/s for some of the test sets to better assess the relationship between wind speed and half-life cooling times. The test orientation of the unit in relationship to the Testoterm reference is shown in Figure 27. Although the environmental test conditions observed in the earlier breadboard testing of Wand 5, were not exactly duplicated in this validation session, the test matrix focused on creating the greatest temperature and humidity extremes afforded by the wind tunnel facility. Furthermore, operation of the sensor suite module at each wind speed setting was conducted in half the time span [approximately six (6) minutes]. This was done to minimize the effects of temperature and humidity drift on wind speed measurement, if any, and, to more closely simulate the intended field operation of the EHM, which employs a nine-cycle, three-minute average. Table 4 summarizes the average temperature and humidity conditions of the wind tunnel environment for each test set conducted for the prototype sensor suite module.

63
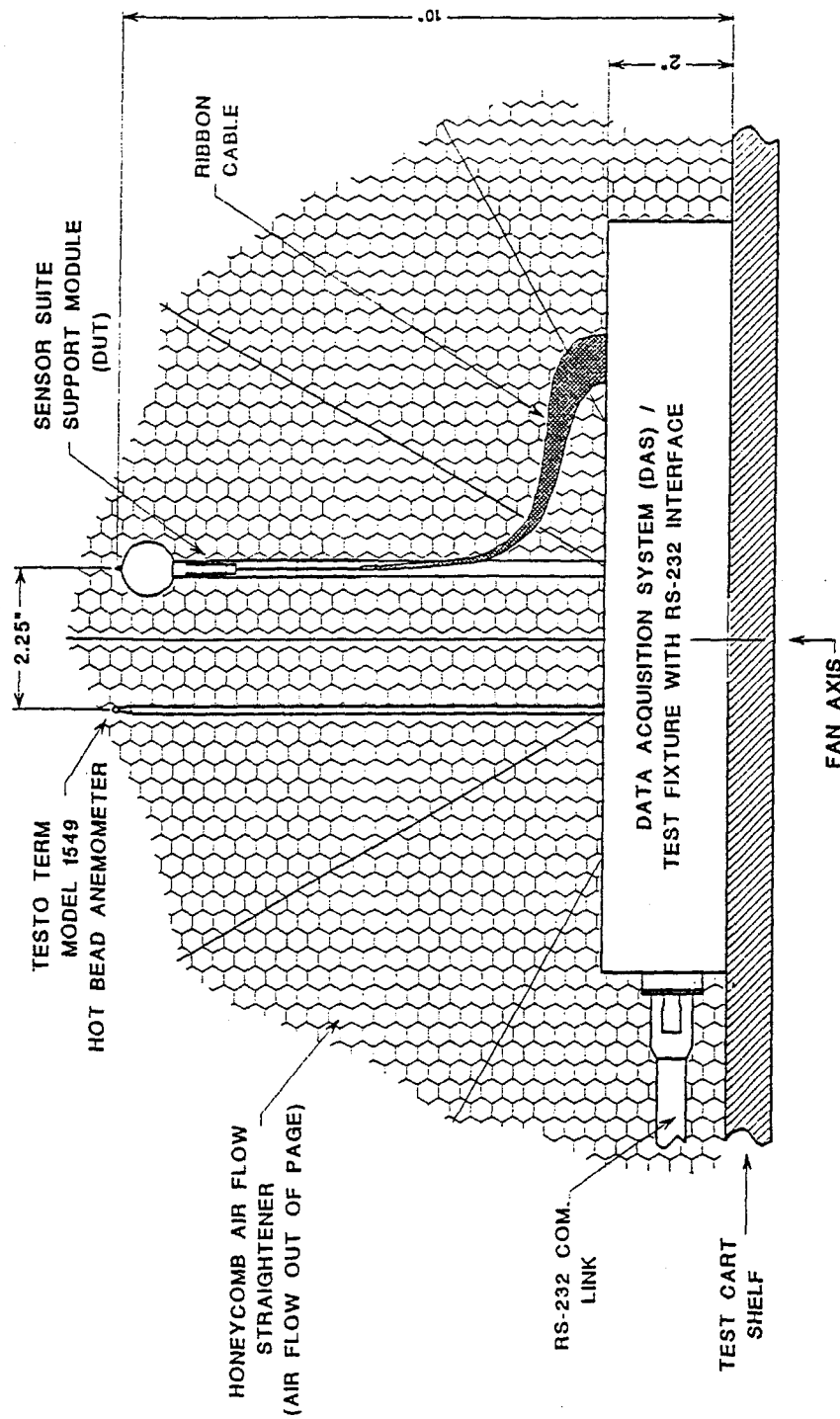
Figure 27. Orientation of Sensor Suite Support Module Assembly and Testo Term Reference Probe

The following labels appear in the figure:

- .01"
- .2"
- RIBBON CABLE
- SENSOR SUITE SUPPORT MODULE (DUT)
- TESTO TERM MODEL 1549 HOT BEAD ANEMOMETER
- 2.25"
- DATA ACQUISITION SYSTEM (DAS) / TEST FIXTURE WITH RS-232 INTERFACE
- FAN AXIS
- HONEYCOMB AIR FLOW STRAIGHTENER (AIR FLOW OUT OF PAGE)
- RS-232 COM. LINK
- TEST CART SHELF
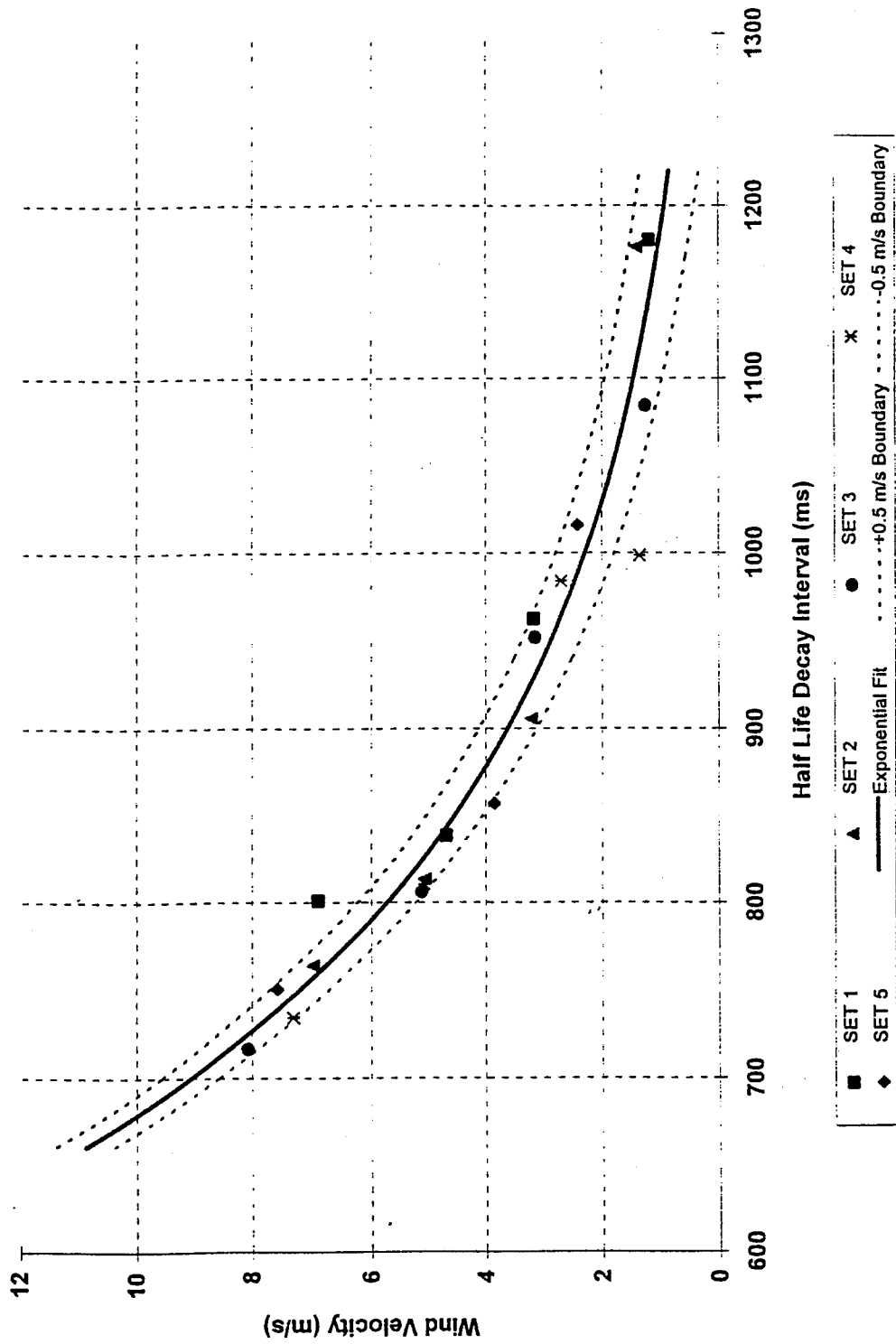
Figure 28. Wind Speed Test Results for the Breadboard Sensor Suite Module Using WAND 5

Test Set	Average Temperature Testoterm 1549 (°C)	Average Humidity Sling Psychrometer (%RH)
1	25.9	58
2	6.6	64
3	38.3	42
4	45.1	83

Table 4.   Average Temperature and Humidities for Test Sets of Prototype Sensor Suite Module at RTI

5.3.3 Test Results. Test data were analyzed according to environmental conditions by comparing the average half-life cooling interval and the average wind-speed velocity recorded at each wind-speed setting for each of the two sensor suite configurations tested. Figure 28 illustrates the relationships among the data acquired for the integrated BGT/hot-bead anemometer; data are presented in terms of wind speed as a function of cooling rate. As observed, the data appear to correlate well with wind speed. Further, the performance of the anemometer did not appear to be directly affected by temperature or humidity changes. The shape of the half-life decoy curve suggests an exponential function of the form:

$$V(t_{1/2}) = A \cdot e^{\frac{t_{1/2}}{B}}, \tag{7}$$

where A and B are empirical constants obtained using curve-fitting algorithms. The dashed lines indicate the upper and lower 0.5 m/s boundaries for this particular fit, which are representative of the proposed wind-speed measurement specification. A similar curve, Figure 29, was obtained for actual prototype sensor suite module. The resulting exponential fit closely resembles the half-life cooling interval performance for the Wand 5 IBGA test probe. Measured velocities for both of the sensor suite module assemblies are tabulated in Appendix E as a function of the various environmental test conditions.

The computed ambient temperature measurement for both the breadboard module and the prototype module fell within the required $\pm$ 0.5°C limits as compared to the Testoterm temperature reference. These results are shown in Figures 30 and 31, respectively, and are also found in Appendix E.

66
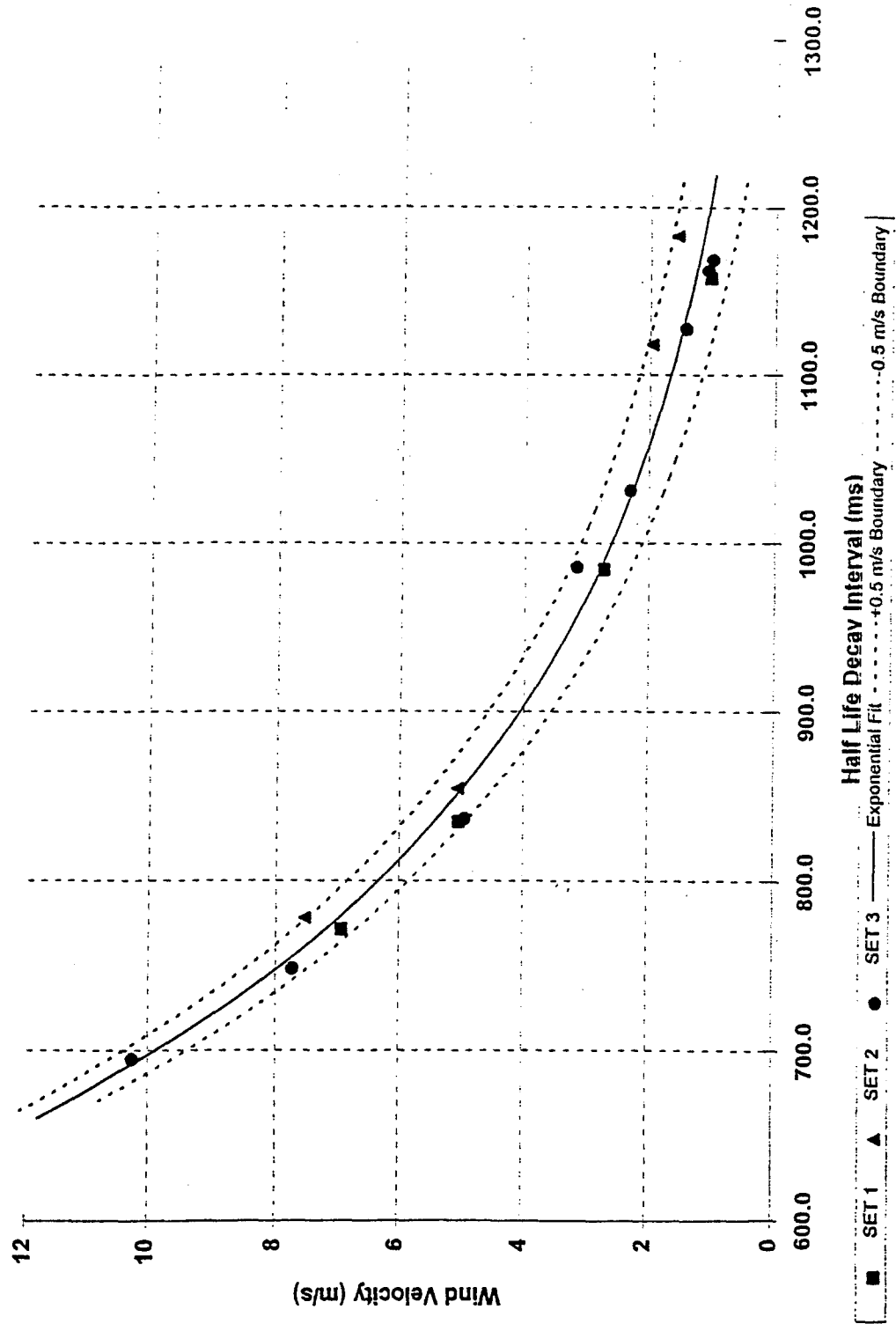
Figure 29. Wind Speed Test Results for the Prototype Sensor Suite Unit No. 2
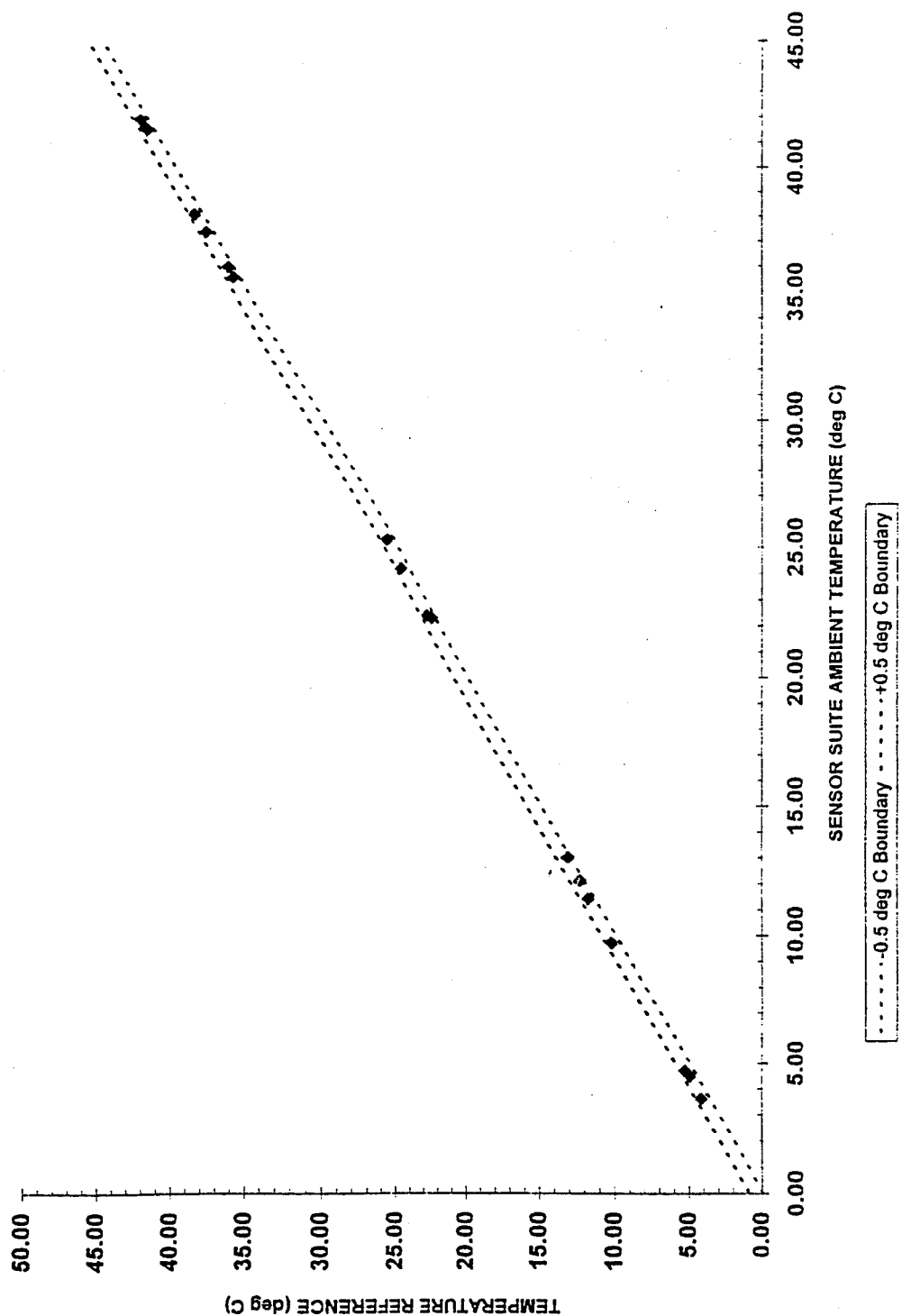
Figure 30. Ambient Temperature Test Results for the Breadboard Sensor Suite Module
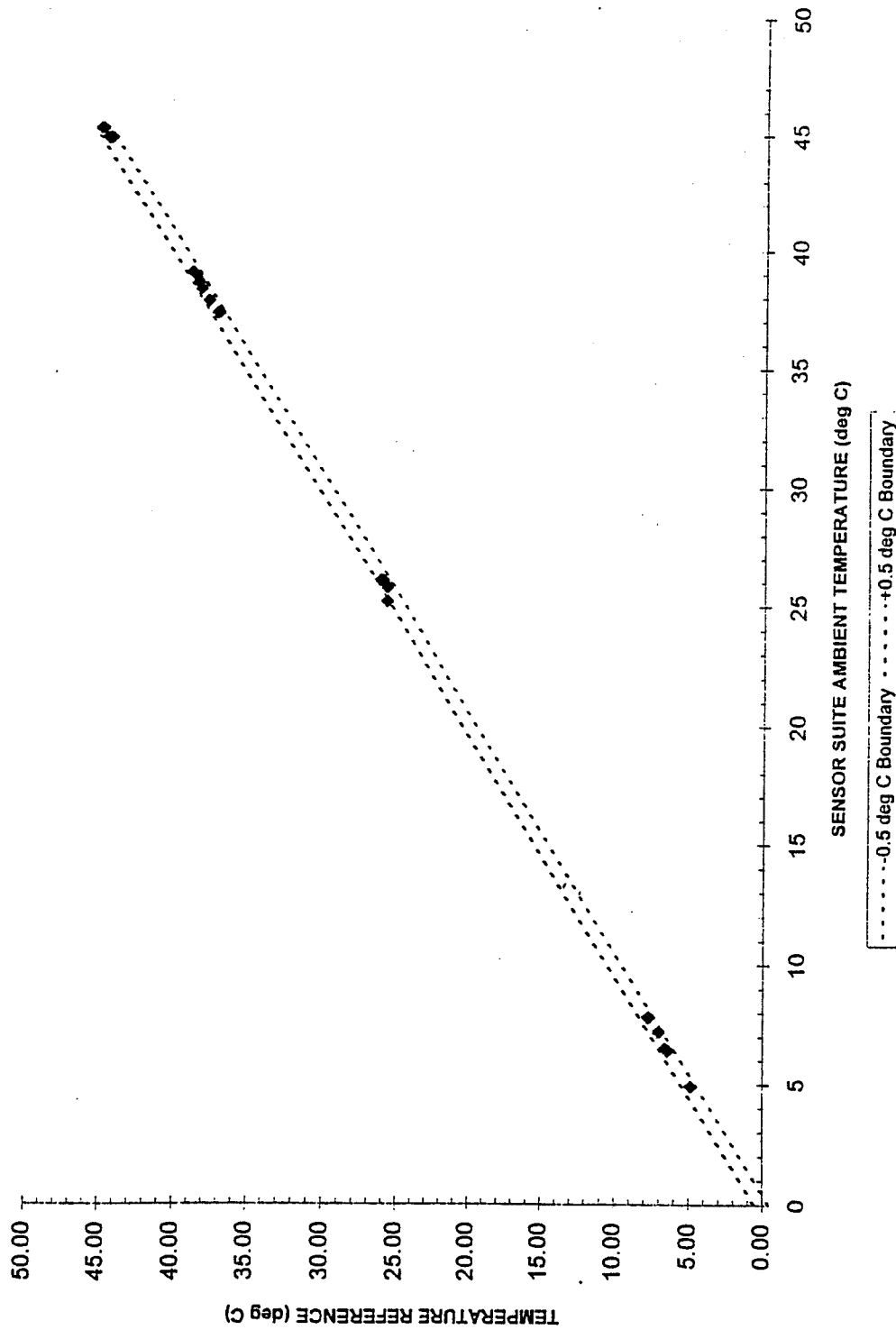
Figure 31. Ambient Temperature Test Results for the Prototype Sensor Suite Module-Unit No. 2

Prior to the scheduled validation testing, the Testoterm humidity probe reference had malfunctioned and could not readily be repaired. Therefore, the humidity performance for both the breadboard version and prototype version sensor suite modules was based on earlier calibration using the HyCal IH-3602-A integrated circuit humidity sensor, HyCal 1, and the Testoterm relative humidity reference at Veritay (refer to Figure 10). Both wet and dry bulb readings were taken using a sling psychrometer prior to each wind speed test; however, these measurements were used to approximate the humidity conditions of the wind tunnel facility (Figure 25). Since the psychrometer measurement was performed below the test platform level to avoid the direct air flow of the fan, the humidity measurements obtained are not necessarily representative of the humidity conditions at the site of the Sensor Suite Device Under Test (DUT). In fact, the humidity as determined by the wet and dry bulb readings was often much higher than the value recorded by the humidity sensor on the Sensor Suite (refer to Figure Eb, Appendix E). Although a slight change in humidity would be expected according to the temperature differential between the two locations, it does not account for the significant variations observed. It is more likely that the moisture content of the air within the facility is nonuniform, rather than a discrepancy in the calibration of the instrumentation.

6. CONCLUSIONS AND RECOMMENDATIONS

Conclusions. In accordance with contract requirements, this effort culminated in the delivery of one prototype advanced temperature sensor suite suitable for the acquisition of four key meteorological parameters: ambient temperature, radiant energy, relative humidity, and wind speed. These data are acquired, stored, and processed in a manner suitable for use with heat stress decision aids; the unit may also be used for conveniently monitoring local weather conditions and can be upgraded to provide WBGT index data. The prototype sensor suite currently does not have this WBGT feature implemented.

The sensor suite as currently configured provides single-point measurements of air temperature and relative humidity (RH) as called for in discrete menu steps for data displayed by the device. Approximately two (2) minutes are required to obtain a black globe temperature reading and another two minutes to obtain a wind speed reading. Both utilize short term averaging of discete data points in order to smooth the effects of wind fluctuations on individual readings. In effect, therefore, real-time values currently displayed by the sensor suite are single points measured (with some averaging) over about a four minute period.

By reprogramming the sensor suite controller, different time sequencing of the measurements could be readily achieved.

The prototype sensor suite was developed using off-the-shelf, pre-calibrated, sensors and sensor components to achieve logistics, dual-use, and cost objectives. It achieves target size and weight objectives; the prototype is approximately the size of a cigarette pack and weighs 151 grams with a standard 9-volt battery.

Sensors and sensor components were successfully integrated into "plug-in" modules to maximize available space, to prevent interference among sensor functions, and to achieve easy "upgradeability." Validation testing demonstrated that there was no interference either among sensors or between sensors and case.

Several configurational and operational decisions were made to permit easy upgrade, repair, and low-cost maintenance. Design modularity permits the replacement of components in the field, if necessary. Sensor module electronic design allows for one-to-one replacement; there will be no need for re-calibration at either the user or depot level.

Power requirements were minimized by incorporating a novel anemometer into the sensor suite. The radiant energy measurement is performed using a miniature black globe. The readings from this miniature black globe have been successfully calibrated to the readings from a standard 6-inch black globe.

71

The relative humidity and ambient temperature readings are achieved using small sensors available commercially. These off-the-shelf sensors are precalibrated.

Sensor readings were successfully validated during testing both at Veritay and at Research Triangle Institute, Research Triangle Park, NC.

Recommendations. The following actions are recommended on the basis of findings during this Phase II SBIR program:

- Conduct heat stress/heat-strain field tests using the prototype advanced temperature sensor suite to determine its field usability with various heat-stress algorithms and decision aids and to identify potential Phase III upgrades desired in production units.

- Conduct Phase III development to implement the RS-232 compatible communications link between EHM instrument and PC systems. This development would involve:

    - Upgrading the EHM software to utilize existing serial I/O circuitry onboard the DAS support unit.

    - Installing an infrared view-port window on the back side of the EHM enclosure to facilitate optical transmission between EHM instrument and the following base unit.

    - Fabricating an external infrared transceiver base unit that interfaces with the EHM instrument to convert optical data to standard RS-232 RxD and TxD serial I/O.

- Perform a Phase III code optimization on all software modules to improve overall computation speed.

- Consider Phase III development of a practical and inexpensive exclosure for the sensor-suite unit to achieve greater ruggedization.

- Consider Phase III development and test of power management software in conjunction with a real-time clock to increase battery longevity.

- Consider potential Phase III modification of the sensor modules necessary to adapt usage for cold-weather trauma and other potential applications.

- Evaluate efficacy and viability of implementing minor changes to the user interface to enhance ergonomic performance in subsequent models.

- Consider integration of a heat-strain predictive model for dual-use applications in the commercial sector.

72

REFERENCES AND SELECTED BIBLIOGRAPHY

Bristow, K.L., Campbell, G.S., "On the Relationship Between Incoming Solar Radiation and Daily Maximum and Minimum Temperature," Agricult. Meteorol., 1985, 31, 159-166.

Burno, R., "A Correction Procedure for Separating Direct and Diffuse Insolation on a Horizontal Surface," Solar Energy, 1978, 20, 97-100.

Campbell, G.S., An Introduction to Environmental Biophysics, New York: Springer-Verlag. 1977.

Chambers, A.B., "A Psychometric Chart for Physiological Research," J. Appl. Physiol., 1970, 29, 406-412.

Duffie, J.A., and Beckman, W.A., Solar Energy Thermal Processes, New York: John Wiley Sons, 1974.

Fritschen, L.J., "Miniature Net Radiometer Improvements," J. Appl. Meteorol., 1965, 4, 528-532.

Gagge, A.P., Nishi, Y., "Physical Indices of the Thermal Environment," ASHRAE Journal, January 1976, 47-51.

Goldman, R.F., Green, E.B., Iampietro, P.F., "Tolerance of Hot, Wet Environments by Resting Men," J. Appl. Physiol., 1965, 20, 271-277.

Goldman, R.F., "Standards for Human Exposure to Heat," in Environmental Ergonomics, Sustaining Human Performance in Harsh Environments, (Edited by Igor B. Mekjavic, Eric W. Banister, and James B. Morrison), Philadelphia: Taylor & Francis, 1988, 99-104.

Gonzalez, R.R., Sexton, G.N., and Pandolf, K.B., "Biophysical Evaluation of the Wet Globe Temperature Index (Botsball) at High Air Movements and Constant Dew Point Temperature," Commonwealth Defence Conference on Operational Clothing and Combat Equipment, Australia, 1985.

Gonzalez, R.R. , Santee, W.R., and Endrusick, T.L., 1992. "Physiological and biophysical properties of a semipermeable hood attached to a chemical protective garment," in The Performance fo Protective Clothing: Fourth Volume, ASTM STP 1133 J.P. McBriarty and N.W. Henry (Eds.) American Society for Testing and Materials, Philadelphia, PA, pp. 557-582.

Graichen, H., Rascati, R., Gonzalez, R.R., "Automatic Dew-Point Temperature Sensor," J. Appl. Physiol., 1982, 52, 1658-1660.

Greenspan, L., "A Pneumatic Bridge Hygrometer for Use As a Working Humidity Standard," in Humidity and Moisture: Measurement and Control in Science and Industry. Fundamentals and Standards, (Edited by A. Wexler and W.A. Wildhack) New York: Reinhold, 1965, 433-443.

Haines, R.W.,"How to Construct High Altitude Psychrometric Charts," Heating, Piping, and Air-Conditioning, October 1961, 114-116.

Herrington, J.B., "Solar Radiation in a Clear-Cut Strip: A Computer Algorithm," Agricult. Meteorol., 1984, 33, 23-39.

Harrison, L.P., "Some Fundamental Considerations Regarding Psychrometry," in Humidity and Moisture: Measurement and Control in Science and Industry. Fundamentals and Standards, (Edited by A. Wexler and W.A. Wildhack),New York: Reinhold, 1965, 71-103.

Harrison, L.P., "Fundamental Concepts and Definitions Relating to Humidity," in Humidity and Moisture: Measurement and Control in Science and Industry. Fundamentals and Standards, (Edited by A. Wexler and W.A. Wildhack), New York: Reinhold, 3-69.

Ideriah, F.J.K., "A Model for Calculating Direct and Diffuse Solar Radiation," Solar Energy, 1981, 26, 447-452.

Idso, S.B., "Transformation of a Net Radiometer into a Hemispherical Radiometer," Agricult. Meteorol., 1971, 9, 109-121.

Idso, S.B., "Simplifications in the Transformation of Net Radiometers into Hemispheric Radiometers", Agricult. Meteorol., 1972, 10, 473-476.

Irgum, K., "Instrument for Relative Humidity Measurement," Anal. Chem., 1983, 55, 1186-1187.

Incropera, F., DeWitt, D.P., <u>Fundamentals of Heat and Mass Transfer</u>, New York: John Wiley and Sons, 1985.

ISO, "Thermal Environments---Instruments and Methods for Measuring Physical Quantities," International Standard ISO 7726, 1985, Inter. Org. for Standardization, Switzerland.

Kilbourne, E.M., "Background Information on Heat-related Health Effects and Recommendations for the Prevention of Injury Control," Centers for Disease Control, 1988.

Kleinhanz, C., Pickarski, C., Haug, E., "Recording and Processing of Various Climate Parameters," <u>Biomed. Technik.</u>, 1980, <u>25</u>, 12-26, (in German).

Kraning, K.K. II, "A Computer Simulation for Predicting the Time Course of Thermal and Cardiovascular Responses to Various Combinations of Heat Stress, Clothing and Exercise," U.S. Army Research Institute of Environmental Medicine, Natick, MA 01760-5007, Technical Report No. T13-91, June 1991.

Krueger, G.P., Cardinal, D.T., and Stephens, M.E., "Publications and Technical Reports of the United States Army Research Institute of Environmental Medicine (US ARIEM), 1961-1992," 30 September 1992.

Kusuda, T. "Algorithms for Psychometric Calculations," National Bureau of Standards, No. 9818, 1969, 1-22.

Leone, O.J., "Improvements in Dew-Point Measurements of Gases by Use of Peltier Devices," in <u>Humidity and Moisture: Measurement and Control in Science and Industry. Principles and Methods of Measuring Humidity in Gases</u>, (Edited by R.E. Ruskins), New York: Reinhold, 1965, 635-642.

Martens, Alexander E., "Solar Radiation Detectors and Anemometer Technologies, Review of Data Base References," June 1995.

Matthew, W.T., and Santee, W.R., "Weather Effects on the Soldier System: Heat Stress," Paper presented at Third Workshop on Battlefield Intelligence in Air/Land Operations, May 27-29, 1992, Los Cruces, New Mexico. In press.

McNally, Richard E., Stark, Maureen M., and Ellzy, Diane T., "Verification and Usage of the Goldman-Givoni Model: Predicting Core Temperature and Casualty Generation in Thermally Stressful Environments," SAIC Report prepared for Contract No. MDA903-88-D-1000, April 1990.

Military Specification, "Monitor, Heat Stress," MIL-M-24605A (SH), 21 June 1988.

Milne-Thomson, L.M., Theoretical Hydrodynamics, Third Edition, New York: MacMillan, 1955, 443.

Minard, D.H., Belding, H.S., Kingston, J.R., "Prevention of Heat Casualties," J. Am. Med. Assoc., 1957, 165, 1813-1818.

Mitchell, J.W., "Heat Transfer from Spheres and Other Animal Forms," Biophy J., 1976, 6, 561-569.

Onkaram, B., Stroschein, L.A., Goldman, R.F., "Three Instruments for Assessment of WBGT and a Comparison with WGT (Botsball)," Amer. Indust. Hyg. Assn. J., 1980, 41, 634-641.

Onkaram, B., Stroschein, L.A., and Goldman, R.F., "A Comparison of Four Instruments for Measuring WBGT Index Correlations of Botsball with WBGT," Technical Report T4/78, United States Army Research Institute of Environmental Medicine (US ARIEM), September 1978.

Pandolf, K.B., et al., "Prediction Modeling of Physiological Responses and Human Performance in the Heat," Comput. Bio. Med., 1986, 15, No. 5, 319-329.

Peters, Wendell R., Darilek, Glenn T., and Herzig, Francis X., "Survey of Environmental Parameter Sensors for a Personal Heat Stress Monitor," Southwest Research Institute Report prepared for U.S. Department of Health, Education and Welfare, Public Health Service, Center for Disease Control, National Institute for Occupational Safety and Health Division of Physical Sciences and Engineering, March 1976.

Powers, M.H. and Hull, S.E., "Gas Monitoring Transducers: Relative Humidity Sensors," J. of Computers in Mathematics and Science Teaching, 1988, 7, 66-69.

Roller, W.L., and Goldman, R.F., "Estimation of Solar Radiation Environment," Int. J. Biometerol., 1976, 11, 329-336.

Santee, W.R. and Gonzalez, R.R., "Characteristics of the thermal environment," Human Performance Physiology and Environmental Medicine at Terrestrial Extremes, (Edited by K.B. Pandolf, M.N. Sawka and R.R. Gonzalez), Indianapolis Benchmark Press, 1988, 1-43.

Santee, W.R., Matthew, W.T., and Tharion, W.J., "Simulated Approach Marches During Thermal Stress: a P^2NBC^2 Study," US Army Research Institute of Environmental Medicine (US ARIEM), Natick, MA 01750-5007, Technical Report No. T12-92, September 1992.

Scott, D., Dave Scott's Triathalon Training, New York: Simon & Schuster, 1986.

Stribley, R.F. and Nunneley, S.A., "Fighter Index of Thermal Stress: Development of Interim Guidance for Hot-Weather USAF Operations," Technical Report SAM-TR-78-6, USAF School of Aerospace Medicine, Brooks AF Base, February 1978.

United States Environmental Protection Agency (EPA)/Occupational Safety and Health Administration (OSHA), "A Guide to Heat Stress in Agriculture," EPA-750-b-92-001, May 1993.

Vernon, H. M., "The Measurement of Radiant Heat in Relation to Human Comfort," J. Ind. Hyg., 1932, 14, 95-111.

Weiss, A., Norman, J.M., "Partitioning Solar Radiation into Direct and Diffuse, and Visible and Near-infra-red Components," Agricult. Meteorol., 1985, 34, 205-213.

Wenzel, H.G., Forsthoff, A., "Modification of Vernon's Globe Thermometer and its Calibration in Terms of Physiological Strain," Scand. J. Work Environ. Health, 1989, 15 47-51.

Wexler, A., and Hyland, R., "The NBS Standard Hygrometer," in Humidity and Moisture: Measurement and Control in Science and Industry. Fundamentals and Standards, (Edited by A. Wexler and W.A. Wildhack),New York: Reinhold, 1965, 389-432.

Winslow, C. A., Herington, L.P., Gagge, A.P., "A New Method of Partitional Calorimetry," Am. J. Physiol., 1936, 116, 641-655.

Wood, L.A., "The Use of Dew-Point Temperature in Humidity Calculations," J. Res. Nat. Bureau Standards, 1970, 74, 117-122.

Woodcock, A.H., Pratt, R.L., Breckenridge, J.R., "Theory of the Globe Thermometer," Res. Study Rpt. BP-7, Quartermaster R & E Command, US Army Natick Labs., Natick, MA, 1960.

Wylie, R.G.,"The Properties of Water-Salt Systems in Relation to Humidity," in Humidity and Moisture: Measurement and Control in Science and Industry. Fundamentals and Standards, (Edited by A. Wexler and W.A. Wildhack),New York: Reinhold, 1965, 507-517.

APPENDIX A

A.1 Background

Defense downsizing, troop-strength reductions, the reformulation of fighting doctrines in response to the end of the Cold War, and a growing emphasis in the Pentagon on dual use and operations other than war[5] have all underscored the need for smaller, better trained, and more mobile fighting units capable of achieving mission objectives rapidly, reliably, and cost effectively. The reality of the chemical/biological threat simultaneously dictates a need for a high level of individual protection equipment, which can bring with it problems associated with equipment interference and individual performance degradation.

Heat stress is a significant contributor to both non-battle injuries and performance degradation, particularly in hostile environments requiring protective attire. The U.S. Army recently addressed a variety of issues associated with heat injury under the U.S. Army Chemical School's P^2NBC^2 program. P^2NBC^2 is an acronym for the Physiological and Psychological Effects of the NBC Environment and Sustained Operations on Systems in Combat. Of particular interest continues to be the impact of heat stress on the performance of soldiers attired in MOPP (Mission Oriented Protective Posture) chemical protection.

Work conducted under the P^2NBC^2 program has indicated general agreement between observed physiological response to heat stress and results predicted from the P^2NBC^2 Heat-Strain Decision Aid (HSDA). This decision aid has its foundation in the databases, predictive algorithms, and heat-strain prediction modeling efforts performed by the U.S. Army Research Institute of Environmental Medicine (USARIEM) over the past two decades.[6] Recent field studies and model validation efforts indicate that model performance generally improves with the quality of meteorological inputs.

---

[5] "HASC [House Armed Services Committee] Members Encourage Dual Use for Law Enforcement as Authorization Bill Goes to Conference," Technology Transfer Week, July 26, 1994, Vol. 1, No. 25. p. 1-2.

[6] W.R. Santee, W.T. Matthew, and W.J. Tharion, "Simulated Approach Marches During Thermal Stress: a P^2NBC^2 Study," US Army Research Institute of Environmental Medicine, Natick, MA 01750-5007, Technical Report No. T12-92, September 1992.

The adverse impact of heat stress on human performance has long been recognized. Since the early part of the 20th century, researchers have approached the difficulty of dealing with the multiplicity of variables that contribute significantly to the heat-stress problem from a variety of perspectives :

- Absolute physical standards
- Instrumentation standards
- Statistical sampling techniques
- Consensus derived from experimental data or field experience
- Consensus based only on expert opinion

A.2 Heat Strain

Goldman provides a chronological list of indices striving to achieve a number expression integrating the various factors contributing to heat stress that dates to 1905.[7]

HEAT IMPAIRS MARKSMANSHIP

"The solider who is required to fire a rifle under a chemical threat in a sustained operation has a number of stressors which are likely to affect his success. The effects of heat, clothing, and exercise state can have profound effects on marksmanship performance. Heat impairs marksmanship accuracy due to degradation of muscular control (Johnson and Kobrick, 1988). Furthermore, it has been shown that soldiers exercising in the heat that lost the greatest amount of body weight or who did not rehydrate fully, had the most severe decrements to rifle marksmanship accuracy (Tharion, et al., 1989).

W.R. Santee, et al.. September 1992.

Each index attempts to provide a decision aid to be used for the purpose of limiting the duration of exposure, reducing the level of work allowed, or requiring that the worker meet certain standards of heat acclimation and/or fitness. Methodologies employed include:

1. Physical indices based on one or more of the physical factors of the environment (humidity, temperature, air motion, and radiant load);
2. Subjective indices based on assessments of thermal sensation;
3. "Rational" indices based on the human heat balance equations; or
4. Physiological indices based on physiological strain (e.g., percent sweated area, predicted rectal temperature, predicted heart rate, etc.).

The first three approaches are based on the capacities or demands for heat transfer of the environment (occasionally adjusted for heat production demanded of the worker but with few adjustments for clothing or work).

---

[7] Ralph F. Goldman, "Standards for Human Exposure to Heat," in *Environmental Ergonomics, Sustaining Human Performance in Harsh Environments*, Edited by Igor B. Mekjavic, Eric W. Banister, and James B. Morrison (Philadelphia: Taylor & Francis, 1988), pages 99-104.

Professional research performed since the early 1970s has introduced the importance of the capacities of the work force (as modified by acclimation, hydration, physical fitness, clothing, etc.). Goldman concluded in the late 80s that

> "...the most promising approach for resolution of heat stress problems is through prediction modeling. Such modeling can build on the concept that heat stress results from an imbalance between the demands imposed on the worker by the task and the environment, and the worker's capacity to eliminate the heat load as modified by clothing."[8]

Building on this approach, researchers at USARIEM have made significant progress toward establishing a data base and developing a series of predictive equations for deep body temperature, heart rate, and sweat loss responses of clothed soldiers performing physical work at various environmental extremes in recent years.[9,10,11,12]

A.3 Sensor Suites

Significantly less work has been devoted, however, to the development of a small, compact, low-cost sensor suite capable of acquiring and reporting meteorological data in real time, and suitable for incorporation into a hand-held environmental monitoring system. An initiative was undertaken by USARIEM to develop individual heat-stress monitors that could be used to provide an immediate, local measurement of environmental conditions for direct input into the heat strain prediction model.

---

[8] Goldman, p.100.

[9] Pandolf, Kent B. et al., "Prediction Modeling of Physiological Responses and Human Performance in the Heat," Comput. Bio. Med., Vol 15 No. 5, pp 319-329, 1986.

[10] Kenneth K. Kraning II, "A Computer Simulation for Predicting the Time Course of Thermal and Cardiovascular Responses to Various Combinations of Heat Stress, Clothing, and Exercise," U.S. Army Research Institute of Environmental Medicine, Natick, MA 01760-5007, Technical Report No. T13-91, June 1991.

[11] William R. Santee and Richard R. Gonzalez, "Characteristics of the Thermal Environment," in Human Performance Physiology and Environmental Medicine at Terrestrial Extremes, edited by Pandolf, Sawka, and Gonzalez (NY: Benchmark Press, 1988), pages 1-43.

[12] Gerald P. Krueger, Donna T. Cardinal, and Marie E. Stephens, "Publications and Technical Reports of the United States Army Research Institute of Environmental Medicine, 1961-1992," 30 September 1992.

The standard sensor suites have used a black globe that is 15 cm in diameter for the measurement of sky radiation (T_g). IST manufactures WBGT monitoring instrumentation that uses a black globe that is 1-5/8 inches in diameter. The measured globe temperature (T_{IST}) is then used to calculate the standard black globe temperature (T_g) according to the following:

$$T_{IST} = \frac{2}{3} T_g + \frac{1}{3} T_a \qquad (2)$$

$T_a =$ Temperature-air
$T_g =$ Temperature - 15-cm BLK globe
$T_{IST} =$ Temperature - IST BLK globe

The IST sensor suite is still relatively large and requires a water reservoir for measuring natural relative humidity. A validation survey conducted by the NASA RTTC in June 1995[13] confirmed that a miniaturized sensor suite is not currently commercially available (Appendix E).

A.4   Heat Stress and the Dynamic Thermal Environment

Heat tolerance problems may arise from a variety of physiological and environmental factors that act independently or interactively to affect the balance of heat production or loss experienced by an individual. The former includes metabolic heat production, heat input from environmental sources, and the rate of physical work; whereas the latter includes the rate of water intake and favorable opportunities for heat exchange with the environment. In particular, protective clothing inhibits both insensible (evaporative) and sensible (convective, conductive, and radiative) heat exchange. When body heat exceeds cooling capability (because of environmental, clothing, task, and/or physical/physiological variables), increased core temperatures can generate performance degradation, unconsciousness, or even death.

In 1988 Goldman identified the following as key factors influencing the heat tolerance of individuals and identified predictive modeling as the methodology having the best potential for resolving the large number of variables involved:

- Environmental parameters (air temperature, humidity, air motion, and radiant temperature);

---

[13] Alexander E. Martens, Executive Director, Upstate New York CTC, National Aeronautics and Space Administration (NASA) Northeast Region Technology Transfer Center (RTTC), "Solar Radioactive Detectors and Anemometer Technologies," June 1995.

- Clothing parameters (insulation, moisture permeability and pumping coefficient);
- Task variables (load weight, placement or lift, and frequency, speed of movement, terrain and grade); and
- Physical and physiological variables of the worker (weight, surface area, age, physical fitness, level of acclimatization, state of hydration).

Significant advances in database generation and predictive algorithm development have occurred in the wake of Goldman's observations. The next level of model refinement may be dependent to a significant extent on achieving an improved understanding the dynamic nature of the thermal environment (i.e., air temperature, humidity, wind speed, and radiant energy) as it impacts human performance. The subject temperature sensor suite was developed to address this need.

APPENDIX B. LITERATURE REVIEW: SENSOR TECHNOLOGY

ADVANTAGES AND DISADVANTAGES OF VARIOUS SENSOR TECHNOLOGIES AS APPLIED TO THE SUBJECT SENSOR SUITE

SENSOR: Wind Speed

TECHNOLOGY	ADVANTAGES	DISADVANTAGES
1. Hot Wire (Constant Temperature) or Hot Film	1.1 Small 1.2 Sensitivity and resolution 1.3 Hot-film on a conical substrate generates an omni-directional sensor.	1.1 Requires a large power drain to maintain the hot wire at an elevated temperature for 3 minutes. 1.2 For increased accuracy and resolution, moisture content (grams of water vapor/cc) is required to perform heat transfer calculations. 1.3 Not omni-directional as hotwire.
2. Hot Wire (Pulsed) or Hot Film	2.1 Small 2.2 Does not require large power drain. The hotwire element is heated with a given amount of energy. A measurement is made of the temperature that the hot wire reaches and the rate that the hotwire elements cools. The combination of these two data points can be used to calculate the wind speed based upon heat transfer calculation.	2.1 Requires S/W development. 2.2 Technique has not been used in the past. It must be proven and validated. 2.3 Sensitivity, resolutions and accuracy are unknown.
3. Impeller	3.1 Small unit 3.2 Requires little power demand.	3.1 Mechanical device may not be good at low wind speed due to friction. 3.2 Not omni-directional. Requires two at right angles and use vectoring to determine wind speed.

B-2

ADVANTAGES AND DISADVANTAGES OF VARIOUS SENSOR TECHNOLOGIES
AS APPLIED TO THE SUBJECT SENSOR SUITE

SENSOR: Wind (Con't)

TECHNOLOGY	ADVANTAGES	DISADVANTAGES
4. Rotating Cup	4.1 Mechanical 4.2 Hardened instrumentation 4.3 Requires minimal power. 4.4 Omni-directional	4.1 Cup arms may be fragile. 4.2 Low speed limitations 4.3 Maintenance to keep the cup/vane mechanism free to rotate.

ADVANTAGES AND DISADVANTAGES OF VARIOUS SENSOR TECHNOLOGIES
AS APPLIED TO THE SUBJECT SENSOR SUITE

SENSOR: Temperature

TECHNOLOGY	ADVANTAGES	DISADVANTAGES
1. Thermocouple/thermopile	1.1 Miniature size 1.2 Does not require power to measure temperature	1.1 A very small electrical signal is generated. The resultant amplification generates a very poor S/N level. This may be overcome by using a multiple of thermocouples in series: called a thermopile. 1.2 Requires a reference temperature junction referred to as the cold junction.
2. Thermistor	2.1 Miniature size 2.2 Good S/N level of output of thermistor 2.3 Can be precalibrated to +/- 0.1 °C	2.1 Fragile and must be protected from physical harm and rough handling.
3. Liquid Thermometer	3.1 None	3.1 Optical viewing required with no electrical feedback for datalogger. 3.2 Low resolution 3.3 Fragile unit

B-4

ADVANTAGES AND DISADVANTAGES OF VARIOUS SENSOR TECHNOLOGIES
AS APPLIED TO THE SUBJECT SENSOR SUITE

SENSOR: Relative Humidity

TECHNOLOGY	ADVANTAGES	DISADVANTAGES
1. Dew Point - Mirror Device	1.1 Very accurate and precise data on the measurement of dew point. This, with the ambient DB temperature, will give relative humidity.	1.1 Large size. The unit can not be miniaturized. 1.2 Large power drain to constantly chill the mirror and operate the optical sensing detector. 1.3 High cost of supporting electronics.
2. Wet Bulb	2.1 Can be used for both non-aspirated (natural) relative humidity or aspirated relative humidity.	2.1 Requires a wetted wick around one of the temperature probes. This generates a requirement for a fresh water reservoir to be with the RH probe. 2.2 Aspirated RH probe requires that air be drawn over the wetted probe at a speed greater than 3+ MPH. This generates a power demand that is large for a long sampling period. 2.3 The wick material becomes contaminated with atmospheric salts and salts in the water supply. This effects the evaporation rate of the wick which results in a false reading.
3. Capacitor Devices	3.1 Small miniature size 3.2 Very little power drain 3.3 Covers a wide range of RH by measuring absolute humidity or water content in a polymer film that is at equilibrium with the surrounding air vapor content. 3.4 Field hardened OTS devices 3.5 Have built in IC units for signal processing.	3.1 Time constant may be slow due to equilibrium between the air and the reactive polymer film. 3.2 Hysteresis effect may exist to generate some measurement error.

ADVANTAGES AND DISADVANTAGES OF VARIOUS SENSOR TECHNOLOGIES
AS APPLIED TO THE SUBJECT SENSOR SUITE

SENSOR: Relative Humidity (Con't)

TECHNOLOGY	ADVANTAGES	DISADVANTAGES
4. Differential cooling of heated thermistors	4.1 Small 4.2 Calibrated to give absolute water vapor content in air. 4.3 Field hardened 4.4 Hybrid Integrated Chip (HIC) has been built that controls the heating, monitoring the cooling of the two thermistors, and the generation of the analog signal for a data logger. 4.5 Comes with a metal , PEi, or metal+PE porous protective shield.	4.1 Requires power to heat thermistor to a temperature significantly above ambient air temperature such that the cooling rate can be measured.

ADVANTAGES AND DISADVANTAGES OF VARIOUS SENSOR TECHNOLOGIES AS APPLIED TO THE SUBJECT SENSOR SUITE

SENSOR: Solar/Radiant

TECHNOLOGY	ADVANTAGES	DISADVANTAGES
1. Differential Energy Absorption: Star, concentric circles or stripped pattern of alternating white and black coated metal substrate connected by thermocouples forming a thermopile (pyranometer)	1.1 Wide viewing angle 1.2 Simplicity of measurement. Ambient air temperature is compensated for by measurement technique. One part of the thermocouple is painted black and the other side is painted white. The radiation will reflect from the white piece and absorb on the black piece. Thus the temperature difference is the result of the absorbed radiation and independent of ambient air temperature. 1.3 The detector scheme is a series of thermocouples that form a thermopile to give adequate S/N level. 1.4 Compensates for self-heating due to black body radiation.	1.1 Observation solid angle is governed by Lambert's cosine law. Thus viewing angle from side is very small compared to direct viewing 1.2 Requires bandpass filters to allow only solar (glass) or near infrared (Pt) to be measured.
2. Total Energy Absorption Sensor	2.1 Small size of sensor. Can be the size of a TO-5 can or about 10 mm diameters. 2.2 Ambient air temperature compensated. 2.3 Compensates for self-heating due to black body radiation.	2.1 Has a limited viewing angle of less than 120° 2.2 Requires a bandpass filter or transparent cover over opening in the TO-5 tin 2.3 Large S/N due to thermocouple

ADVANTAGES AND DISADVANTAGES OF VARIOUS SENSOR TECHNOLOGIES
AS APPLIED TO THE SUBJECT SENSOR SUITE

SENSOR: Solar/Radiant (Con't)

TECHNOLOGY	ADVANTAGES	DISADVANTAGES
3. Black Globe	3.1 Integrates radiant/solar energy. 3.2 Considers wind convective cooling (correlates with man).	3.1 Very slow time constant to come to equilibrium. 3.2 Does not differentiate between solar and radiant energy.

APPENDIX C. SENSOR/ELEMENTS RECOMMENDED FOR EVALUATION AND SOURCES OF COMMERCIALLY AVAILABLE SENSOR TECHNOLOGY

RECOMMENDED SENSOR ELEMENTS FOR EVALUATION

PARAMETER	TECHNOLOGY	SENSOR/MANUFACTURER
Temperature	Thermistor	Multi-sources
Wind Speed	Mechanical	Testoterm
	Hot bead	Sierra, Testoterm,Dantec
	Hot wire	Cole-Parmer
	Differential Cooling	Custom fabricated [Microsen]*
Humidity	Differential Cooling	Shibaura
	Thin Film Cap.	Panametrics, HYCAL Elan, Omic
	Resistive Polymer Film	Victory Engineering
Black Globe Probe [Integrated Solar/Rad]	Black Globe Thermometer	IST
Solar (0.4 to 0.8µ) Filter: 0.4 to 2µ	Thermopile	Armtec
	Photocell	Hamamatsu, Victory Eng.
Radiant (8 to 14µ) Filter: 2 to 20µ	Thermopile	Armtec
	Photocell	Hamamatsu

* Requires significant Research and Development

COMMERCIAL SOURCES FOR RECOMMENDED SENSORS/ELEMENTS

RH	WS	S	R	BGT	Name	Telephone No
X	X				Alnor	708.677.3500
X					Analite Incorporated	516.752.1818
		X	X		AMP	215.666.3500
X					AMETEK	302.456.4400
	X				Applied Technologies, Inc.	303.530.4977
		X	X		Armtec Industries Inc	603.669.0940
X	X				Barnant	800.637.3739
				X	Bruel & Kjaer	513.753.1657
		X	X		Centronic	805.499.5902
X	X				Climatronics Corp	516.567.7300
	X				Climet Instruments	909.793.2788
X	X				Cole-Palmer	800.323.4340
	X				Dantec Measuremet Tech	201.512.0037
X	X			X	Davis Instruments	800.368.2516
X					Elan Technical Corp	203.335.2115
X	X				Earth and Atmospheric Sci	800.543.9930
X					EG&G	617.270.9100
		X	X		Eplab Laboratory	401.847.1031
X					Extech Instruments	617.890.7440
X					General Eastern	800.225.3208
	X				Gardco	305.946.9454
		X	X		Hamamatsu	908.231.0960
	X				Honeywell-Microswitch	800.537.6945
X		X	X		HY-CAL	818.444-4000
X	X			X	IST	716.266.9003
X	X	X	X	X	Kahl Scientific Inst	619.444.0207
X					Kahn	203.529.8643

COMMERCIAL SOURCES FOR RECOMMENDED SENSORS/ELEMENTS

RH	WS	S	R	BGT	Name		Telephone No
X					Leeds and Northrup		215.699.2000
		X	X		Li-COR		402.467.3576
X					Newport Scientific, Inc		301.496.6700
X		X	X		Omega		800.826.6342
X					Ohmic Instruments		800.626.7713
	X				Ohmcraft (Micropen)		716.586.0823
		X	X		Optronics Laboratories, inc		407.422.3171
X	X				Pacer		800.283.1141
X					Panametrics		617.899.2719
X					Phys-Chem Scientific Corp		212.924.2070
X					Protimeter		516.864.5643
X	X				Qualimetrics		916.928.1000
X	X				Shibaura Electronics	Tel	048.852.6661 (Japan)
						Fax	048.852.4324 (Japan)
	X				Simeri Instruments		410.849.2505
	X				Sierra Instruments		800.866.0200
X	X				Solomat		203.849.3111
X					Taylor Environmental Inst		704.684.5178
X					Tesco International		415.572.1683
X	X				Testoterm, Inc		800.227.0729
X					Thunder Scientific Corp		800.872.7728
	X				TSI		800.TSI.2811
X					Vaisala		617.933.4500
X					Victory Engineering		201.379.5900

APPENDIX D. VALIDATION REVIEW AND SURVEY OF CANDIDATE SENSORS FOR TECHNOLOGY TRANSFER

CTC
Upstate New York

104 Nettlecreek Road • Fairport, NY 14450
Voice (716) 223-2632 • Fax (716) 223-4177

SOLAR RADIATION DETECTORS
AND
ANEMOMETER TECHNOLOGIES

REVIEW OF DATA BASE REFERENCES

Prepared for

Dr. Kathy Bernard
Veritay Technology, Inc.
East Amherst, New York

Prepared by

Alexander E. Martens
Executive Director

Reference: Contract No. DAMD17-92-C-2053
Phase II SBIR
U.S. Army Research Institute of Environmental Medicine

June 1995

1.0 Introduction

Per your request I have carried out a review of literature and of activities at various Government Research Centers, Universities and private companies in the fields of solar radiation detection and wind speed measurement. In addition, for sake of comparison, I studied the sub-systems developed by Veritay for measurement of solar radiation and wind speed, to be incorporated in the portable Environmental Health Monitor (EHM). **The purpose of the present effort was to make sure that no potentially useful technology was overlooked during the development and that optimum choices were made.**

I reviewed a large number of references and contacted a number of organizations. My conclusion is that Veritay's solutions to the measurement of at least the wind speed measurement and, possibly, of total solar radiation, are probably unique (though two references regarding the use of thermistors in anemometers are included) and are, for a number of reasons, especially well suited for the application in the EHM.

2.0 Methodology

I commissioned data-base searches by NTTC, CTC, and MTAC. CTC has conducted a preliminary search and an in-depth search, based on the results of the first effort. About one half of the results of these searches was relevant to the subjects of interest.

The following organizations have been contacted for additional information:

- NASA Langley Research Center (Mike Scott, Aerodynamic Measurement Branch)
- NASA Jet Propulsion Laboratory (James Schroeder)
- NASA Goddard Space Fight Center (June Dea)
- NIST Radiometric Physics Laboratory
- NOAA Aeronomy Laboratory (Dr. R. Trotter)
- University of Nebraska at Lincoln (Drs. B. Blad, S. Verma, Ken Hubbard)
- National Renewable Energy Laboratory (Dr. Dana Moran)
- Center for Aerospace Information (Maria Zimmerman)
- Lawrence Berkeley National Laboratory (Dr. C. Fradiadakis)
- NTIS (Harry Samos at LaRC)
- NCAR (Natl. Ctr. for Atmosph. Res.) (S.L. Potter, B. Donaldson)

3.0 Results

3.1 Solar Radiation Detectors

The information I received describes several types of solar radiation detectors:

<u>Active cavity radiometers</u>

Sophisticated, precise, expensive and rather complex instruments used to measure total solar irradiance (optical energy) without spectral discrimination. Employed in spacecraft and terrestrial solar radiation measurements.

References:

Hudson, H.S., California U. at LaJolla (work supported by NASA), ""Helioseismology with ACRIM instrument on the Solar Maximum Mission (Active cavity radiometer irradiance monitor)", COSPAR Plenary Meeting reported in *Advances in Space Research*, v. 11, no. 4, 1991

Kundu, M.B., U. of Maryland, College Park (work supported by NSF), "Measurement of microwave radiation as a proxy for solar irradiance", *Report to NSF Div. of Atmospheric Science.*

Mahan, J.R. et al, NASA Langley R.C., "Comparison of the measured and predicted response of the Earth Radiation budget Experiment active cavity radiometer during solar observations", 1989, *Appl. Optics*, v. 28

Mecherikunnel, A., NASA Goddard SFC, "A comparative study of total irradiance measured by active cavity radiometers", *Metrologia*, v. 30, no. 4, 1993

Moore, R., NASA Marshall SFC, "Active cavity radiometer", 1986, NTIS HC A03/mf A01

Priestly, K.J. et al, NASA Langley RC, "An uncertainty analysis for the ERBE active cavity radiometers", *SPIE Proc.*, v. 1938, 1993

Willson, R.C., NASA JPL, "Active cavity radiometer", 1988, NTIS N89-29413/6, PC A04/MF (Also used tow types of pyrheliometers for comparison of performance).

Wilson, R.C., NASA JPL, "Active cavity radiometer", *NASA report, NTIS HC A04/MF A01*, 1988

Wilson, R.S. et al, NASA Langley RC, "In-flight calibration of shortwave active cavity radiometers -- approach and results", *SPIE Proc. op. cit..*

Because of their complexity, weight, size and cost, these instruments or the sensors employed in them are not suited for the application in EHM.

Pyrheliometers and pyranometers

Both types of these sophisticated instruments are reported to be used in space craft for the measurement of solar radiation. Pyrheliometers measure only the energy of direct sunlight, whereas pyranometers detect the total solar irradiance. These instruments use photodetectors or other optical energy detectors, such as thermopiles.

References:

Bannehr, L., Clover, V., Ntl. Ctr. f. Atmospheric Research, Boulder, CO., "Preprocessing of airborne pyranometer data", 1991, NTIS PB92-119627/HDM, report No. NCAR/TN-364+STR.

Bauman, F. et al, Lawrence Berkeley Ntl. Laboratory, "Integrating pyranometer for beam daylighting measurements in scale-model buildings", 1985, NTIS DE87001884/HDM, report No. LBL-19594.

Crescenti, G.H. et al, Woods hole Oceanographic Institution, "Improved meteorological measurements from buoys and ships (IMET): preliminary analysis of solar radiation and motion data from IMET test buoy", 1989, NTIS PB90-241894/HDM, report No. WHOI-89-45

Flowers, E.C., NOAA, Boulder, CO, "Test and evaluation of the performance of solar radiation sensors at inclination from the horizontal under laboratory and field conditions", 1977, Report No. DSE/1041-1.

Mecherinkunnel, A.T. et al, NASA Goddard SFC, "Solar constant data from Earth radiation budget measurements", 1991, NTIS N91-12456/0, PC AL6/MF A16.

Myers, D.R., Solar Energy Research Inst. (SERI), Golden, CO, "Uncertainty analysis for thermopile pyrometer and pyrheliometer calibrations performed at SERI", 1988, Report SERI/TR-215-3294

NASA, Washington, D.C., Tech Note, "Inexpensive meter for total solar radiation", (A pyranometer containing solar cells measures the combined intensity of direct light from the Sun and diffuse light from the sky), 1987, NASA NPO-16741/TN.

Tsilingiris, P.T., Ntl. Tech. U., Athens, Greece, "Low-cost, non-selective, solar-radiation detectors", 1993. J. Inst. of Electrical Engineers, UK, v. 45, no. 4; (The theory of a low-cost, flat response thermoelectric detector is presented, which can be adapted for use as a pyranometer or net radiometer. The analysis allows the calculation of the responsivity and optimal design of a detector. Theoretical results are corroborated by experimental data.)

Other solar radiation monitors

References:

Pacific Northwest Laboratory, DOE, "Inexpensive device to measure solar radiation", 1993, Doc. no. 000031679. (An inexpensive device designed for low-maintenance operation is available to help scientists who need to assess solar energy resource, monitor atmospheric visibility or track global climate changes. This microprocessor controlled device is a rotating shadowband radiometer; it uses a single detector to record total, diffuse and direct solar radiation. The sensor head consists of an arc-shaped metal band (the shadowband) that rotates, driven by a stepper motor around a silicon cell.)

Breault Research Organization, Inc. Tucson, AZ, has developed for Los Alamos NL a novel radiometer called "LARI". Information has been requested.

Note: Additional brief references to information available form INSPEC on the topics of instruments and sensors to measure solar radiation are included in the Appendix.

3.2 Anemometers

The majority of references to wind speed measuring devices that have no moving parts describe hot-wire, hot-film, or hot-bead sensors. I have encountered only two references (Way, C.M. and Fujita, H.) where a thermistor circuit (as a hot bead) is used to measure water flow.

Heated element anemometers

In these wind speed sensors the rate of cooling of a pre-heated element, due to air movement is measured.

References:

"Hot wire and hot film anemometry (latest citations from the COMPENDEX database)", 1993, NTIS No. PB93-867224, price $65.00. (A bibliography containing citations concerning the design and applications of thermal anemometers.)

Bailley, E.L., Department of the Army, "[Hot-wire anemometer] gyro pick-off", 1980, Patent applied for. (A Wheatstone bridge circuit is described.)

Bridson, D.W., Exeter U., England, "Wind speed measurement for wind turbine testing", 1979, *Proc. of Wind Energy Workshop*, Multi-Science Publishing Co., Ltd., England. (The fragile sensor wire was imbedded in resin.)

Dubbleday, P,S., Naval Res. Lab., Orlando, FL, "Relaxation behavior of a hot-film anemometer under imposed bias flow", 1989, *Review of Sci. Instr.*, v. 60 no. 8.

Frota, M., Moffat, R.J., Stanford U., "Instrumentation for the measurement of turbulence components in a three-dimensional flow field", 1978, Rep. no. AD-AO73954

Gilmore, D.C., McGill U., Montreal, Canada, "The probe interference effect of hot wire anemometers", 1967, Rep. no. TN-67-3. Avail. from AIAA Tech. Libr.

Gray, D.L., NASA Langley RC, "Improved circuit for hot-film anemometer", 1993 (A Wheatstone bridge configuration of hot-film elements is employed). Report No. LAR 14856.

James, J.R. et al, School of Aerospace Medicine, Brooks AFB, TX, "A miniature environmental monitor (portable equipment for environmental monitoring of cabin atmosphere in cockpits)", Rep. no. AD-A017208, Avail. from AIAA Tech. Libr. (A portable suite of sensors -- hot wire anemometer, hygrometer, ambient temp. probe, absolute pressure transducer-- packaged in a medium-sized aluminum suitcase).

Jones, G., NASA LaRC, Tech. Info Sheet, TOPS Exhibit #115, (Multi-sensor hot thin film anemometric sensors are used to measure and separate velocity, density, temperature, and flow direction).

Kinns R., Cambridge U., England, "Calibration of a hot-wire anemometer in velocity perturbation measurement", *J. of Phys. E - Scientific Instr*, v. 6, March 1973.

Kukharets, V.P., "Aircraft dc thermoanemometer (wind velocity measurement)", 1975, *Meteorology and Hydrology*, no. 2, 1975. (Dc and constant temp. anemometers are compared).

Lynch, J.W., Reed, W.H. III, NASA Langley RC, "Anemometer for unsteady wind velocity measurement", 1963, *J. Appl. Meteorology*, v. 2, no. 3.

Maddalon, D.V., NASA Langley RC, "Measurement of crossflow vortex structure: microthin multiple hot-film sensors yield data on crossflow wavelength", U.S. Pat. 5,209,111, Ref. LAR-14824.

McKenzie, R., NASA Ames RC, "Further studies of hot-wire anemometry: measurements of fluctuations of temperature and density are complicated by spurious effects", 1993, Rep. no. ARC-12104.

Messerole, L.T., U.S. Navy Primary Standards Lab., San Diego, CA, "Engineering considerations in anemometer calibration", Proc. 31st Int'l Instrumentation Symposium, May 1985, ISA. (Performance of hot-wire anemometers and those with moving parts was compared).

NASA Ames RC, "Accuracy of [hot-wire] anemometry in supersonic turbulence: the sensitivity of a [hot-wire] probe is compared to laser-induced fluorescence measurements", 1989, Rep. no. ARC-11802/TN.

NASA, Washington, DC, Tech. Note, "Portable airflow meter: a matrix of tubes reduces turbulence in a relatively short length", 1989, Tech. Support Package MSC-21200/TN. (A compact hand-held instrument to measure air flow is a hot wire anemometer in a flow-straightening tube to reduce swirling).

Nishioka, M., Osaka Prefecture U., Japan, "Hot-wire technique for measuring velocities at extremely low wind speed", 1973, *JSME Bull.*, v. 16.

Sakao, F., Hiroshima U., Japan, "Two point calibration of the lineariser for hot-wire anemometer", 1980, *J. of Phys. E - Scientific Instr.*, v. 13. Avail. from AIAA.

Scott, M.A., NASA LaRC, Tech. Info Sheet, TOPS Exhibit #115, (The thin-film sensor array serves as an advanced diagnostic tool in various flow conditions. Two types of sensor arrays: direct-deposited and glued-on. The arrays are made using polymide-based materials and metals.)

Smart, J.C., University of California, L.A., "Micromachined hot-wire anemometer", 1993, (Silicon micro-machining techniques were applied to make arrays of hot-wire sensors that, because of their small dimensions allow for a greater spatial resolution, sensitivity, and response. Low cost of $1 per unit is predicted, vs. $100 for a conventional hot wire anemometer). Report No. UOC-LA93-080-01.

Stannek, T.H., Dantec Measurement Technology, A/S, Denmark, "A new calibrator for improved performance of hot-wires [anemometers]", 1993, 15th Int'l Congress on Instrumentation in Aerospace Simulation Facilities, Saint-Louis, France, Proc. published by IEEE.

Stellema, L., Sydney U., Australia, "A constant temperature hot-wire anemometer", 1978, Rep. no. ATN-7803, Avail. from AIAA Tech. Libr.

Sundberg, G.R., NASA Lewis RC, "Microtronic flow transducer", 1993, Report LEW-14654. (A device similar or identical to the one by J.C. Smart is described).

Symposium on thermal anemometry, 1987, at the Conference on ASM Applied Mechanics, Bioengineering, and Fluids Engineering. Table of contents is included in the Appendix.

Takagi, S., Ntl. Aerospace Lab., Japan, "Design and experimental study of low-noise anemometer with constant current mode", 1982, Rep. no. NAL-TR-697; ISSN-0389-4010, (Novel circuitry, including a low-noise amplifier and a frequency compensation circuit are described).

Other types of anemometers without moving parts.

Various references describe laser Doppler anemometers, sonic anemometers, UVW anemometers, scanning elastic-backscatter lidar, sound detection and ranging (SODAR), Pitot tube.

Watmuff, J.H., NASA Ames RC, "Frequency response of hot-wire anemometers: effects of various circuit parameters are discussed", 1993, Rep. no. ARC-12469.

Way, C.M. et al, Army Engineer Waterways Experiment Station, "Development and application of a thermistor current meter", 1994, NTIS AD-A275 816/7/UDM. A hot-bead thermistor current meter for the measurement of water flow and a calibration system are described)

3.3 Other related instruments, devices, services.

Fujita, H., Kurabe Ind. Co., Ltd., Hamamatsu, Japan, "Environmental sensor", 1994, Proc. IEEE Instrumentation and Measurement Conference", IEEE publication. (To measure the parameters of thermal environment, i.e. temperature, humidity, and air flow rate, a novel RH sensor and a miniature thermistor have been developed. These devices are integrated with their signal-processing circuits. Specifications are given.)

Potter, S.L., NCAR, "Portable Automated Mesonet System", 1993, Doc. no. 000024153. (Portable, solar-powered, automated weather observing system, include temperature, wind speed, humidity, etc., is described)

NCAR carries out environmental instrument development and testing. Contact: Bruce Donaldson, Tel. 303-497-8587.

4.0 Conclusions

Prior art exists describing the use of thermistors as hot-bead devices for wind speed measurement. It appears, however, that Veritay came up with a novel implementation of this technology that improves the response of the sensor and, at the same time, drastically reduces power use, a critical aspects for a miniature, portable instrument.

I have not found any references to solar radiation sensor of the type used in EMH.

I recommend that a patent search should be conducted for both technologies. Upstate CTC can carry out such search.

28/6/10   (Item 10 from file: 2)
04335174 INSPEC Abstract Number: A9305-9385-058
   Title: Investigation of the aging rate of a star-type pyranometer due to
the discoloration of the receiver

28/6/12   (Item 12 from file: 2)
04259213 INSPEC Abstract Number: A9222-9385-078
   Title: Pyranometer frequency response measurement and general correction
scheme for time response error

28/6/13   (Item 13 from file: 2)
04253960 INSPEC Abstract Number: A9222-8610K-008, B9211-8250-022
   Title: Rotating shadow band pyranometer irradiance monitoring for
photovoltaic generation estimation

28/6/14   (Item 14 from file: 2)
04253959 INSPEC Abstract Number: A9222-8610K-007, B9211-8250-021
   Title: Joint EPRI/SERI project to evaluate solar radiation measurement
systems for electric utility solar radiation resource assessment

28/6/15   (Item 15 from file: 2)
04054155 INSPEC Abstract Number: A9203-9385-020
   Title: Spectral and temperature correction of silicon photovoltaic solar
radiation detectors

28/6/16   (Item 16 from file: 2)
03950529 INSPEC Abstract Number: A91113015
   Title: Determination of the optical thickness and effective particle
radius of clouds from reflected solar radiation measurements. II. Marine
stratocumulus observations

28/6/17   (Item 17 from file: 2)
03909640 INSPEC Abstract Number: A91083937
Title: Calibrating a solar calorimeter as pyranometer

28/6/18   (Item 18 from file: 2)
03578754 INSPEC Abstract Number: A90042822, B90019243
   Title: Spectral and temperature correction of silicon-photodiode solar
radiation detectors

28/6/19   (Item 19 from file: 2)
03560152 INSPEC Abstract Number: A90030813, B90019237
   Title: An improved electrothermal model for the ERBE nonscanning
radiometer: comparison of predicted and measured behavior during solar
observations

28/6/20   (Item 20 from file: 2)
03452607 INSPEC Abstract Number: A89111494
  Title: Determination of beam, diffuse and reflected insolation components
through use of a multi-pyranometer array

28/6/21   (Item 21 from file: 2)
03429617 INSPEC Abstract Number: A89104158, B89058819
  Title: Comparison of the measured and predicted response of the Earth
Radiation Budget Experiment active cavity radiometer during solar
observations

28/6/22   (Item 22 from file: 2)
03379431 INSPEC Abstract Number: A89067656
  Title: A simple method for correcting the solar radiation readings of a
Robitzsch-type pyranometer

28/6/23   (Item 23 from file: 2)
03263298 INSPEC Abstract Number: A89004172
  Title: Analysis of solar radiation measurements at Sana'a University
weather station (15 degrees N, 44 degrees E)

28/6/24   (Item 24 from file: 2)
03094093 INSPEC Abstract Number: A88046053, B88023180
  Title: On the accuracy of global solar radiation measurements using
bimetallic pyranographs in India

28/6/25   (Item 25 from file: 2)
03080216 INSPEC Abstract Number: A88034897, B88018085
  Title: Empirical corrections to a rotating shadowband silicon cell
pyranometer

28/6/26   (Item 26 from file: 2)
03024927 INSPEC Abstract Number: A88004142
  Title: Determination of the scaled optical thickness of clouds from
reflected solar radiation measurements

28/6/27   (Item 27 from file: 2)
02997781 INSPEC Abstract Number: A87134028, B87071359
  Title: Empirical radiometric correction of a silicon photodiode rotating
shadowband pyranometer

28/6/28   (Item 28 from file: 2)
02997773 INSPEC Abstract Number: A87134027
Title: A solar radiation distribution sensor

28/6/29   (Item 29 from file: 2)
02903603   INSPEC Abstract Number: A87079537
  Title: Solar radiation received by a spherical body, determined by
pyranometer measurements

28/6/30   (Item 30 from file: 2)
02865984   INSPEC Abstract Number: A87055218, B87029938
  Title: Characteristics of network measurements solar radiation measurement

28/6/31   (Item 31 from file: 2)
02798229   INSPEC Abstract Number: A87014381, B87009000
  Title: Performance characteristics of active cavity radiometers in
unshuttered applications

28/6/32   (Item 32 from file: 2)
02634519   INSPEC Abstract Number: A86042012, B86025433
  Title: A multisensor pyranometer for determination of the direct component
and angular distribution of solar radiation

28/6/33   (Item 33 from file: 2)
02504442   INSPEC Abstract Number: A85098321
  Title: Solar radiation measurements at the Egadi Islands

28/6/34   (Item 1 from file: 8)
04090661
  Title: Theoretical analysis on thermal lag effect of TBQ-2 pyranometer

28/6/35   (Item 2 from file: 8)
04090660
  Title: Further study on calibration of spectral pyranometer

28/6/36   (Item 3 from file: 8)
04081765
  Title: Calibration of a shortwave reference standard by transfer from a
blackbody standard using a cryogenic active cavity radiometer
  Conference Title: Proceedings of the 1994 International Geoscience and
Remote Sensing Symposium. Vol 4 (of 4)

28/6/37   (Item 4 from file: 8)
03990274
  Title: Validation of bidirectional and hemispherical reflectances from a
geometric-optical model using ASAS imagery and pyranometer measurements of
a spruce forest

APPENDIX E. ENVIRONMENTAL TEST FACILITY AT
RESEARCH TRIANGLE INSTITUTE

Set No.	Test No.	T_i (deg C)	T_f (deg C)	Average Velocity[3] (m/s)	Relative Humidity[2] (%)	Hot Bead[2] INIT (deg C)	Tamb[2] INIT (deg C)	RH Comp[2] INIT (deg C)	BGT[2] INIT (deg C)	Relative Humidity[2] INIT (%)	Average 1/2 Life Interval[4,5] (ms)
				TestoTerm Probe Model 1549	Sling psychrometer	BREADBOARD SENSOR SUITE MODULE USING WAND 5 BGT (DUT)					
1	1	4.10	4.80	6.84	55.00	4.35	na	na	na	na	800.70
	2	4.70	4.60	4.78	59.00	4.38	5.30	5.11	5.20	54.04	838.50
	3	4.50	4.40	3.18	59.00	4.59	4.98	4.97	4.98	53.84	962.60
	4	3.60	3.40	1.18	59.00	3.48	4.18	4.13	3.97	55.99	1179.75
2	5	9.70	10.10	1.40	90.00	10.26	10.26	10.44	10.19	74.37	1175.50
	6	11.40	11.40	3.22	87.00	11.95	11.79	11.61	11.56	84.61	905.30
	7	12.10	12.30	5.08	87.00	12.31	12.34	12.38	12.27	86.37	813.50
	8	13.00	13.20	6.99	88.00	12.83	13.13	13.07	13.13	85.60	763.50
	9	22.30	21.60	7.11	72.00	22.35	22.50	22.46	22.52	65.10	na
3	10	35.60	35.60	8.08	49.00	35.52	35.91	35.87	35.98	41.50	716.75
	11	36.00	36.30	5.14	47.00	36.09	36.25	36.23	36.29	41.18	805.95
	12	37.40	37.70	3.16	47.00	37.35	37.79	37.31	37.68	38.88	951.90
	13	38.10	38.40	1.25	45.00	38.14	38.59	38.49	38.23	37.66	1084.55
4	14	41.50	41.60	1.34	83.00	41.38	41.88	41.95	41.60	74.66	998.45
	15	41.90	41.90	2.70	84.00	41.84	42.29	42.33	42.18	74.79	983.90
	16	41.60	41.70	5.10	84.00	41.43	42.00	41.98	42.10	74.02	810.50
	17	41.50	41.80	7.31	84.00	41.38	41.84	41.85	41.96	75.91	734.50
5	18	25.30	24.70	7.58	71.00	25.17	25.71	25.69	25.90	67.28	750.35
	19	24.20	23.30	3.85	70.00	23.93	24.75	24.75	25.05	67.47	857.05
	20	22.40	21.60	2.42	69.00	21.89	22.86	23.02	22.93	67.44	1015.75

NOTES:

1) T_i and T_f are temperature readings taken before and after each wind speed test.
2) Sling Psychrometer and Sensor Suite humidity and temperature readings were taken before each test.
3) The TestoTerm velocity measurement represents a 12 minute (approx.) average taken over the course of a single wind speed test.
4) The Pulsed duty cycle anemometer half-life decay cooling interval falls between 15 degrees above ambient to 7.5 degrees above ambient.
5) Half-life intervals are based on a twenty sample average.

E-2

Figure Ea. Validation Test Results Obtained at Research Triangle Institute for Sensor Suite Breadboard Using Wand 5

Set No.	Test No.	T_i (deg C)	T_f (deg C)	Average Velocity[3] m/s TestoTerm Probe Model 1549	Wet Bulb Temp[2] deg C	deg F	Dry Bulb Temp[2] deg C	deg F	Relative Humidity[2] %	Hot Bead[2] INIT deg C	Tamb[2] INIT deg C	BGT[2] INIT deg C	Relative Humidity[2] %	Average 1/2 Life Interval[4,5] (ms)
					Sling psychrometer					PROTOTYPE SENSOR SUITE MODULE UNIT #2 (DUT)				
1	1	25.2	25.7	6.95	19.4	67.0	24.2	75.5	64	25.58	25.83	25.46	53.1	771.3
	2	25.8	25.9	5.04	18.9	66.0	24.7	76.5	57	25.92	25.83	25.96	48.20	835.0
	3	26.1	26.1	2.74	18.9	66.0	25.0	77.0	56	26.00	26.11	26.04	47.75	984.4
	4	26.1	26.0	1.05	18.9	66.0	25.3	77.5	54	26.12	26.29	26.06	46.74	1157.4
2	5	4.9	5.5	1.67	3.9	39.0	6.4	43.5	66	4.58	4.88	4.71	63.64	735.0
	6	6.4	6.2	1.98	3.9	39.0	6.7	44.0	63	6.37	6.44	6.25	61.26	1117.7
	7	7.2	7.5	5.05	4.2	39.5	4.2	39.5	63	7.14	7.06	6.64	59.96	854.6
	8	7.8	8.0	7.55	4.4	40.0	4.4	40.0	64	7.70	7.73	7.73	59.44	778.0
repeat of test 5	9	6.5	6.4	1.58	n/a	n/a	n/a	n/a	n/a	6.46	6.63	6.74	65.37	1182.7
3	10	38.7	38.9	1.03	25.6	78.0	37.5	99.5	39	38.74	38.65	38.17	30.84	1168.5
	11		39.1	1.09	n/a	n/a	n/a	n/a	n/a	39.18	n/a	n/a	n/a	1162.2
	12	39.1	39.0	1.44	26.1	79.0	37.8	100.0	39	39.15	39.09	38.89	31.20	1127.0
	13	38.9	38.7	2.32	n/a	n/a	n/a	n/a	n/a	39.00	38.83	38.70	32.20	1031.4
	14	38.4	38.3	3.18	n/a	n/a	n/a	n/a	n/a	38.60	38.46	38.50	33.25	985.7
	15	37.9	37.7	4.95	26.1	79.0	36.9	98.5	43	38.06	37.93	38.14	34.59	836.9
	16	37.4	37.4	7.74	26.1	79.0	36.4	97.5	45	37.49	37.33	37.55	35.89	748.3
	17	37.4	37.2	10.26	26.1	79.0	36.4	97.5	45	37.46	37.20	37.33	36.54	695.0
4	18	44.9	45.1	1.11	40.3	104.5	43.3	110.0	83	44.98	44.70	44.33	73.38	1066.9
	19	45.3	45.4	1.27	40.8	105.5	43.9	111.0	84	45.55	45.18	44.87	73.18	1138.1
	20	45.3	45.6	2.80	41.1	106.0	43.9	111.0	84	45.53	45.28	45.21	73.51	1097.0
	21	45.3	45.1	4.54	40.6	105.0	43.9	111.0	81	45.63	45.22	45.43	72.47	978.1
	22	44.9	44.8	6.74	40.6	105.0	43.9	111.0	81	45.28	44.86	45.07	72.69	842.0
	23	44.9	44.7	10.55	40.6	105.0	43.6	110.5	84	44.96	44.58	44.77	74.26	784.7

NOTES:

1) T_i and T_f are temperature readings taken before and after each wind speed test.
2) Sling Psychrometer and Sensor Suite humidity and temperature readings were taken before each test.
3) The TestoTerm velocity measurement represents a 6 minute (approx.) average taken over the course of a single wind speed test.
4) The Pulsed duty cycle anemometer half-life decay cooling interval represents a half-life decay cooling interval falls between 15 degrees above ambient to 7.5 degrees above ambient.
5) Half-life intervals are based on a twenty sample average.

E-3

Figure Eb. Validation Test Results Obtained at Research Triangle Institute for Prototype Sensor Suite Unit No. 2

APPENDIX F. ERGONOMICS STUDY

PRELIMINARY ERGONOMIC ANALYSIS

OF

THE ADVANCE TEMPERATURE SENSOR SUITE

The Advance Temperature Sensor Suite [ATSS] is an environmental measurement instrument developed to measure air temperature, relative humidity, wind velocity, and radiant energy according to the functional specification of the sponsoring agency, to be the size of a cigarette package according to the configuration specification, and to be operated by a single person. This report addresses ergonomic issues with the current design of the ATSS.

The method of generating the ergonomic data was to have two consultants review the current mockup of the ATSS. Each consultant has a PhD in Human Factors and over 20 years as an active research in the field of ergonomics. The first consultant's professional interest is in the design of machines to maximize the man-machine interface. The second consultant's professional interest is in training with emphasis on the man-machine interface.

The physical and functional aspect of the instrument was described to them so that they would have a feeling of how the instrument was to be used. After this briefing, they commented on the ergonomic issues based on the ATSS mockup model. The majority of the ergonomic issues are related to the membrane keypad and its menu.

The format of the report will be to list the ergonomic issues that were identified and not to give a summary of them. In this fashion, the critical nature of each issue can be weighted by Veritay to determine if
    1: Action should be taken to satisfy the current SBIR sponsor;
    2: Action should be delayed for consideration in the commercial model, or
    3: No action at all.

Figure 1 is a drawing of the physical form of the ATSS. This will be used as a reference when physical ergonomic issues are discusses. Figure 2 is a schematic of the display flowchart that describes the operational nature of the ATSS.

SUMARY

The majority of the comments were on the display/keypad function flowchart. The emphasis was on making display/keypad flow in a more operational manner as the instrument would be used as a field instrument for R&D purposes as implied by the multi choices in the menu. It was not clear how the ATSS would be placed in the environment to take data.

The overall impression was that the design was very well conceived to meet the use of a miniature hand-held device.

RECOMMENDATIONS

The display/keypad functions should be readdressed with emphasis on symbols that are easier to understand and fit international or military configuration. It is also recommended that a separate ONN/OFF switch be used and not part of a dual functional keypad entry point.

The ATSS should have printed on it both the display/keypad functions flowchart and operating instructions.
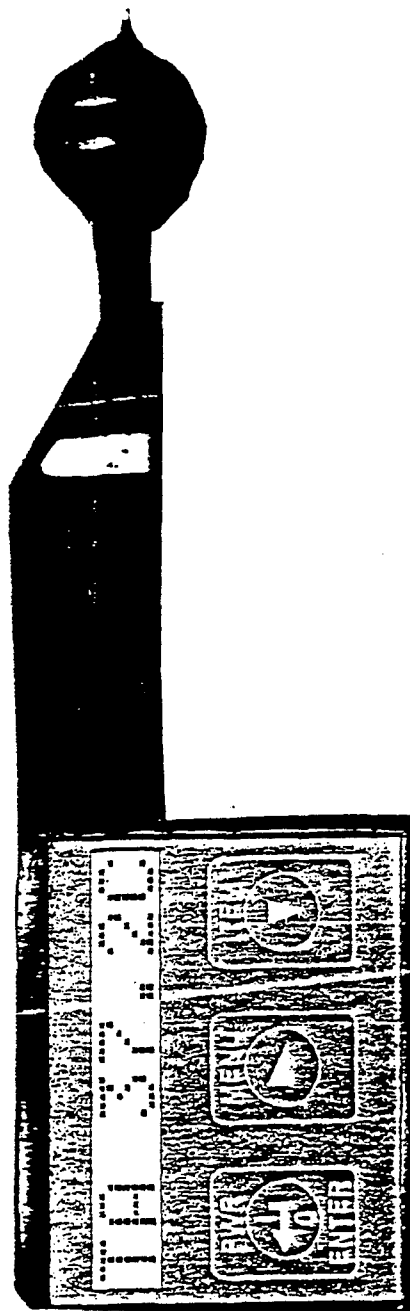
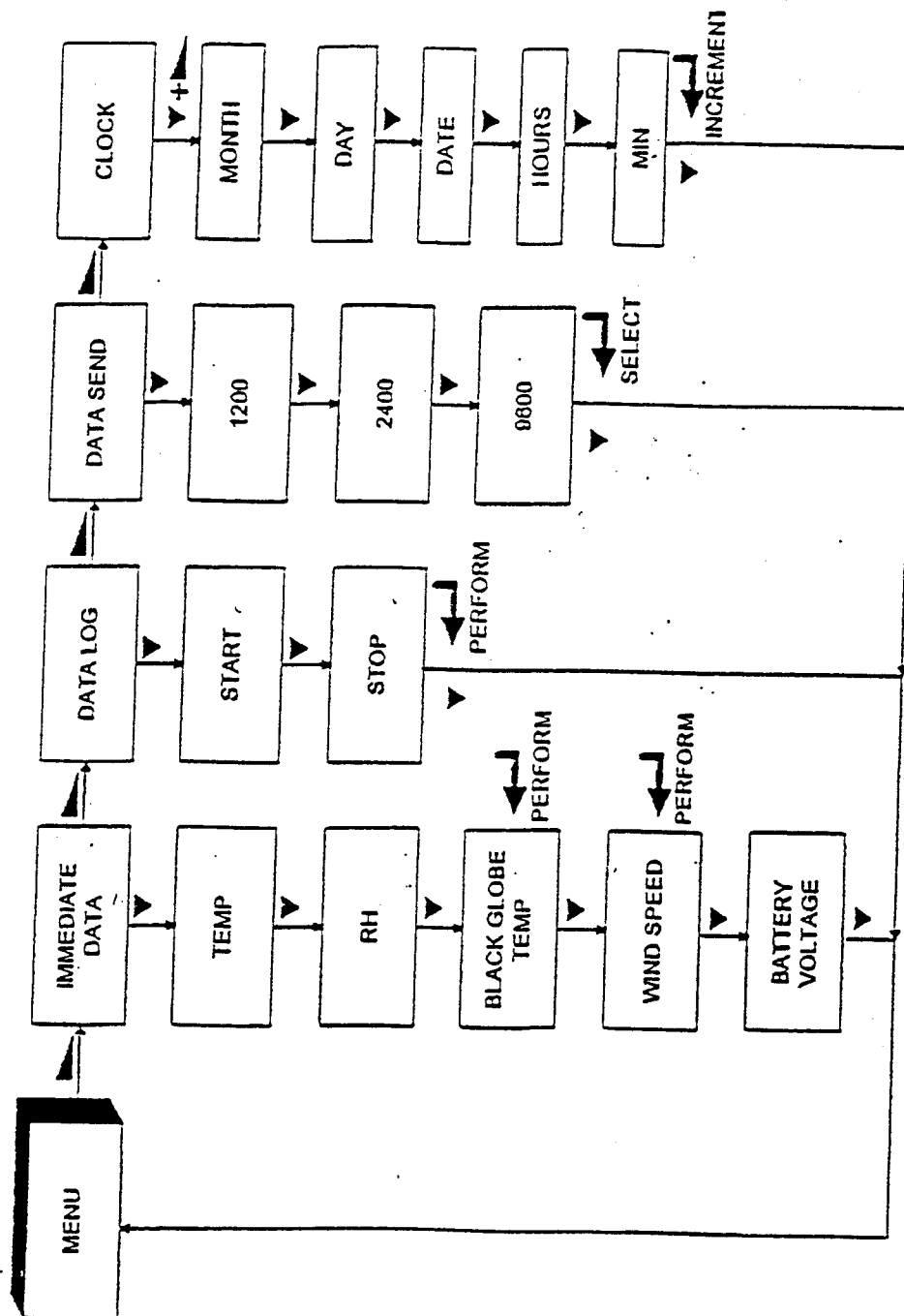FIGURE 1 DRAWING OF ADVANCE TEMPERATURE SENSOR SUITE

FIGURE 2:   FLOW CHART OF DISPLAY / KEYPAD FUNCTIONS

F-4

ERGONOMIC COMMENTS

1. The overall package configuration was very pleasing to the eye and easy to hold. The question was raised about if the soldier or person would be wearing NBC protective ensemble or operate the equipment with NBC gloves being worn.

2. There should be a separate power switch that is ""ON/OFF" or "I/O". It is not a good idea to have multiple duty switches for the military. Is it possible for them to accidentally turn the instrument off when they really mean to do something else.

3. If this is to be used as a field instrument for gathering data, where is the RS-232 port located?

4. As a field instrument for taking data during a man-in-the-loop test, is there going to be a special holder to hold the instrument up in the air or is it just going to sit on the ground?

5. There were several comments on the display/keypad
      a. Clock had several subitems that did not seem to be needed. The subitems can be shortened as follows:
            1. Eliminate MONTH and DAY
            2. Have date as MM/DD/YR
            3. Replace HOURS and MIN with 24hr clock with time zone indicator
            This would be HH:MM:TZ   HH=hour 00 to 23, MM=min from 00 to 59 and TZ
            would be ES for Eastern Standard time or ED for Eastern Daylight Savings,
            or IT for international time.
            4. Add a subitem that would allow the time to be entered manually. The mechanism
               of using two keys as in a digital watch would be acceptable.

      b. Change MENU to something SELECT

      c. Change ITEM to SCROLL

      d. Do not have ON/OFF and the ENTER key on the switch or keypad.

      e. How do you start to store data or do you continuously store data until the memory is full and then it is FIFO (first in - first out) protocol? How is data cleared from memory? Do you have a protocol that stamps date/time followed with the data run then with another date/time stamp or followed with a space.

      f. Move the display to the side of the unit and move the keypad up to the location of the display. This would allow a flowchart of the display information and instructions to be printed underneath the keypad. The backside could have a detailed instruction of how to operate all of the function the entire ATTS.

      g. Eliminate the BATTERY VOLTAGE and have the display unit flash when battery is low or have the display flash BATTΔLOW

      h. The keypad marking should be a single marking that outlines where the active area of the pad is. It is not desirable to have a circle area within a square. Thus if the area within the single marking is touched, then the pad has been activated.

      i. If there is a RS-232 port, is it also available to override the keypad or is it only used to download data?

j. The menu DATA LOG meaning is not clear from its verbiage. It should be changed to something like ACQΔDATA. Under this menu the first subitem would be for starting. The display would show READY or START. After one presses ENTER, the display could be showing elapse time or just show RUNNING. When one wants to stop they would scroll to STOP and press ENTER.

k. There is a lot of room on the membrane keypad. The words should be spelled out, such as POWER not PWR. Only mil or international symbols should be used.

l. If one scrolls to Black Globe or Wind Speed and there is a required time delay before the data is taken, i.e.2 min or 3 min. then the display should indicate that a data run has been started by either flashing the display or have a clock counting down such as WAITΔXXX with X displaying time as seconds left.

m. The sequence of menu should be in the order that data would be taken:
> Set clock
> Start Data Run
> Observe Data
> Send Data

n. It would be better to have a separate ON/OFF switch with the other membrane pads being in this order: Menu - Item - Entry

6. Is there a built in delay between when the machine is turned on and when the data is to be taken to allow for the black globe and wind speed to come to equilibrium and take realistic data that is not effected by the residual storage.

7. If the arm with the sensors are always to be completely folded out, then there should be a locking mechanism that would hold them in place.

8. A question about the hot ball temperature and burning the skin. If the temperature was to be raised 20°C above ambient then it could be possible to have the ball temperature greater than 140°C which the skin should not be allowed to experience. Is there a built in mechanism that limits the amount of energy that the ball can obtain and is the mass of the ball small enough that there would not be significant energy transfer?

9. What does the storage or packing case look like?

10. Is the ATSS easily taken out of the packing case without causing interference of the temperature sensors from the person operating the ATSS?

11. How much time does it take for the ATSS to come into environmental equilibrium after it is taken from the packing/storage case? The Mil-Std-810D has a test for storage at 70°C (165°F) and then the unit must function after removal from storage container.

OPERATING INSTRUCTIONS FOR THE ENVIRONMENTAL HEALTH MONITOR (PROTOTYPE UNIT, Ver. 1.03)
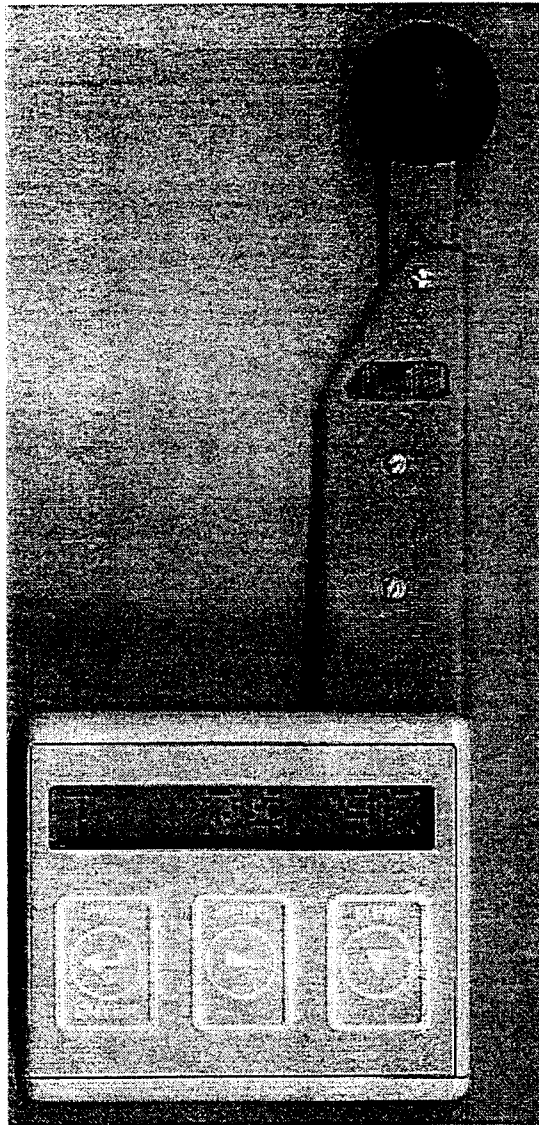
INTRODUCTION

The following instructions pertain to the prototype Environmental Health Monitor (EHM) unit which is operating under the program revision V1.03. This particular software version implements only the basic features of the instrument's capabilities and is intended for purposes of demonstrating the functionality of the Sensor Suite Support Module (SSSM) detachable probe in conjunction with the Data Acquisition System (DAS) base unit. At present, the following measurements have been made available:

- Ambient Temperature

- Relative Humidity

- Black Globe Temperature

- Wind Speed

OPERATION

The EHM instrument is shown in the various SSSM arm positions in Figure 1. The first, or closed position is the typical configuration when the instrument is not in use or in shipment. This configuration also helps protect the Black Globe and Anemometer sensors. The fully deployed position should be used when taking measurements.

NOTE: The EHM instrument is shipped with the SSSM arm attached to the DAS base. *The EHM unit will not power ON with it removed.*

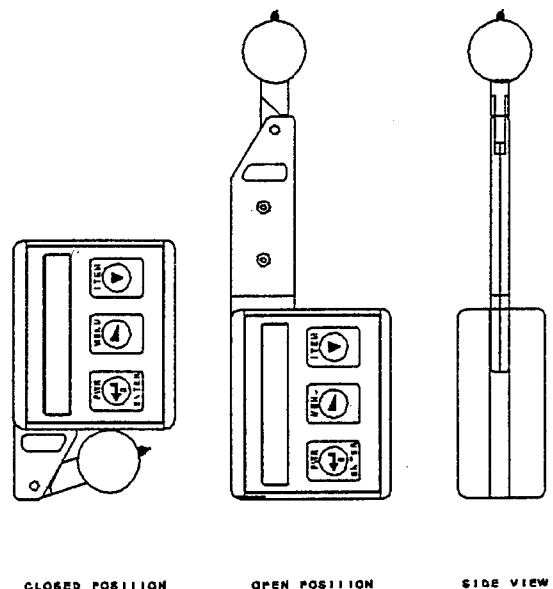CLOSED POSITION   OPEN POSITION   SIDE VIEW

Figure 1. Sensor Suite Arm Positions

2

To operate the instrument, extend the SSSM arm by rotating it into the open position as shown in Figure 1. Turn the unit *ON* by depressing the PWR-ENTER ↵ key (refer to Figure 2) for approximately two to three seconds until the LCD is completely annunciated, followed by the Battery Voltage indication (BT). The battery level will remain on the display until the PWR-ENTER ↵ button is released, permitting the unit to advance to the *Imm Data* menu heading. Menu functions can now be selected by following the Keyboard Menu illustrated in Figure 3.
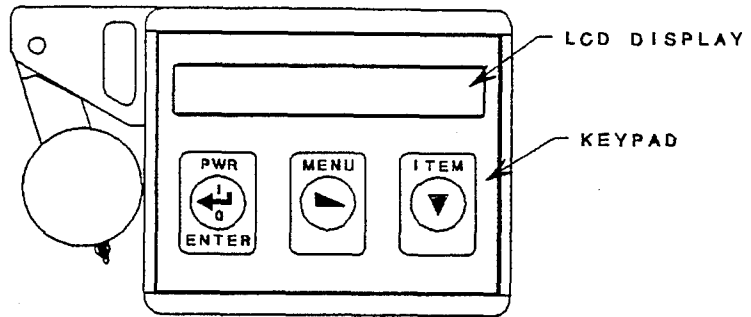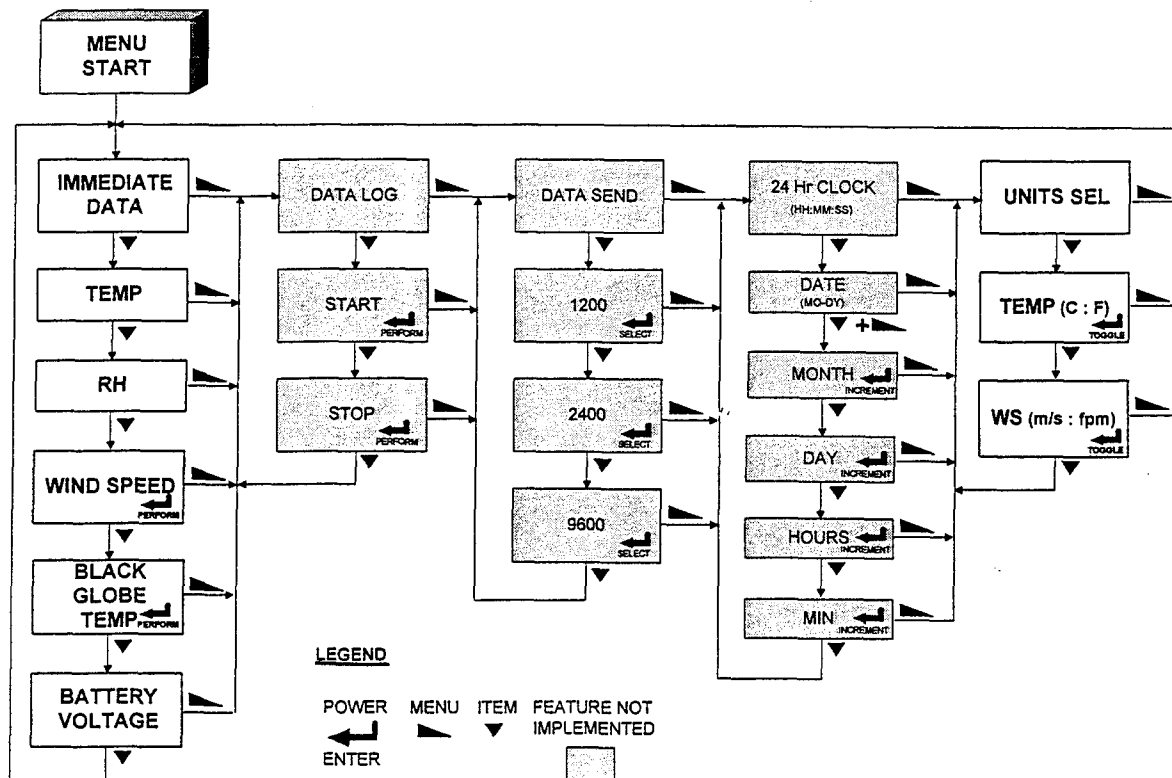

Figure 2

Figure 3. EHM Menu and Keypad Functions

3

Advancing (across) to the next menu selection takes place during the release action of the MENU► button. Advancing (downward) to the next sub-menu selection takes place during the release action of the ITEM▼ button. Measurement of Ambient Temperature (T) and Relative Humidity (H) will be immediately displayed when scrolling down the Immediate Data menu column. Black Globe Temperature (G) and Wind Velocity (V), however,
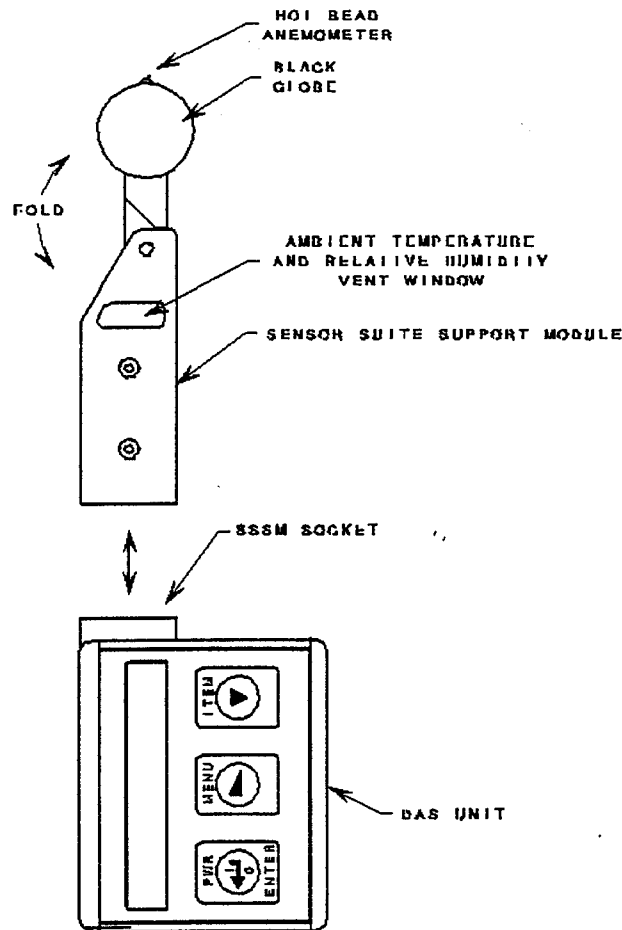
Figure 4

4

require approximately two minutes each to compute an average measurement and display the results. Black Globe Temperature and Wind Velocity measurements are initiated by depressing the PWR-ENTER ← button at the appropriate menu selection and can be skipped over entirely by depressing the MENU▸ or ITEM▾ button. During Black Globe Temperature measurement, the display will prompt the user of the remaining sample time before an average value is computed and displayed. During Wind Velocity measurement, the display will indicate the number of anemometer readings remaining in the two-minute sampling interval and will report a run-time-averaged wind speed at the end of each reading. The keypad will be inoperable during Wind Speed and Black Globe Temperature measurement. Keypad functionality will return after the display of these results. The last selection of the *IMM DATA* menu is the battery level indication in Volts. Depressing the ITEM▾ button once more will return the unit to the top of this menu column. The displayed units of measure for both Ambient Temperature and Wind Velocity can also be changed. This is performed by advancing the menu selection using the MENU▸ key until the *UNITS SEL* menu appears. Depressing the ITEM▾ button selects the function to be changed and the PWR-ENTER ← button toggles the units displayed. Depressing the MENU▸ key will return the EHM back to the top of the menu, *IMM DATA*. The EHM unit can be powered *OFF* at any menu or sub-menu level except during Black Globe and Wind Velocity measurement and, is achieved by holding the PWR-ENTER ← key down for approximately two to three seconds until the LCD is completely blanked.

EHM PROTOTYPE SPECIFICATIONS

DISPLAY FORMAT

The following illustrates the display format for each unit of measure. A blank digit is indicated by an underscore (_).

	Low	High
Range>		
Digits>	12345678	12345678
Temperature:	T___5.0C	T__65.0C

5

```
                           T__41.0F   T_149.0F

Rel. Humidity:             H___5.0%   H__95.0%

BGT:                       G___5.0C   G__77.0C

Wind Velocity:             V_0.0m/s   V_9.9m/s
                           V____0ft   V1949fpm   (ft/min)

Natural Wet Bulb:          N___0.0C   N__77.0C (Software not implemented
                                               this version)
Battery:                   BT__6.2V   BT_10.5V
```

PHYSICAL

Operating Temperature   5 °C to 65 °C (proposed)

Storage Temperature   -10 °C to 65 °C

Battery Type   Standard 9V

Weight   Dry: 104.6 g (3.7 oz)
                    w/Battery: 150.8 g (5.3 oz)

Size (LxWxH)   Open: 17.6 cm x 5.74 cm x 3.11 cm (6.93 in x 2.26 in x 1.23 in)
                    Closed: 9.26 cm x 5.74 cm x 3.11 cm (3.65 in x 2.26 in x 1.23 in)

6

BATTERY REPLACEMENT

The instrument will display *LOW BATT* if the battery voltage level falls below 7.0V (the actual Battery Voltage can be read by selecting it from the Immediate Data menu column). The EHM unit is capable of operating down to a battery level of 6.3 Volts. Changing the 9V battery should be done carefully as opening the prototype unit will expose static sensitive circuitry. This is done by removing case screws and sliding the bottom half of the case cover (Figure 5). Remove battery directly without dislodging circuit board and insert new battery making sure thin plastic insulator isolates battery from circuit components. Replace cover making sure both case halves mate correctly and wires are not pinched before securing screws.
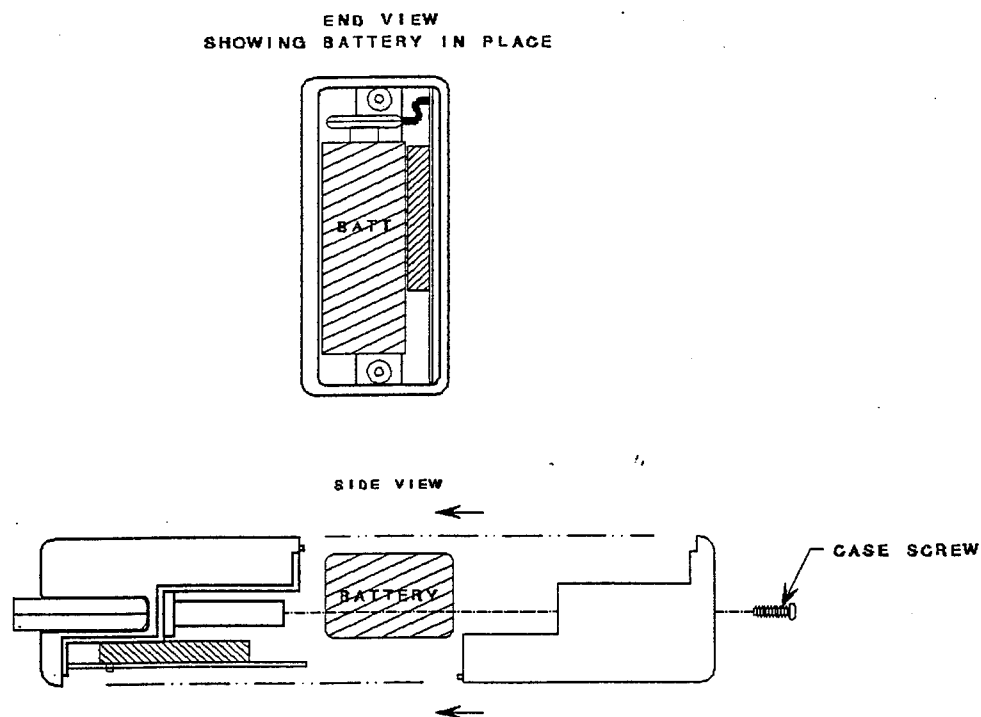
END VIEW
SHOWING BATTERY IN PLACE

SIDE VIEW

CASE SCREW

Figure 5. Location of 9V Battery

7

DEPARTMENT OF THE ARMY
US ARMY MEDICAL RESEARCH AND MATERIEL COMMAND
504 SCOTT STREET
FORT DETRICK, MARYLAND 21702-5012

REPLY TO
ATTENTION OF:

MCMR-RMI-S   (70-1y)   21 Jan 00

MEMORANDUM FOR Administrator, Defense Technical Information
            Center, ATTN: DTIC-OCA, 8725 John J. Kingman
            Road, Fort Belvoir, VA 22060-6218

SUBJECT: Request Change in Distribution Statement

1. The U.S. Army Medical Research and Materiel Command has
reexamined the need for the limitation assigned to technical
reports written for the attached Awards. Request the limited
distribution statements for Accession Document Numbers listed be
changed to "Approved for public release; distribution unlimited."
These reports should be released to the National Technical
Information Service.

2. Point of contact for this request is Ms. Virginia Miller at
DSN 343-7327 or by email at virginia.miller@det.amedd.army.mil.

FOR THE COMMANDER:

Encl   PHYLIS M. RINEHART
as   Deputy Chief of Staff for
                                     Information Management